MOLECULAR ENGINEERING OF POLYCARBONATES DERIVED FROM POLYHYDROXYL NATURAL PRODUCTS AS RESOURCEFUL MATERIALS

A Dissertation

by

ALEXANDER LONNECKER

Submitted to the Office of Graduate and Professional Studies of
Texas A&M University
in partial fulfillment of the requirements for the degree of

DOCTOR OF PHILOSOPHY

Chair of Committee,	Karen L. Wooley
Committee Members,	David E. Bergbreiter
	Donald J. Darensbourg
	Arul Jayaraman
Head of Department,	Simon North

December 2017

Major Subject: Chemistry

ABSTRACT

Utilizing renewable resources can address toxicological and environmental issues associated with commodity plastics and engineering materials. In addition, scientists can exploit the various structures and chemistries of naturally occurring feedstocks to create a myriad of polymers with unique functionalities and tunable properties. With this in mind, linear polycarbonates incorporating glucose into the main chain were synthesized by AA'/BB polymerizations of phosgene, diphosgene or triphosgene and one of four different glucose-based regioisomeric diols. Each monomer exhibited unique reactivities and produced polymers with varying thermal properties. Monomers bearing hemiacetal functionalities produced polymers with low molecular weights, (>10,000 Da), whereas the remaining monomers permitted higher molecular weights (>30,000 Da). Polymers with the carbonate linkage connected to the anomeric center of the glucose ring were more thermally sensitive, with onset decomposition temperatures (T_ds) ranging from 137 to 230 °C. TGA-MS analysis revealed early degradation was due to loss of carbon dioxide and benzyl protecting groups. In addition, by modifying the monomer synthetic scheme to produce AA'A'A bis-adducts, regioregular polymers possessing high molecular weights (>100,000 Da) and elevated glass transition temperatures were obtained.

Functional linear polycarbonates bearing an endocyclic alkene were formed *via* organocatalyzed ring-opening polymerization of a six-membered carbonate monomer synthesized from D-glucal. Using 1,5,7-triazabicyclo[4.40]dec-5-ene catalyst (1 mol %)

a polymer with a molecular weight of 9900 Da and polydispersity of 1.21 was obtained, whereas a 1,8-diazabicyclo[5.4.0]undec-7-ene and 1-(3,5-bis(trifluoromethyl)phenyl)-3-cyclohexyl-2-thiourea cocatalyst system (2 mol%) afforded a polymer with a molecular weight of 5000 Da and a unimodal polydispersity of 1.20. Both catalyst systems reached full conversions in dichloromethane under argon at 30 °C in fewer than ten minutes, forming amorphous polymers with a T_g at 65 °C and T_ds *ca*. 200 °C.

Tunable three-dimensional polycarbonate networks were synthesized from quinic acid, a polyhydroxyl natural product, similarly structured to glucose. Solvent-free thiol−ene chemistry was utilized in the copolymerization of tris(alloc)quinic acid and a variety of multifunctional thiol monomers to obtain poly(thioether-*co*-carbonate) networks with a wide range of achievable thermomechanical properties including glass transition temperatures from −18 to +65 °C. Addition of diallyl carbonate was explored as a comonomer, which allowed for the lowering of glass transitions (38 to 65°C), without altering rubbery modulus. Control force cyclic testing demonstrated excellent shape memory; high percent recoverable strains were obtained, reaching 100% recovery during fourth and fifth cycles.

DEDICATION

This work is dedicated to my family.

Thank you so much Mom, Dad, Mark, Matthew, Jeffrey, and Grandmother for all of your love and support. I could not have done this without all of you.

ACKNOWLEDGEMENTS

This work would not have been possible without the mentorship of my advisor, Prof. Karen L. Wooley. I thank her for the guidance and motivation, and never allowing me to be satisfied with the bare minimum. Throughout my career, I will carry the work ethic and standards that were instilled in me during my tenure as a student in her lab.

I would like to thank my dissertation committee, Dr. David E. Bergbreiter, Dr., Donald J. Darensbourg, and Dr. Arul Jayaraman, for their comments and suggestions make advances in my research. I would also like to thank the staff at Texas A&M for providing the facilities and business logistics that helped make conducting research and graduating possible, including: Steve Silber, Vladimir Bakhmoutov and K. P. Sarathy (NMR Facility), Yohannes Rezenom and Vanessa Santiago (Laboratory for Biological Mass Spectrometry), Philip Wymola and Melvin Williams (Stockroom), Bill Merka (Glass Shop), Sanding Manning (Graduate Advising) and everyone from the business office.

I had the unique opportunity to conduct a multi-disciplinary project that included synthetic organic chemistry, analytic chemistry, and materials science. I would like to acknowledge my collaborators outside the Wooley laboratory that helped contribute to the vision and execution of these projects. Working with Taylor Ware at UT Dallas, I was able to expand my research interest from strictly synthetic organic chemistry to also include materials and biomedical sciences. I also worked with Keith Hearon on many different projects, who encouraged me to push continually the envelope and strive to

create the most novel and impactful research possible. Much of what I learned about materials science comes from working with him in the Maitland lab. I will forever be grateful for these experiences.

I was privileged to work alongside many talented graduate students and post-doctoral associates that helped teach many synthetic and analytical skills, as well as challenge me to do quality research. Céline Besset, who was a post-doctoral researcher when I first joined the lab showed me the ropes and is responsible for teaching me many synthetic techniques and skills. More importantly, she was a great mentor and I owe my work ethic and drive to her. Simcha Felder and Young Lim, two extremely talented graduate students helped with the completion and publication of my first project. Laruen Link was an invaluable lab mate and collaborator and critical in the expansion and application of our crosslinked polymers. I would also like to thank all other Wooley Lab members, particularly Kevin Pollack, Adriana Pavia Sanders, Marco Giles, Amandine Noel, and Guorong Sun, for everything from answering a quick question to taking time out of the day for a bigger task, or maybe just for a casual chat, all of which helped make my day-to-day experience in this lab memorable. Outside the Wooley lab, I would like to thank my colleagues Keith Hearon and Marc Rufin for their support, advice, and friendship during our time in College Station.

Finally, I want to thank my incredible family for their never ending love and support. My parents always put my education and well-being before all else. I would not have been able to have such academic successes without their unwavering encouragement and sacrifices throughout my life. I want to thank my Grandmother, who has been a

constant support throughout my undergraduate and graduate experiences, whether it is chemistry or swimming. I want to thank my brothers, Mark, Matthew, and Jeffrey, who are all nuts, but a constant source of encouragement and distraction. I am very lucky to have a great family that has taught me good values and shaped me into the man that I am today.

CONTRIBUTORS AND FUNDING SOURCES

Contributors

This work was supported by a dissertation committee consisting of Professors Karen L. Wooley (Advisor), David E. Bergbreiter, and Donald J. Darensbourg of the Department of Chemistry and Professor Arul Jayaraman of the Department of Chemical Engineering.

This dissertation includes several collaborative projects between members of the Wooley and Maitland laboratories at Texas A&M University. In Chapter II, synthetic strategies for the *1,4*-monomer as well as the initial screening method for polymerization found were developed by Céline J. Besset. In addition, Simcha E. Felder and Young H. Lim contributed to the polymer synthesis and characterization. In Chapter IV, Young H. Lim contributed to the characterization of monomeric units and precursors. Chapter V includes collaborative work between the Wooley and Maitland labs at Texas A&M University. Quinic acid cyclic lactone synthesis was developed by Céline J. Besset. Mechanical testing *via* dynamic mechanical analysis (DMA) was performed alongside Keith Hearon and tensile testing was performed with Keith Hearon and Lauren A. Link. Thermomechanical analysis (TGA) and differential scanning calorimetry (DSC) of select samples were performed by Lauren A. Link. Significant studies, although not discussed in Chapter V, were reported in the cited article found in the chapter and conducted by L. Link. Small molecule mass spectral analysis for all projects was performed by the Texas

A&M University for Biological Mass Spectrometry. All other work conducted for the dissertation was completed by the student independently.

Funding Sources

Financial support provided by the National Science Foundation (CHE-1610311) and the Welch Foundation (A-0001) is gratefully acknowledged.

NOMENCLATURE

1,2-EDT	1,2-Ethanedithiol
1,6-HDT	1,6-Hexanedithiol
2,3-BDT	2,3-Butanedithiol
AFM	Atomic Force Microscopy
Alloc	Allyloxycarbonyl
APC	Aliphatic Polycarbonate
ATR	Attenuated Total Reflection
Bn	Benzyl
$CDCl_3$	Deuterated Chloroform
d	Doublet
DBU	1,8-diazabicyclo[5.4.0]undec-7-ene
DCM	Dichloromethane
dd	Doublet of Doublets
ddd	Doublet of Doublet of Doublets
dddd	Doublet of Doublet of Doublet of Doublets
DNA	Deoxyribonucleic Acid
dt	Doublet of Triplets
DCM	Dichloromethane
DP	Degree of Polymerization
CD_2Cl_2	Deuterated Dichloromethane

DBU	1,8-diazabicyclo[5.4.0]undec-7-ene
DMA	Dynamic Mechanical Analysis
DMAP	4-Dimethylaminopyridine
DMF	*N*,*N*-Dimethylformamide
DMPA	2,2-Dimethoxy-2-Phenylacetophenone
DMSO	Dimethylsulfoxide
DSC	Differential Scanning Calorimetry
ESI	Electron Spray Ionization
EtOH	Ethanol
FTIR	Fourier Transform Infrared
GPC	Gel Permeation Chromatography
HH	Head-to-Head
HRMS	High-Resolution Mass Spectrometry
HT	Head-to-Tail
IPA	Isopropyl Alcohol
IR	Infrared
m	Multiplet
MALDI	Matrix Assisted Laser Desorption Ionization
Me	Methyl
M_n	Number-Average Molecular Weight
M_w	Weight-Average Molecular Weight
MeOH	Methanol

MS	Mass Spectrometry
NaOMe	Sodium Methoxide
NMR	Nuclear Magnetic Resonance
PCL	Poly(ε-Caprolactone)
PEG	Poly(Ethylene Glycol)
PETMP	Pentaerythritol Tetrakis(3-Mercaptopropionate)
PDI	Polydispersity Index
PDLA	Poly(D-Lactide)
PDLLA	Poly(D,L-Lactide)
PDGC	Poly(ᴅ-Glucose Carbonate)
PGA	Poly(Glycolic Acid) or Poly(Glycolide)
PLA	Poly(Lactic Acid) or Poly(Lactide)
PLGA	Poly(Lactide-*co*-Glycolide)
PLLA	Poly(L-Lactide)
PTMC	Poly(Trimethylene Carbonate)
pyr	Pyridine
q	Quartet
R_f	Retention Factor
ROP	Ring-Opening Polymerization
s	Singlet
sept	Septet
SEC	Size Exclusion Chromatography

SS	Stainless Steel
t	Triplet
TAQA	Tris(alloc)Quinic Acid
TBD	1,5,7-Triazabicyclo[4.40]dec-5-ene
TBS	*tert*-Butyl Silyl
TBSCl	*tert*-Butyl Silyl Chloride
td	Triplet of Doublets
T_d	Onset Decomposition Temperature
TEGBMP	Tetraethylene Glycol Bis-(3-Mercaptopropionate)
TIPS	Triisopropylsilyl Ether
T_g	Glass Transition Temperature
TGA	Thermogravimetric Analysis
TGA-MS	Thermogravimetric Analysis Coupled Mass Spectrometry
THF	Tetrahydrofuran
TLC	Thin Layer Chromatography
TMPTMP	Trimethylolpropane Tris(3-Mercaptopropionate)
ToF	Time of Flight
TT	Tail-to-Tail
TU	1-(3,5-Bis(Trifluoromethyl)-Phenyl)-3-Cyclohexyl-2-Thiourea
UV	Ultraviolet
VOC	Volatile Organic Compound
XRD	X-Ray Diffraction

TABLE OF CONTENTS

Page

LIST OF EQUATIONS

Page

LIST OF FIGURES

Page

Page

Page

LIST OF SCHEMES

LIST OF TABLES

CHAPTER I

INTRODUCTION

1.1 Background and Motivation

Over the past few decades, there has been a significant push by researchers and various consumer markets to utilize polymers that originate from natural products, in order to diminish dependence on petrochemical resources, reduce landfill accumulation of waste, and curtail CO_2 emissions. Moreover, demand for renewable polymers is growing, the production and commercialization of renewable bio-based polymers are expected to continuously grow by 2030. In fact, the bio-based plastics market is expected to reach *ca*. €5.2 billion by 2030.[1] Although, it has been the general goal for renewable polymers to resemble and replace existing polymeric materials derived from petrochemicals, the discussion does not need to be limited to the discussion to the development of new commodity plastics. One area of research that can not only utilize renewable resources as a cost effective feedstock, but could also benefit from their use as synthetic starting materials, is the development of biomedical materials, specifically those as degradable orthopedic implants for bone fixation.

Bone tissue is susceptible to fracture as a result of trauma, pathology, and resorption.[2,3] In fact, every year more than 5.5 million orthopedic surgeries are performed in the United States alone, with open reduction of fractures by internal fixation representing 80,000 of those.[4] Internal fixation entails the use of implants such

as plates, screws, pins and wires holding bone fragments in place during bone healing; for rigid fixation, plates and screws are most commonly used.[5] Types of materials that are used for bone fixation can be classified into two groups according to their degradation profiles: bio-inert and biodegradable.[6,7] Bio-inert fixation and repair devices are fabricated with stainless steel, titanium, cobalt-chromium, and their alloys, which have been employed successfully for the majority of fracture fixation devices,[8-10] albeit with several issues. First of all, there is a remarkable difference in the mechanical properties of the metals used and cortical bone (Table 1.1), which leads to a condition called stress-shielding. The compressive stress-shielding at the fracture-interface immediately after fracture-fixation delays callus formation and bone healing leading to lower density bone tissue around the fixation device. Likewise, the tensile stress-shielding of the layer of bone underneath fixation plates can cause osteoporosis and decrease in tensile strength of the bone.[11] In several cases where spinal cages were used during spinal fusion surgery, stress-shielding from metal implants retarded the vertebrae fusion process, eventually leading in pseudoarthrosis, corrosion, wear, and ultimately implant migration.[12-14] This drawback combined with the findings such as corrosion leading to reduced mechanical strength and toxic by-products have led to the pursuit of alternate materials.[15] Finally, the main disadvantage associated with metal implants is the need for secondary surgical removal of hardware, which not only increases the hospitalization time and health care cost but also elevates the chance of infection and other complications.

In many surgical applications, tissue requires temporary augmentation or fixation while regrowth of natural tissue occurs. In such circumstances, degradable polymers are being increasingly used in place of traditional metallic materials. There are multiple reasons for the use of a degradable material, but the most basic begins with the simple desire to have a device that can be used as an implant and will not necessitate a second surgery for removal. In addition to eliminating the need for surgical removal, long-term implant-related complications are averted. Bioabsorbable polymers typically retain strength to support the tissue into which they are placed for defined periods of time, which may vary from a few days to several months. The degradation products must be compatible with living tissue, at least at the concentration in which appear, so that the healing process may occur unimpeded. Development of biodegradable polymers has generally been accomplished by incorporating hydrolytically unstable linkages throughout the backbone. Common hydrolytically labile linkages include anhydrides, orthoesters, carbonates, amides, and, most commonly, esters.[16] As a result, several polymers have been investigated and used clinically as degradable orthopedic implants. Today, nearly every orthopedic manufacturer has an extensive line of bioresorbable devices to offer, predominantly composed of two polyesters, poly(glycolic acid) (PGA) and poly(lactic acid) (PLA).

1.2 Biodegradable Polymers Used in Orthopedic Materials

Biodegradable polymer materials were introduced in surgical sutures over 40 years ago and the idea of using them for surgical implants was proposed as early as 1966.[17] Although a wide variety of polymers have been used for biomedical applications, polyesters are most extensively investigated due to their biocompatibility and tunable degradation properties. In fact, they laid the foundation for the development of the first synthetic degradable sutures and implants. The first biodegradable bone fixation implant was a degradable rod made out of PGA, which was first employed to treat an ankle fracture in 1984.[18] PGA is the simplest aliphatic polyester, with a single methylene group in the polymer backbone. Polymers can be prepared by the polycondensation of glycolic acid, however it is not the most efficient method, as it leads to low molecular weight products. Alternatively, PGA can be produced from the glycolide monomer, which is synthesized from the dimerization of glycolic acid, and polymerized through ring-opening polymerization to form high molecular weight materials with high crystallinity (45-55%), high melting points (220-225 °C) and glass transitions temperatures ranging from 35 to 40 °C.[10] With a high degree of crystallinity, PGA has low solubility in most solvents, with the exception of highly fluorinated organic solvents such as hexafluoroispropanol.[19] As a result, use of PGA homopolymers is limited. Fibers from PGA exhibit high strength and modulus but are too stiff to be used as sutures, except as a braided material. To avoid these problems, PGA has been used as self-reinforced foam[20] or is copolymerized with other degradable polymers to

reduce stiffness in the final material. PGA materials hydrolytically and enzymatically degrade back into glycolic acid, which is either hepatically metabolized into CO_2 and H_2O, or excreted renally.[21] Biodegradation, low aggregation, and lack of cytotoxic response have been the main advantages for using PGA as a degradable material; however complications have arisen when PGA materials have been used clinically.

Table 1.1. Mechanical properties of bone and clinically used implant materials.[19,22-27]

						In vivo loss times	
Material	T_g (°C)	T_m (°C)	Tensile Modulus (GPa)	Tensile Strength (MPa)	Strain to Failure (%)	Strength (weeks)	Mass (months)
Cancellous bone	-	-	0.2-0.5	10-20	5-7	-	-
Cortical bone	-	-	3.3-17.0	51-193	1-3	-	-
SS (316L)	-	1375-1400	200	550-965	20-50	-	-
Ti	-	1650-1700	100	620	18	-	-
PGA	35-40	225-230	4.0-7.0	75-142	15-20	3-6	6-12
PLLA	56-65	170-178	2.7-5.1	40-140	5-10	12-26	>24 (up to 10 years)
PDLLA	55-60	Amorphous	1.9	42-51	3-10	12-16	12-36

PGA has a high degradation rate due to its hydrophilic nature and its mechanical strength after implantation drops significantly, limiting the usefulness for load bearing applications. Several clinical studies have reported issues with PGA implant degradation, which includes fluid accumulation, sinus formation, and osetolysis.[28] In

certain cases, side reactions were severe enough to require revision surgery or arthrodesis. PGA continues to be used for a variety of biomedical applications, however it is often copolymerized with other polymers in order optimize the mechanical and degradation properties to produce materials more suitable for orthopedic applications.

Since PGA was observed to degrade too rapidly for orthopedic applications, slower degrading polylactic acid (PLA) became widely utilized material for orthopedic fixation implants. PLA, an aliphatic polyester, is predominantly synthesized in a similar fashion to PGA from the cyclic monomer, lactide, which exists as two isomers D-lactide, and L-lactide. The two different isomers allow for control over the final polymer properties, allowing for PLA to be tailored to a wider variety of applications than PGA.[29] The homopolymer of L-lactide (PLLA) is a semicrystalline polymer and, like PGA, exhibits high tensile strength and low elongation. Consequently, PLLA has a high modulus that makes it more applicable than other amorphous polyesters for orthopedic fixation devices and sutures. Unlike PLLA, the random distribution of both isomers found in poly(DL-lactide) (PDLLA) prevents the polymer from arranging into a crystalline organized structure. The amorphous nature of PDLLA gives the material a lower tensile strength, higher elongation, and a much more rapid degradation time.[30] Ability for tuning through control of stereoregularity, crystallinity, molecular weight, molecular weight distribution and morphology has made PLA materials attractive for a variety of applications, however there are limitations to the use of PLA as an orthopedic material. PLA has poor toughness and is a very brittle material with less than 10% elongation at break.[31] The poor toughness limits its use in applications that need plastic

deformation at higher stress levels experienced by orthopedic fixation devices.[32] PLA, additionally, is relatively hydrophobic, which in turn affects degradation and cell affinity. The degradation rate is often an important selection criterion for biomedical applications. Slow degradation rate leads to a long i*n vivo* life time, which could several years in some cases. There have been reports of a second surgery almost three years after implantation to remove PLA-based implants.[28]

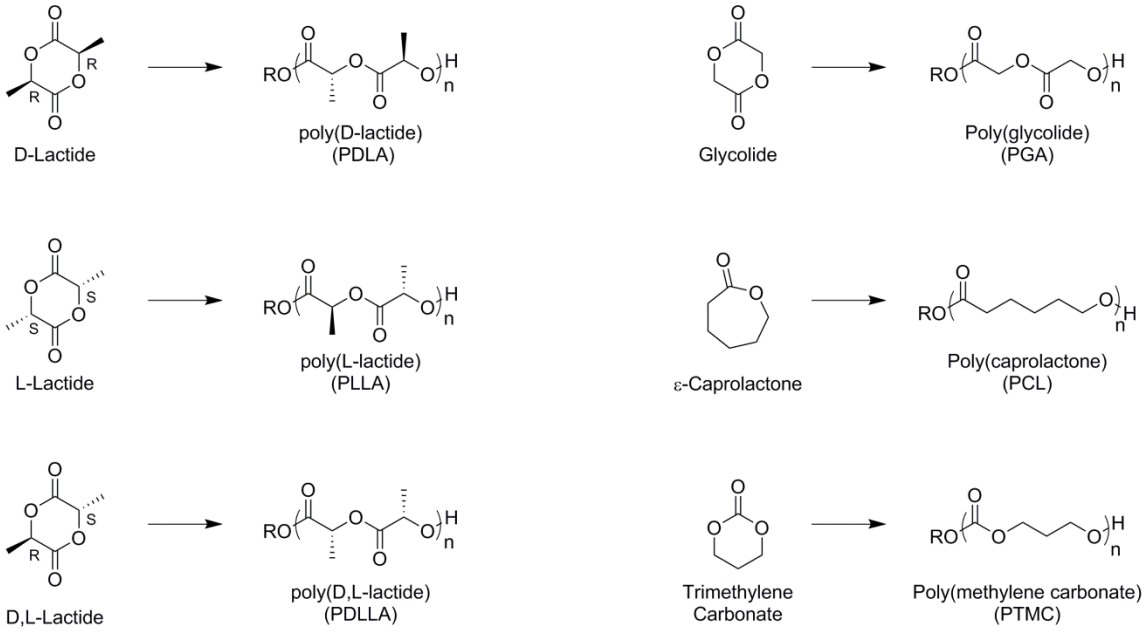

Figure 1.1. Structures of commonly used degradable polymers for orthopedic materials.

In order to produce suitable PLA materials, PLA is often copolymerized with other polyesters or bulk-modified, the most common of which is the copolymer is poly(lactide-*co*-glycolide) (PLGA). Although PLGA has been extensively used in a

variety of clinical applications, its use is limited in the field of orthopedics.[33] The reason for this is notably due to hydrophobic nature of PLGA which does not support cell adhesion for promoting bone in-growth.[34] By altering the monomer ratio of glycolide to lactide and the molecular weight, biodegradation and mechanical strength can be controlled, but even with optimization, PLGA is not an ideal candidate to be used for load bearing applications due to the low mechanical strength.[33]

The degradation kinetics and brittleness of PGA and PLA can be improved by using polymers that have a lower glass temperatures, such as poly(ε-caprolactone) (PCL), polyethylene glycol (PEG), or poly(trimethylene carbonate) (PTMC).[10] PTMC, its copolymers, and its derivatives have been extensively studied for use in biomedical applications. PTMC can be prepared by a ring-opening polymerization (ROP) of trimethylene carbonate using both conventional organometallic catalysts[35-38] and emerging organocatalysts.[39,40] PTMC is a hydrophobic non-crystalline polymer with a glass transition temperature (T_g) of around −20 °C. Therefore, PTMC is usually used as a soft material in a scaffold application for soft tissue regeneration. In addition, resistance to non-enzymatic hydrolysis, generation of nonacidic degradation products, and enzymatic degradation with a surface erosion mechanism, allows PTMC to be used applications in biomedical devices that could not be achieved with traditional aliphatic polyesters.[41] However, progress in current medical technologies has led to the requirement for more complex and higher level functional materials. Thus, the integration of multiple functions has been explored for synthetic biodegradable polymers by various approaches, including polymer blends, composites, copolymerization, and

functional pendant groups, in order to respond to a broad range of applications. These aims can be achieved by utilizing alternate monomer saccharide-based feedstocks, which would ultimately lead to hydroxyl decorated polymers that allow formation of hierarchical structures through hydrogen bonding and also post-polymerization.

1.3 Development of Saccharide-Based Aliphatic Polycarbonates

Although, aliphatic polycarbonates were first synthesized by Carothers over 80 years ago,[42] research and development of polycarbonates have almost exclusively focused around aromatic compounds. With their characteristic low melting points and high susceptibility to hydrolysis, which were considered inferior to the properties displayed by many other polymers [*e.g.*, polyester, polyamide, poly(methyl methacrylate)] developed in the era for fiber production and commodity plastics, aliphatic polycarbonates were not pursued commercially. Unlike aromatic polycarbonates, which garnered immediate commercial attention when bisphenol-A polycarbonates was first developed, aliphatic polycarbonates remained largely unexplored commercially and received little attention from the research field until the 1990s. Early studies of aliphatic polycarbonates focused on the improvement of mechanical properties and thermal stabilities of the readily available PTMC through its blending with polymers having complementary properties for applications such as engineering thermoplastics, albeit with limited commercial success.[43] Despite the relatively slow development of aliphatic polycarbonates, they have received significant

renewed interest in recent years. An increasing demand for more versatile, degradable materials has revived interest in aliphatic polycarbonates for biomedical applications,[44,45] for which their degradability, low glass transition temperatures, and elasticity, once perceived as major drawbacks, lend them a competitive advantage over existing polymer systems.[44,45] In addition the recent surge in aliphatic compounds has also resulted from new progress in polymerization techniques,[39,46-51] functional monomer synthesis,[52-62] and the new applications being explored.[63-66]

Within this same time frame, interests in the development of polycarbonate feedstocks based on renewable materials, namely carbohydrates, has intensified, due to the low biodegradability of petroleum-based polymers and the exhaustible nature of the oil reserved. Carbohydrate-based polymers that retain the chiral, cyclic main chain structure of natural polysaccharides and that can be prepared by controlled synthetic methods are of interest for both basic studies and applications. Specifically, novel polymeric structures having a hydrophilic pyranose backbone not joined with ether linkages are interesting because these materials are not found in nature and provide new molecular architectures to be explored. In addition, polymers based on naturally occurring products represent promising new materials, with novel technical potential and enhanced properties with regard to biocompatibility and biodegradability. Consequently, the production of environmentally friendly and sustainable materials and the development of biomass-based polymers constitute a steadily growing field of attention.

Unfortunately, polymerization of monomers derived from sugars is not straightforward. First of all, the multifunctionality of saccharides must be minimized, by removal or masking through use of appropriate protecting groups, to prevent side reactions leading to undesirable products. Secondly, in order to obtain regio- and stereoregular polymers, strict control throughout the course of monomer synthesis and polymerization is required. Otherwise, random orientation of chiral units can lead to ill-defined atactic polymers. Much work has focused on the development of synthetic carbohydrate-based polymers and glycopolymers, however they predominantly rely on poly(vinylsaccharides)s and other conventional functionalized polymers having sugars as groups pendant from the main chain of the polymer.[67-71] Our focus is the development is the synthesis of sugar-based monomers which will lead to polycarbonates having sugar units incorporated into the main chain. The interest in this kind of carbohydrate-based polymer has been steadily increasing and a considerable number of papers have been published on the subject during the last few years.[72] The following sections reports on the synthesis and polymerization of this type of sugar-derived monomers in the past and present work.

1.3.1 Polycondensation of Anhydroalditols

Research of polycarbonates sourced from anhydroalditols, namely isosorbide, precluded the recent surge in aliphatic polycarbonate development by several decades as a potential replacement for poly(bisphenol-A carbonate) and related plastics.

Poly(bisphenol-A carbonate) is widely used for engineering materials and commodity plastics due to its outstanding toughness, transparency, heat resistance, thermal oxidative stability, and electrical properties.[73] Its rigid aromatic backbone that provides excellent thermal stability and mechanical properties as well as a flexible carbonate linkage that provides improved processability and toughness. The combination of high toughness and good transparency makes it a promising material when producing special function materials, such as prescription glasses, aircraft windows, and bullet-proof glass. The high refractive index, clarity, and UV absorption makes poly(bisphenol-A carbonate) an ideal material for eyewear, lenses, and safety glasses.[74] Despite its commercial success and attractive thermomechanical and physical properties, bisphenol-A is not a sustainable monomer from two different viewpoints. Bisphenol-A represents a non-renewable and potentially harmful feedstock, as it is derived from petroleum and can act as an endocrine disruptor.[75-77] Isosorbide, on the other hand, is derived from the reduction and dehydration of glucose and is non-toxic. The use of isosorbide and other dianhydrohexitols (isomannide and isoidide) in polymers, more specifically polycondensates, can be motivated by several features; they are rigid molecules, chiral, non-toxic, thermally stable, and readily available. For these reasons, there are expectations that polymers with high glass transition temperatures and/or with special optical properties can be synthesized. Also, the innocuous character of the molecules opens the possibility of additional applications in areas of packaging or medicine.

The interfacial polycondensation of bisphenol-A with phosgene or diphosgene, the technique used to obtain over 90% of the poly(bisphenol-A carbonate) produced,[78] is

not useful with alditols because they are extremely hydrophilic and less acidic than diphenols. Much effort has gone into finding alternative methods to synthesize isosorbide polycarbonates. The synthesis of poly(isosorbide carbonate) homopolymers may be carried out through other methods, such as transesterification of isosorbide with diphenyl carbonate[79-82] and dimethyl carbonate.[83] This method requires high reaction temperatures (220-300 °C) and long reaction times, which, often with heterocyclic diols, leads to branching and cross-linking, forming brown non-homogenous material. Solution-based polymerization has been primarily attempted because it can precisely control chemical reaction heat and viscosity and prevent auto-acceleration reactions. Condensation with phosgene,[84,85] diphosgene,[79,84] or with bischloroformate functionalized isosorbide comonomers[86] proved to be more successful at producing high molecular weight polymers, with few side reactions. Isosorbide-based polycarbonates generally exhibit relative resistance to hydrolysis and high T_gs, reaching 175 °C.[87] This can be explained by the rigid fused-ring structure of the isosorbide monomer which would lead to low mobility of the poly(isosorbide carbonate) polymer chain.

1.3.2 Polycondensation of O-Protected Saccharides

The most common *O*-protecting groups of the secondary hydroxyl groups found on the saccharide monomers are acetal, ester, and ether groups. The ether group is the most resistant *O*-protecting group of the alditol monomers under the polycondensation reaction conditions, but also the most difficult to remove from the resulting polymers.

Sugar-based polymers, protected alditol derivatives, can be prepared from commercially available diethyl L-tartrate, pentoses (arabinitol, xylitol and ribose), and hexitols (mannitol) to prepare various aliphatic polycarbonates.[88-90]

Biodegradable polymers having pendant functionalities are of particular interest, being capable of covalent prodrug formation and other functionalities. With derivatization of pendant functional groups, variations in hydrophobicity, physical properties, and biodegradation can be achieved. This concept was explored in various studies in which functional polycarbonates were synthesized from four, five, and six carbon sugars. Biodegradable poly(hydroxyalkylene carbonate)s from optically active and racemic 2,3-*O*-ispropylidene-threitol and 2,4:3,5-di-*O*-isopropylidene-D-mannitol were prepared[91] with diethyl carbonate in the presence of diethyl tin oxide. After isopropylidene protecting groups were hydrolyzed, polymers with free hydroxyl groups were derivatized with esters, orthoesters, and carbamates producing polycarbonates with varying physical properties. Deprotected polycarbonates were water-soluble, and degraded in a few weeks by a mechanism in which hydroxyl groups were shown to participate. Similarly structured threitol-based polycarbonates with pendant isopropylidene functional groups were synthesized from L-tartaric acid, a natural compound found in a large variety of fruits, by the enzymatic catalyzed ring opening of a seven membered cyclic carbonate.

Galbis *et al* have described the use of 2,3,4-tri-*O*-methyl-L-arabinitol and 2,3,4-tri-*O*-methyl-xylitol in the synthesis of polycarbonates and polyesters.[92] These pentitols were polycondensed using a commercial solution of phosgene in toluene (20% phosgene

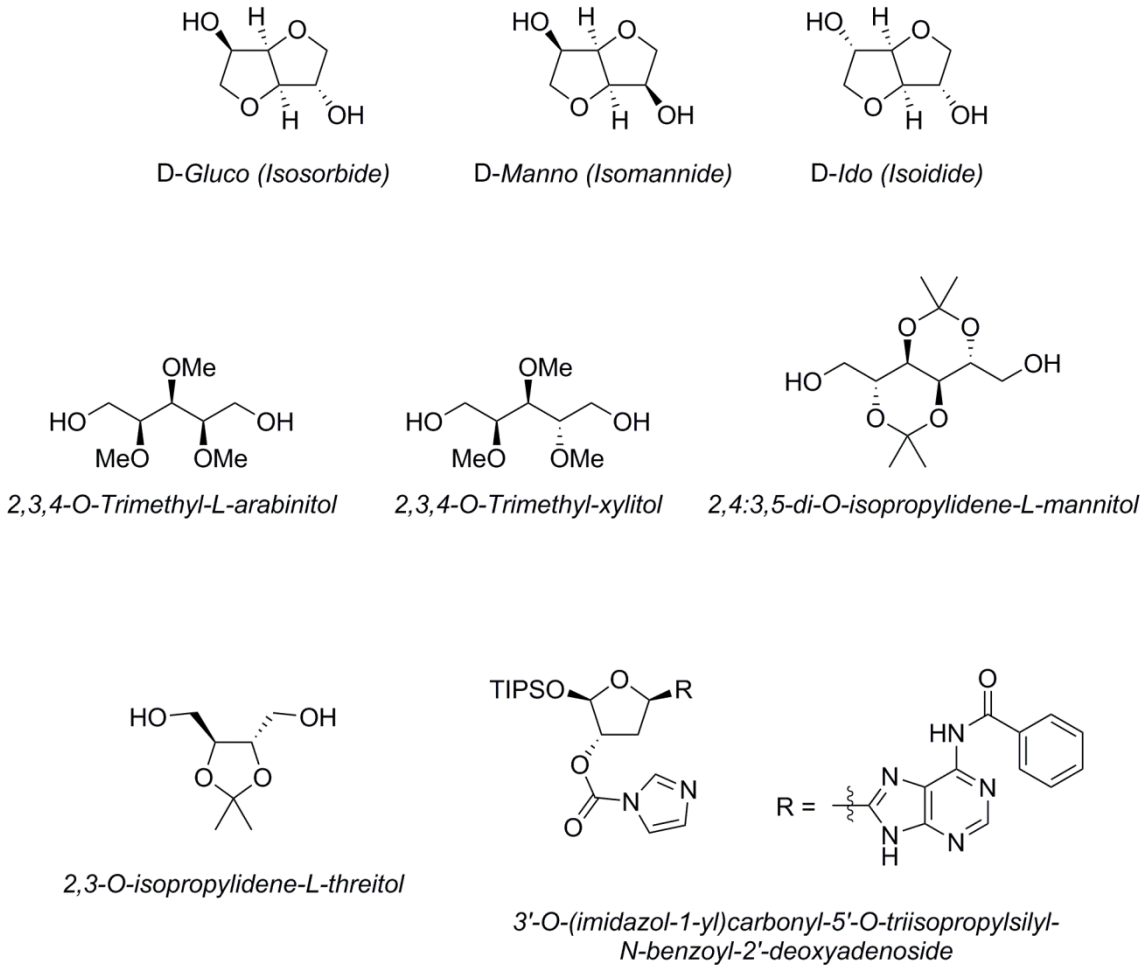

Figure 1.2. Protected alditol monomers used to form saccharide-based polycarbonates *via* AA-BB and AB polycondensation.

in toluene); whereby, sugar-based homopolycarbonates and copolycarbonates with bisphenol-A were obtained in high yields. Both showed high resistance to chemical hydrolysis, however, they were enzymatically degraded in different degrees. The fastest degradation promoted by lipase B from *Candida antartica* was observed for the fully

xylitol-based polycarbonate, followed by copolycarbonates also based on xylitol, which revealed a marked stereospecificity of the enzyme towards this sugar.

In addition to utilizing saccharides to form functional polycarbonates for biomedical applications, synthetic DNA analogues have been synthesized from poly(2'-*O*-deoxyadenosine carbonate)s *via* AB polycondensation.[93] Protected monomers were synthesized with triisopropylsilyl (TIPS) ether and carbonylimidazolide at the 3'- and 5'-positions of the 2'-deoxyribonucleoside ring. In the presence of cesium fluoride, removal of the TIPS protecting group afforded a reactive alkoxide *in situ*, which in turn attacks the carbonylimidazolide group, affording the corresponding polycarbonate together with the cyclic oligomers. However, the deprotection of the *N*-benzoyl group resulted in the scission of the polymer main chain. Thus, the *N*-unprotected 2'-deoxyadenosine monomers were examined for polycondensation. This led to undesired reaction between the adenine amino group and the carbonylimidazolide to form the carbamate linkage. In order to exclude this unfavorable reaction, dynamic protection was employed. Strong hydrogen bonding was used in place of the usual covalent bonding for reducing the nucleophilicity of the adenine amino group, allowing for the production of polycarbonates with the almost regular 3'-5' carbonate linkages.

1.3.3 Ring-Opening Polymerization of Cyclic Furanoses and Pyranoses

Carbohydrate-based polymers that retain the chiral, cyclic main chain structure of natural polysaccharides that can be prepared by controlled synthetic methods are of

interest for various applications. Specifically, novel polymeric structures having a hydrophilic pyranose backbone joined with carbonate linkages are interesting because these polymers provide rigid molecular architectures that may lead to robust materials with high glass transition temperatures. A number studies from the Gross lab have investigated the synthesis and characterization of polycarbonates and poly(ester-*co*-

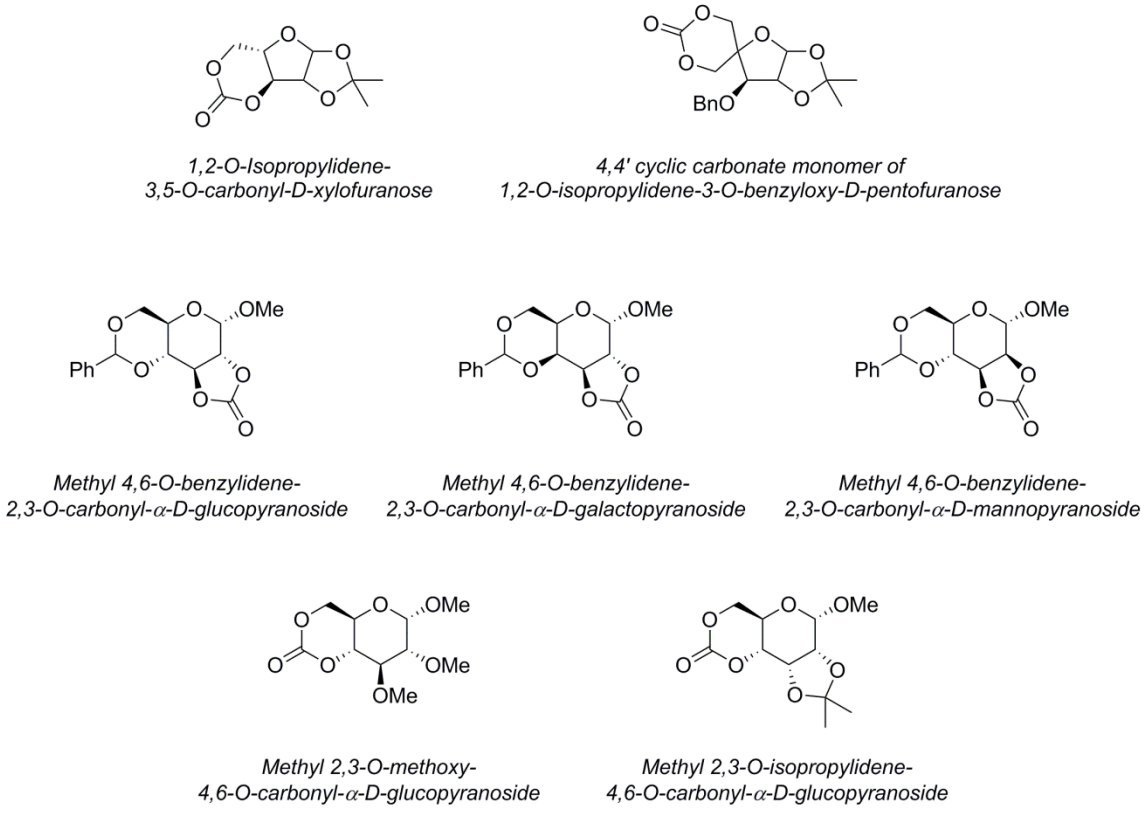

Figure 1.3. Sugar derived five-membered and six-membered cyclic carbonate monomers used to form polycarbonates *via* ROP. Unlike previously synthesized saccharide linear polycarbonates, these polymers incorporate intact saccharide rings into the main chain of the polymer.

carbonate)s derived from the natural sugar, xylose. Chen and Gross synthesized high-molecular weight derived from L-lactide and 3,5-cyclic carbonate of 1,2-*O*-isopropylidene-D-furanose[94] in the presence of organometallic catalyst, $Sn(Oct)_2$. Even though the monomer reactivity ratio of L-lactide is much greater than that of the xylose monomer, short xylose segment lengths were formed. This observation was explained by intramolecular exchange reactions, xylose monomer insertion reaction during propagation, or by other more complicated phenomena. The same xylose monomer was also used to form homopolymers[95], though even with different organometallic catalysts such as methylaluminoxane (MAO), isobutyl aluminoxane (IBAO), $AlEt_3$-0.5 H_2O, $ZnEt_2$-0.5 H_2O, Et_2AlOEt, and $Y(O\text{-}i\text{-}Pr)_3$ the investigators failed to recreate polymers of similar chain length from the previous study. In addition, anionic catalyst, *tert*-butoxide, an effective catalyst for the polymerization of ε-caprolactone and other cyclic esters, was also tested, however polymerization for the xylose monomer occurred at a much slower rate, which was attributed to steric constraints imposed by the vicinal ketal-protected diol. The polymers created exhibited high glass transitions (T_g) for aliphatic polycarbonates and three different types of carbonate linkages (head-head, head-to-tail, and tail-to-tail) in ratios that indicate a random propagation mechanism. Following this study, the same authors also polymerized the xylose monomer with trimethylene carbonate in the presence of organometallic catalyst.[96] Copolymers containing 8 to 83% of xylose presented an alternating structure and amorphous nature. The ketal deprotection was also carried out and the resulting polymers were soluble in dimethylformamide (DMF), indicating low degree of cross-linking. The original

polymers presented increased T_gs as the xylose content increased, whereas the T_g of the unprotected compolymers decreased, further supporting original claims of the T_g elevating effect by the substituents attached to the 1,3-dioxane-2-one-ring.[95]

Additional functional copolymers with control of the quantity and the proximity of hydroxyl groups along the main chain were synthesized by copolymerization of L-lactide with a six-membered cyclic carbonate monomer derived from glucose.[97] The new 4'4-cyclic carbonate monomer of 1,2-isopropylidne-3-benzyloxy-ᴅ-pentofuranose was copolymerized with L-lactide in the presence of $Sn(Oct)_2$ at 130 °C. The benzyl ether and ketal groups were selectively removed by hydrogenolysis or acid catalyzed hydrolysis so that the units within the copolymers could have one, two, or three free hydroxyl groups.

More recently, the Endo group has focused on the ring opening polymerization of glucose-based monomers with five-membered cyclic carbonates.[98,99] It is known that anionic ring opening polymerizations of six- and seven-membered cyclic carbonates, such as trimethylene carbonate and tetramethylene carbonate easily proceed under anionic conditions. Anionic ring-opening polymerizations of five-membered cyclic carbonates, on the other hand, usually require more vigorous conditions with higher temperatures, and often proceed with the elimination of carbon dioxide resulting in poly(carbonate-*co*-ether)s. Despite the unfavorable thermodynamic nature of anionic ROP of five-membered cyclic carbonates, Haba *et al* were able to produce polycarbonates from a five-membered cyclic carbonate containing glucopyranoside *via* anionic polymerization by potassium-*tert*-butoxide (*t*-BuOK) and 1,8-

diazabicyclo[5.4.0]undec-7-ene (DBU), without elimination of carbon dioxide.[98] DBU proved to be a more effective initiator, however, the polymerization proceeded in a non-controlled fashion as polymers with relatively high polydispersity indexes (>1.4) were formed. Further investigations showed that the rate and mechanism was dependent on both initiator and solvent used. Polymerizations initiated with *n*-BuOLi, *t*-BuOLi, *n*-BuONa, *n*-BuOK, and DBU proceeded smoothly to yield corresponding polycarbonates in high yields. Interestingly though, when using DBU as an initiator in DMF rather than THF, the polymerization proceeded at a faster rate and under an alternate zwitterionic mechanism. In fact, when copolymerized with L-Lactide, methyl 4,6-*O*-benzylidene-2,3-*O*-carbonyl-α,D-glucopyranoside (MBCG) shared similar reactivity ratio and copolymers were composed of a random distribution of monomer units in ratios that corresponded to their respective monomer feed ratios.[100]

The unusually good ability of the reported MBCG to polymerize was reported to be caused by the ring strain of the five-membered ring, more specifically, due to the trans-fusing to the pyranose ring.[101] The same phenomenon was observed when applied to other pyranoside monomers. To investigate the relationship between steric structures and stereochemistry of five membered cyclic carbonates, the anionic ring-opening polymerization of three different monomers: MBCG, methyl 4,6-*O*-benzylidene-2,3-*O*-carbonyl-α,D-galactopyranoside (MBCGa), and methyl 4,6-*O*-benzylidene-2,3-*O*-carbonyl-α,D-mannopyranoside (MBCM).[102] Similar to previous polymerizations of MBCG, the polymerization of MBCGa proceeded without the elimination of CO_2, while the polymerization of MBCM did not proceed. Ring-closing reactions revealed the

preference of the mannopyanoside-based hydroxycarbonate to produce cyclic carbonate, while others did not give cyclic carbonates. This finding along with X-ray crystallography data indicated that the *trans*-fused carbonate rings of MBCG and MBCGa are less stable than that of the *cis*-fused MBCM carbonate ring, and thus more favorable for ROP.

Mannose was also used as a starting material for the synthesis of cyclic carbonates, which could undergo ROP to yield renewable linear polycarbonates.[103] Interestingly, the authors utilized a novel approach to form the cyclic carbonate that does involve the use of dangerous compounds, such as phosgene. Reaction of the protected mannose (methyl-2,3-*O*-isopropylidene-α-D-mannopyranoside) with carbon dioxide in the presence of DBU, afforded the six-membered cyclic carbonate in relatively good yields (57%). The cyclic monomer was subsequently polymerized *via* organocatalyzed ROP with TBD catalyst and methylbenzyl alcohol initiator, producing regioregular homopolymers with T_gs and high-temperature resistance.

The Wooley group has an interest in developing renewable glucose-based polycarbonates having well-defined structures and high thermal stabilities. With the advancement of organocatalyzed ROP of six-membered cyclic carbonates, monomers were synthesized bearing a fused 4,6-cylic carbonate and polymerized with the hydrogen-bonding, bifunctional catalyst, 1,5,7-triazabicyclo[4.4.0]dec-5-ene (TBD), and methylbenzyl alcohol initator.[104] In contrast to the ROP of five-membered glucopyranoside carbonate monomers, the ROP of methyl-2,3-*O*-methyl-4,6-*O*-carbonyl-glucopyranoside afforded well defined amorphous poly(D-glucose carbonate)s

(PDGC) with low PDIs (<1.2) and well-defined end-groups. Polymerization of PDGC homopolymers progressed at an accelerated rate when compared to other six-membered ring systems (full conversion was reached in under 10 min, DP_n = 50, PDI = 1.13), namely due to the torsional strain applied to the carbonate by the bicyclic system. Importantly, the controlled ROP forms PDGC in a rapid and efficient manner and also proved compatible with other polymer systems in the formation of diblock-*co*-polymers,[105] which was carried out *via* chain extension of a polyphosphoester (PPE) macrointiator.[106,107] Polyphosphoester-*block*-poly(glucose carbonate)s represent a new functional architecture prepared from renewable materials that can be rapidly transformed into a diverse array of amphiphilic diblock copolymers, with the potential to break down into natural byproducts.

1.4 Current Work

With advances in biomedical sciences, it is necessary to develop polymers that meet more demanding requirements. In this work we attempt to utilize synthetic organic chemistry to produce a class of renewable polycarbonates that can tackle drawbacks associated with aliphatic polyesters used in biomedical applications. By utilizing polycarbonate linkages, we hope to build robust materials that do not degrade into acidic byproducts. In addition use of polyhydroxyl natural products, namely glucose, have rigid cyclic core units together with polar, hydrogen-bonding hydroxyl groups to lead to strong and tough materials for engineering and biomedical and other applications, where

the combined properties and degradation can be properly utilized. The primary goals of the research in this body of work were:

1. to advance the field of aliphatic polycarbonates by developing novel degradable polymers from naturally occurring polyhydroxyl natural products, namely D-glucose and quinic acid;
2. to synthesize renewable polycarbonates *via* polycondensation containing intact heterocycles in the main chain from various *O*-protected glucopyranoside diols
3. to investigate the structure-property relationship of glucose-based polycarbonates and the effect of regiochemistries on monomer reactivity and the physical properties of the resulting polymers;
4. to develop polycarbonates with "clickable" functionalities *via* ROP of a glucose-sourced, glucal monomer in order to establish a novel multifunctional polymer system that lends itself to facile post-polymerization functionalization
5. to utilize rapid crosslinking methods, specifically incorporation of thiol-ene chemistry, as means to generate robust quinic acid-based three-dimensional crosslinked networks.

Chapter II focuses on the transformation of D-glucose, Nature's building and energy storage block, into monomers for the synthesis of sophisticated degradable polycarbonates. Through a series of chemical transformations, selective hydroxyl

groups on D-glucose were capped with benzyl or methyl protecting groups, and four distinct diol monomers were formed. A series of polymerization conditions were tested with each monomer to determine optimal polymerization conditions. Differences in reactivity of each monomer were assessed by the resulting molecular weight of each polymer. Two monomers where able to give high molecular weights (>20kDa). The two monomers bearing hemiacetal functionalities proved to be less reactive than their counterparts, and thus produced low molecular weight polymers (<10 kDa). The thermal properties of each polymer were analyzed by differential scanning calorimetry (DSC). All polymers exhibited amorphous behaviors with glass transition temperatures ranging from 44-85 °C, depending on regiochemical connectivity and molecular weight. The polymers additionally underwent thermogravimetric analysis (TGA) and it was found that the thermal stability of each polymer also varied, correlating with the differences in chemical makeup of carbonate linkages. Polymers in which the carbonate linkage ran through C1, or in which the carbonate linkage was adjacent to an acetal functional group, had significantly lower onset decomposition temperatures. It was hypothesized that the anomeric center of glucose, played a role in the in thermal breakdown of the polymer, leading to the facile evolution carbon dioxide as a degradation product. However, our originally proposed degradation mechanism was not fully supported, when additional ions were detected at lower temperatures during thermal decomposition. When analyzed by TGA coupled mass spectrometry (TGA-MS), degradation fragments were observed early in the decomposition at

increments of *m/z* 77, 78, 91, 92, 105, and 106, which correspond to phenyl, toluyl, and benzoyl radicals, respectively, signifying a more complicated degradation mechanism.

In **Chapter III,** modifications were made to the monomer structure when various polymerization conditions failed to produce polymers with M_n over 10 kDa. Since the monomers with primary alcohols yielded polycarbonates with higher molecular weights, bis-adducts of two of the previous monomers were synthesized, by incorporating an additional synthetic step to produce monomers with two primary alcohols. These two new monomers proved to be more reactive than previously synthesized glucose-based monomers in Chapter II, yielding polymers with molecular weights reaching over 100 kDa and polydispersities ranging from 1.5 to 1.9. Due to the regioregularity and high molecular weights of the polymers, each regioisomeric poly(glucose carbonate) exhibited relatively high glass-transition temperatures for aliphatic polycarbonates, 92 °C to 101 °C. The polymers also exhibited relatively high thermal stability, with onset decomposition temperatures (T_d) near 300 °C, as revealed by TGA.

Chapter IV moves away from polycondenstion polymers and introduces a new glucal-based monomer with a six-membered cyclic carbonate, suitable for ROP. Unlike, condensation polymerizations, ROP allows for greater control over polymer size and distribution, affording polymers with narrow polydispersity indexes. Recently, the Wooley group developed a glucose-based monomer suitable for ROP by utilizing hydroxyl groups on C4 and C6 to create a six-membered ring. Additionally these polymers could be easily modified by changing the protecting groups and thus adding additional functionality. In this investigation, a cyclic carbonate was synthesized from

tri-acetyl-D-glucal, an abundant glucose derivative commonly used as a chiral feedstock in organic chemistry. Glucal was chosen as the starting material in order to incorporate alkene functionality in the polymer backbone to make post-polymerization modification *via* click-chemistry available. Interestingly, the incorporation of the double bond had an important effect on the thermodynamics of the polymerization. Previously, ROP of glucose-based utilized TBD required 2-5 hours to reach complete conversion. When using similar conditions, polymerization proceeded significantly faster and full conversion was achieved in under a minute. As a result, a milder cocatalyst system of DBU and TU was used in this study to produce well-defined polymers. Finally these polymers were analyzed by TGA and DSC, revealing amorphous polymers with high T_g and early onset decomposition temperatures.

In **Chapter V**, investigations into a rapid, solvent-free, UV-promoted thiol-ene crosslinking reaction was conducted, building upon linear quinic acid-based polycarbonates reported by the Wooley lab. Previously, the synthesis of poly(quinic acid carbonate)s was investigated by copolymerization of *tert*-butyldimethylsilyloxy (TBS)-protected 1,4- and 1,5-diol monomers of quinic acid and diphosgene in pyridine. Although the polymers exhibited high glass transition temperatures [209 °C for poly(1,4-quinic acid carbonate) and 229 °C for poly(1,5-quinic acid carbonate)], they possessed poor mechanical strength, which likely resulted from limited molecular weights and high glass transition temperatures. To introduce mechanically robust polycarbonates, a crosslinking strategy utilizing thiol-ene "click" chemistry to synthesize three-dimensional networks was employed. The synthesis and thermomechanical

characterization of covalently crosslinked networks derived from QA are reported in this study. Transformation of hydroxyl groups on the quinic acid lactone to allyloxy carbonate functional groups was performed by reaction with allyl chloroformate to produce the tris(alloc)quinic acid (TAQA) alkenyl monomer. Solvent-free thiol-ene chemistry was utilized in the copolymerization to obtain poly(thioether-*co*-carbonate) networks with a wide range of achievable thermomechanical properties, including glass transition temperatures from -18 to 65 °C and rubbery moduli from 3.8 to 20 MPa. Further tunability of thermomechanical properties was achieved by varying "ene-content" through the introduction of diallyl carbonate as a comonomer. Networks were synthesized with glass transition temperatures ranging from -15 to 63 °C without significantly varying rubbery moduli. Finally, control force cyclic testing by DMA showed excellent shape memory behavior for 1,2-EDT-*co*-TAQA and 1,2-EDT-*co*-TAQA-*co*-DAC materials. High percent recoverable strains were obtained, reaching 100% recovery during fourth and fifth cycles.

CHAPTER II

REGIORANDOM POLYCARBONATES DERIVED FROM FOUR DISTINCT GLUCOSE-BASED AA' MONOMERS

2.1 Original Publication Information*

This chapter contains excerpts from the article *Four Different Regioisomeric Polycarbonates Derived from One Natural Product, D-Glucose.* Modifications to the original document are cosmetic and used only to conform to the format of this document or provide uniformity of enumeration. Additional studies as well as contents found in the supporting information, which was originally a separate document, have been included in the chapter, and schemes and figures have been renumbered to the style of this document.

2.2 Overview

The design and synthesis of new biomaterials, particularly those derived from biomolecule-based monomers, remains an area of considerable research effort. Herein the synthesis and characterization of polycarbonates based on the renewable resource,

*Reprinted with permission from "Four Different Regioisomeric Polycarbonates Derived from One Natural Product, D-Glucose", by Alexander T. Lonnecker, Young H. Lim, Simcha E. Felder, Céline J. Besset and Karen L. Wooley, **2016**, *Macromolecules*, *49*(20), 7857-7867, DOI: 10.1021/acs.macromol.6b00591), Copyright 2016 by The American Chemical Society.

glucose, are reported. Three different synthetic methods were studied with respect to their ability for the preparation of high molecular weight poly(glucose carbonate)s from four distinct benzyl and methyl protected glucose diols. The polymers possess glass transitions temperatures (T_g) ranging from 44 °C to 85 °C and onset thermal decomposition temperatures (T_d) ranging from 137 °C to 325 °C depending on the regiochemistry of the polymer. Polymers synthesized from monomers possessing hemiacetal functionalities exhibited lower T_gs and significantly lower thermal stabilities. Further investigation of thermal decomposition by tandem TGA-MS showed early degradation due to the loss of carbon dioxide and benzyl protecting groups.

2.3 Introduction

The past few decades have seen a paradigm shift from non-degradable polymeric materials to those with inherent degradability for medical and related applications.[108-110] Examples of these new materials vary widely from sutures and orthopedic devices,[111] to engineered tissues,[110] and drug delivery systems.[112] The major driving force for the development of advanced degradable materials for use in biomedical applications include ethical and technical concerns associated with the long-term biocompatibility of implants generally resulting in follow-up procedures to expedite their replacement or removal.[108] The advancement of degradable polymers in biomedicine has been limited to variations on traditional polymers such as aliphatic polyesters and polyanhydrides,[113,114,115] To create the next generation of biomaterials, with improved

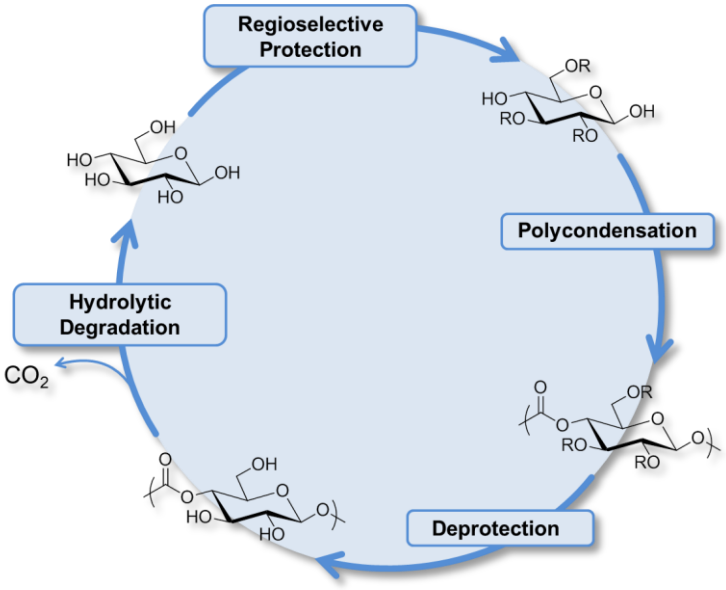

Figure 2.1. Ideal life cycle of glucose-based polycarbonates.

functionality, degradability, and biocompatibility, new monomeric systems should be explored. To improve biocompatibility, the use of biodegradable materials obtained from natural resources, such as monosaccharides,[116] terpenes,[117,118] menthides,[119,120] capable of degrading into bioresorbable products are currently receiving increased attention as an alternative to traditional petroleum based materials.[121]

We envision glucose-based polycarbonates would serve as ideal degradable polymeric biomedical materials, since the starting materials can be obtained from abundant renewable compounds and the degradable byproducts are ubiquitous in the human body, avoiding complex issues with clearance and toxicity. In addition, multiple hydroxyl groups on each saccharide repeat unit would form intermolecular hydrogen bonds with oxygen atoms on neighboring chains, creating strong, reinforced materials.

In naturally occurring support materials like cellulose and chitin, this high-degree of intermolecular bonding leads to the formation of microfibrils with high tensile strength. Our approach to generating natural product-based polymeric materials is to develop saccharide-based polycarbonates. With this in mind there are several reported polycarbonates derived from monosaccharides, often with the saccharide moiety as a side chain substituent,[122,123] as an opened ring in the main chain of copolymers,[91,92] or as an intact saccharide ring in the polymer backbone.[93,96,98,99,124-128] In addition, much interest has been devoted to modified saccharide feedstocks, such as alditols and anhydroalditols,[129] which lend themselves to facile synthetic strategies as well as generation of high performing engineering polymers. Simplification of carbohydrate structures, like in the case of isosorbide, produces monomers that are capable of forming high molecular weight engineering materials, however they lose their structural diversity and multiple functionalities that gives them their interesting bioactivity. This has led us to focus on the development of polymeric materials that are synthesized from, and undergo hydrolytic degradation into, the same natural product starting materials.

In this context, we have investigated the synthesis of polycarbonates built from glucose, an abundant natural product that is prevalent both in nature and the human body, to afford a unique family of bio-sourced, potentially degradable, engineering polymers: poly(ᴅ-glucose carbonate)s (PDGCs). Glucose is an important carbohydrate, acting as an energy source, a metabolic intermediate, and a monomeric repeat unit in many polymeric support structures. These features, along with an established field of carbohydrate protection and deprotection chemistry, make glucose an appealing starting

material for the synthesis of linear polycarbonates. This article reports the design, synthesis, and rigorous characterization of polycarbonates prepared from four different benzyl-protected glucose monomers *via* condensation polymerization to evaluate the efficacy of different glucose monomers to yield high molecular weight polymer and the effect of backbone connectivity on physiochemical and thermal properties.

2.4 Experimental

2.4.1 Materials

Unless otherwise noted, all reagents were used as received. Dichloromethane (DCM) was purified by passage through a solvent purification system (J.C. Meyer Solvent Systems) and used as a dried solvent. Monomers **4**, **8**, **11**, and **12** were dried under reduced pressure, over P_2O_5 and stored under Ar environment. Column chromatography was performed on a combiflash Rf4x (Teledyne ISCO) with RediSep Rf Columns (Teledyne ISCO).

2.4.2 Characterization

The ^{1}H NMR (500 MHz) and ^{13}C NMR (125 MHz) spectra were obtained on an Inova 500 MHz spectrometer using the solvent as an internal reference. Glass transition (T_g) temperatures were measured by differential scanning calorimetry (DSC) on a

Mettler Toledo DSC822e apparatus (Mettler Toledo, Columbus, OH) with a heating rate of 10 °C/min. The measurements were analyzed using Mettler-Toledo Star^{e} v. 10.00 software. The T_g was taken as the midpoint of the inflection tangent, upon the third heating scan. Thermogravimetric analysis (TGA) was performed under an Ar atmosphere using a Mettler Toledo model TGA/SDTA851^{e} apparatus with a heating rate of 10 °C/min that was coupled to a Pfeiffer TermoStar/GSD320T3 mass spectrometer. Ions generated during TGA ranging from 0-300 amu were detected over a span of 30 sec (10ms/amu) during the run of the TGA with a steady flow of Ar (10 mL/min). Gel permeation chromatography (GPC) was conducted on two Waters Chromatography, Inc. (Milford, MA) systems eluted with either tetrahydrofuran (THF) or dimethylformamide (DMF) at a flow rate of 1.00 mL/min. Both GPCs were equipped with an model 1515 isocratic pump, a model 2414 differential refractometer, and a three-column set of Polymer Laboratories (Amherst, MA) Styragel columns (PL_{gel} 5 μm Mixed C, 500 Å, and 104 Å, 300 x 7.5 mm columns) for the THF system equilibrated at 35 °C, or a four-column set of 5 μm Guard (50 × 7.5 mm), Styragel HR 4 5 μm DMF (300 × 7.5 mm), Styragel HR 4E 5 μm DMF (300 × 7.5 mm), and Styragel HR 2 5 μm DMF (300 × 7.5 mm) equilibrated at 70 °C. Polymer solutions were prepared at a known concentration (*ca.* 3 mg/mL), and an injection volume of 200 μL was used. Data collection and analyses were performed with Precision Acquire software and Discovery 32 software, respectively (Precision Detectors, Inc.). The differential refractometer was calibrated with standard polystyrene materials (SRM 706 NIST) for the THF system and poly(ethylene glycol) for the DMF system. IR spectra were recorded on an IR Prestige

21 system (Shimadzu Corp., Japan), equipped with an ATR accessory, and analyzed using IRsolution v. 1.40 software.

2.4.3 Synthesis

Synthesis of Glucose Monomer 4

Methyl 2,3-di-*O*-benzyl-4,6-*O*-benzylidene-α-D-glucopyranoside (2). Methyl-4,6-benzylidene-α-D-glucopyranoside (10.4 g, 36.8 mmol), **1**, potassium hydroxide (14.1 g, 251 mmol), and benzyl bromide (42.8 g, 251 mmol) were suspended in 150 mL of toluene and heated to reflux. Water generated *in situ* was collected with a Dean-Stark apparatus. The reaction was monitored by TLC until complete consumption of starting material and allowed to cool to room temperature after 2 hours. The mixture was washed with water and the aqueous layer was extracted with DCM. The organic layer was dried with magnesium sulfate and concentrated under vacuum. The residue was then purified by column chromatography (SiO_2, 85:15 hexane, acetone) resulting in a white solid (15.6 g, 92%).

*Methyl 2,3-di-O-benzyl-4,6-O-benzylidene-α-D-glucopyranoside (**2**).* ^{1}H NMR (500 MHz, $CDCl_3$) δ 7.50-7.26 (m, 15H), 5.55 (s, 1H), 4.94-4.90 (d, J = 11.2 Hz, -OCH_2Ar, 1H), 4.88-4.84 (d, J = 12.1 Hz, -OCH_2Ar, 1H), 4.85-4.82 (d, J = 11.2 Hz, -OCH_2Ar, 1H), 4.72-4.68 (d, J = 12.1 Hz, -OCH_2Ar, 1H), 4.60-4.59 (d, $J_{1\text{-}2}$ = 3.7 Hz, 1H, H1), 4.29-4.24 (dd, $J_{6eq\text{-}6ax}$ = 9.9 Hz, $J_{6eq\text{-}5}$ = 4.6 Hz, 1H, $H6_{eq}$), 4.08-4.02 (t, $J_{3\text{-}2}$ = $J_{3\text{-}4}$ = 9.3 Hz, 1H, H3), 3.87-3.79 (dt, $J_{5\text{-}4}$ = $J_{5\text{-}6ax}$ = 9.9 Hz, $J_{5\text{-}6eq}$ = 4.6 Hz, 1H, H5), 3.74-3.67

(t, $J_{6ax\text{-}5}$ = $J_{6ax\text{-}6eq}$ = 9.9 Hz, 1H, $H6_{ax}$), 3.63-3.57 (dd, $J_{4\text{-}5}$ = 9.9 Hz, $J_{4\text{-}3}$ = 9.3 Hz, 1H, H4), 3.58-3.54 (dd, $J_{2\text{-}3}$ = 9.3 Hz, $J_{2\text{-}1}$ = 3.7 Hz, 1H, H2), 3.40 (s, 3H, -OCH_3) ppm; ^{13}C NMR(125 MHz, $CDCl_3$): δ 138.7, 138.1, 137.4 (Ar_{ipso}), 128.9, 128.4, 128.3, 128.2, 128.1, 128.0, 127.9, 127.6, 126.0 (Ar), 101.2 (-O*C*HAr), 99.2, (C1), 82.1 (C4), 79.1 (C2), 78.6 (C3), 75.4 (-O*C*H_2Ar), 73.8 (-O*C*H_2Ar), 69.0 (C6), 62.3 (C5), 55.4 (-O*C*H_3) ppm; FTIR (ATR) υ_{max} (neat, cm^{-1}): 3100–3000, 3950–2800, 1450, 1367, 1329, 1175, 1084, 1050, 1028, 964, 732, 692, 652; +ESI MS: calculated $[M + Li]^+$ for $C_{28}H_{30}O_6$: 469.2202, found: 469.2191.

Methyl 2,3,6-tri-*O*-benzyl-α-D-glucopyranoside (3). Compound **2** (14.8 g, 32.0 mmol) was suspended in 500 mL of THF under N_2 and sodium cyanoborohydride (14.5 g, 230 mmol) was added. After stirring for 45 min at room temperature (r.t.), the temperature was decreased to 0 °C and aluminum chloride (38.4 g, 288 mmol) was added. Following an additional hour of stirring the reaction mixture was filtered to remove the aluminum salts. The filtrate was extracted with 500 mL of DCM and washed with water. The aqueous phase was extracted with 250 mL of DCM and the two organic layers were combined, dried with Na_2SO_4, and then concentrated under vacuum. The residue was purified by column chromatography on silica gel, eluting with a 7:3 mixture of hexanes and ethyl acetate, to produce colorless oil (12.6 g, 85%).

*Methyl 2,3,6-tri-O-benzyl-α-D-glucopyranoside (**3**).* ^{1}H NMR (500 MHz, $CDCl_3$) δ 7.38-7.26 (m, 15H, Ar), 5.02-4.99 (d, *J* = 11.4 Hz, 1H, -OCH_2Ar), 4.78-4.76 (d, *J* = 12.0 Hz, 1H, -OCH_2Ar), 4.75-4.72 (d, *J* = 11.4 Hz, 1H, -OCH_2Ar), 4.67-4.62 (d, *J* = 12.0 Hz, 1H, -OCH_2Ar), 4.64-4.63 (d, $J_{1\text{-}2}$ = 3.5 Hz, 1H, H1), 4.60-4.58 (d, *J* = 11.8 Hz,

1H, -OCH_2Ar), 4.55-4.53 (d, J = 11.8 Hz, 1H, -OCH_2Ar), 3.80-3.77 (t, $J_{3\text{-}2}$ = $J_{3\text{-}4}$ = 9.4 Hz, 1H, H3), 3.61-3.58 (dd, $J_{5\text{-}4}$ = 9.5 Hz $J_{5\text{-}6}$ = 3.9 Hz, 1H, H5), 3.57-3.56 (d, $J_{6\text{-}5}$ = 3.9 Hz, 2H, H6), 3.51-3.47 (dt, $J_{4\text{-}3}$ = $J_{4\text{-}5}$ = 9.4 Hz, $J_{4\text{-OH}}$ = 2.1 Hz, 1H, H4), 3.44-3.41 (dd, $J_{2\text{-}3}$ = 9.4 Hz, $J_{3\text{-}1}$ = 3.5 Hz, 1H, H2), 3.39 (s, 3H, -OCH_3), 2.22-2.21 (d, $J_{\text{OH-}4}$ = 2.1 Hz, 1H, $H_{\text{OH-}4}$) ppm; 138.9, 138.2, 138.1 (Ar_{ipso}), 128.7, 128.6, 128.5, 128.3, 128.1, 128.1, 128.0, 127.8, 127.7 (Ar), 98.3, (C1), 81.6 (C3), 79.7 (C2), 75.6, 73.7, 73.3 (-OCH$_2$Ar), 70.8 (C4), 70.0 (C5), 69.6 (C6), 55.4 (-OCH$_3$) ppm; FTIR (ATR) υ_{max} (neat, cm^{-1}): 3456 (broad – OH stretch), 3030, 2915, 2875, 2840, 1496, 1453, 1397, 1359, 1328, 1283, 1242, 1208, 1192, 1158, 1135, 1085, 1069, 1049, 1027, 909, 844, 734, 695; HRMS (+ESI) m/z calc'd for $C_{28}H_{32}O_6$ $[M+K]^+$: 503.18, found 503.1754.

2,3,6-Tri-*O*-benzyl-ᴅ-glucopyranoside (4). Compound **3** (4.0 g, 5.6 mmol) was dissolved in 120 mL of acetic acid at r.t. The solution was heated to 110 °C and 40 mL of HCl (4 N) was added. The reaction was monitored by TLC and stopped after 35 min. The reaction mixture was added into 500 mL of water and neutralized by the addition of 2 M NaOH. The solution was extracted with 500 mL of DCM. The organic layer was dried with Na_2SO_4 and concentrated under vacuum. The residue was purified by chromatography on silica gel, eluting with a 7:3 mixture of hexanes:ethyl acetate and then concentrated under vacuum. The product was recrystallized in a 7:1 mixture of hexanes to ethyl acetate resulting in 1.3 g (32%) of a 1:1 mixture of 2,3,6-tri-*O*-benzyl-α-ᴅ-glucopyranoside and 2,3,6-tri-*O*-benzyl-β-ᴅ-glucopyranoside **4**, which was used without further purification.

*2,3,6-tri-O-benzyl-α-D-glucopyranoside (**4α**).* ^{1}H NMR (500 MHz, $CDCl_3$) δ 7.50-7.26 (m, 15H, Ar), 5.23 (t, $J_{1\text{-}2} = J_{1\text{-}OH}$ = 2.8 Hz, 1H, $H1_{\alpha}$), 5.00-4.96 (d, J = 11.4 Hz, 1H, -OCH_2Ar), 4.78-4.74 (d, J = 11.4 Hz, 1H, -OCH_2Ar), 4.78-4.74 (d, J = 11.8 Hz, 1H, -OCH_2Ar), 4.71-4.67 (d, J = 11.8 Hz, 1H, -OCH_2Ar), 4.62-4.58 (d, J = 12.2 Hz, 1H, -OCH_2Ar), 4.55-4.51 (d, J = 12.2 Hz, 1H, -OCH_2Ar), 4.02-3.96 (td, $J_{5\text{-}4}$ = 9.7 Hz, $J_{5\text{-}6}$ = 4.2 Hz, 1H, H5) 3.82-3.76 (t, $J_{3\text{-}2} = J_{3\text{-}4}$ = 9.2 Hz, 1H, H3), 3.68-3.67 (d, $J_{6\text{-}5}$ = 4.2 Hz, 2H, H6), 3.64-3.60 (dd, $J_{2\text{-}3}$ = 9.4 Hz, $J_{2\text{-}1}$ = 2.8 Hz, 1H, H2), 3.58-3.53 (dd, $J_{4\text{-}5}$ = 9.4 Hz, $J_{4\text{-}OH}$ = 3.5 Hz, 1H, H4), 2.96-2.95 (d, $J_{OH\text{-}4}$ = 3.5 Hz, 1H, OH-4), 2.38-2.37 (d, $J_{OH\text{-}1}$ = 3.0 Hz, 1H, OH-1) ppm; ^{13}C NMR(125 MHz, $CDCl_3$): δ 138.8, 137.9, 137.9 (Ar_{ipso}), 128.7, 128.7, 128.6, 128.5, 128.5, 128.3, 128.2, 128.1, 128.01, 128.0, 128.0, 127.9, 127.9 (Ar), 91.4 (C1), 81.2 (C3), 79.8 (C2), 75.5, 73.8, 73.1 (-O*C*H_2Ar), 71.0 (C4), 70.2 (C5), 69.8 (C6) ppm; FTIR (ATR) υ_{max} (neat, cm^{-1}): 3500–3300, 3100–3000, 2950–2800, 1498, 1453, 1337, 1216, 1132, 1101, 1048, 1024, 910, 865, 755, 695; +ESI MS: calculated $[M + Li]^+$ for $C_{27}H_{30}O_6$: 457.2202, found: 457.2195.

*2,3,6-tri-O-benzyl-β-D-glucopyranoside (**4β**).* ^{1}H NMR (500 MHz, $CDCl_3$) δ 7.50-7.26 (m, 15H, Ar), 5.49-5.46 (dd, $J_{1\text{-}2}$ = 10.0 Hz, $J_{1\text{-}OH}$ = 2.8 Hz, 1H, $H1_{\beta}$), 5.00-4.96 (d, J = 11.4 Hz, 1H, -OCH_2Ar), 4.78-4.74 (d, J = 11.4 Hz, 1H, -OCH_2Ar), 4.78-4.74 (d, J = 11.8 Hz, 1H, -OCH_2Ar), 4.71-4.67 (d, J = 11.8 Hz, 1H, -OCH_2Ar), 4.62-4.58 (d, J = 12.2 Hz, 1H, -OCH_2Ar), 4.55-4.51 (d, J = 12.2 Hz, 1H, -OCH_2Ar), 3.77-3.74 (dd, $J_{5\text{-}4}$ = 8.0 Hz, $J_{5\text{-}6}$ = 3.0 Hz, 1H, H5), 3.68-3.67 (d, $J_{6\text{-}5}$ = 3.0 Hz, 2H, H6), 3.53-3.49 (td, $J_{4\text{-}3} = J_{4\text{-}5}$ = 8.8 Hz, 1H, H4), 3.48-3.45 (t, $J_{3\text{-}2} = J_{3\text{-}4}$ = 8.8 Hz, 1H, H4), 3.39-3.36 (dd, $J_{2\text{-}1}$ = 10.0 Hz, $J_{2\text{-}3}$ = 8.8 Hz, 1H, H2), 3.12 (s, 1H, $H_{OH\text{-}1}$), 2.43-2.42 (d, $J_{OH\text{-}4}$ =

3.5 Hz, 1H, H_{OH-4}) ppm; ^{13}C NMR(125 MHz, $CDCl_3$): δ 138.6, 138.4, 137.8 (Ar_{ipso}), 128.7, 128.7, 128.6, 128.5, 128.5, 128.3, 128.2, 128.1, 128.01, 128.0, 128.0, 127.9, 127.9 (Ar), 97.6 (C1), 84.0 (C3), 82.7 (C2), 75.4, 74.7, 74.3 (-O*C*H_2Ar), 73.7 (C4), 71.2 (C5), 70.2 (C6) ppm; FTIR (ATR) υ_{max} (neat, cm^{-1}): 3500–3300, 3100–3000, 2950–2800, 1498, 1453, 1337, 1216, 1132, 1101, 1048, 1024, 910, 865, 755, 695; +ESI MS: calculated $[M + Li]^+$ for $C_{27}H_{30}O_6$: 457.2202, found: 457.2195.

Synthesis of Glucose Monomer 8

Methyl 2,3,4,6-tetra-*O*-benzyl-α-D-glucopyranoside (6). NaH (60% suspension in mineral oil, 41.2 g, 1.03 mol) was washed with hexanes under N_2. Hexanes was removed and NaH was suspended in dry DMF (500 mL). Methyl glucopyranoside (24.8 g, 0.128 mol) was dissolved in 200 mL of dry DMF and added dropwise the reaction mixture at 0 °C, and allowed to stir for 30 min until bubbles ceased to be produced. *Tert*-butyl ammonium iodide (5.2100 g, 0.014105 mol) was added, followed by the dropwise addition of benzyl bromide (83.2 g, 0.486 mol). The reaction mixture was allowed to warm to room temperature and stir for 22 hours. To quench the reaction, H_2O (100 mL) was added dropwise over 20 min. The mixture was extracted with DCM and washed with brine. The organic layers were collected, dried with $MgSO_4$, filtered, and concentrated under reduced pressure. The resulting residue was purified my column chromatography (SiO_2, gradient hexane:ethyl acetate) to yield the perbenzylated product (58.6 g, 82.7%).

*Methyl 2,3,4,6-tetra-O-benzyl-α-D-glucopyranoside (**6**).* ^{1}H NMR (500 MHz, $CDCl_3$) δ 7.37-7.12 (20H, m, Ar), 4.99-4.97 (d, J = 11.0 Hz, 1H, -OCH_2Ar), 4.84-4.81 (d, J = 10.6 Hz, 1H, -OCH_2Ar), 4.83-4.81 (d, J = 11.0 Hz, 1H, -OCH_2Ar), 4.81-4.78 (d, J = 12.2 Hz, 1H, -OCH_2Ar), 4.67-4.65 (d, J = 12.2 Hz, 1H, -OCH_2Ar), 4.63-4.62 (d, $J_{1\text{-}2}$ = 3.6 Hz, 1H, H1), 4.61-4.59 (d, J = 12.2 Hz, 1H, -OCH_2Ar), 4.48-4.46 (d, J = 12.2 Hz, 1H, -OCH_2Ar), 4.47-4.45 (d, J = 10.6 Hz, 1H, -OCH_2Ar), 4.00-3.96 (t, $J_{3\text{-}2}$ = $J_{3\text{-}4}$ = 9.2 Hz, 1H, H3), 3.76-3.72 (ddd, $J_{5\text{-}4}$ = 9.3 Hz $J_{5\text{-}6a}$ = 3.7, $J_{5\text{-}6b}$ = 2.0 Hz, 1H, H5), 3.74-3.70 (dd, $J_{6a\text{-}6b}$ = 13.6 Hz, $J_{6a\text{-}5}$ = 3.7 Hz, 1H, H6a), 3.65-3.62 (dd, $J_{6b\text{-}6a}$ = 13.6 Hz, $J_{6b\text{-}5}$ = 2.0 Hz, 1H, H6b), 3.65-3.61 (t, $J_{4\text{-}3}$ = $J_{4\text{-}5}$ = 9.3 Hz, 1H, H4), 3.57-3.54 (dd, $J_{2\text{-}3}$ = 9.3 Hz, $J_{2\text{-}1}$ = 3.6 Hz, 1H, H2), 3.38 (s, 3H, -OCH_3) ppm; ^{13}C NMR (125 MHz, $CDCl_3$) δ: 138.9, 138.4, 138.3, 137.0 *(*Ar$_{ipso}$*)*, 128.6, 128.5, 128.4, 128.3, 128.1, 128.0, 128.0, 127.8, 127.8, 127.7 (Ar), 98.3 (Cl), 82.3 (C3), 79.9 (C2), 77.8 (C4), 75.9, 75.2, 73.6, 73.5 (-OCH$_2$Ar), 70.2, (C5), 68.6 (C6), 55.3 (-OCH$_3$) ppm; FTIR (ATR) υ_{max} (neat, cm^{-1}): 3088, 3062, 3030, 2899, 2864, 1496, 1452, 1359, 1325, 1207, 1192, 1157, 1134, 1085, 1070, 1043, 1026, 1002, 910, 850, 732, 694, 650; HRMS (+ESI) m/z calc'd for $C_{35}H_{38}O_6$ $[M+Li]^+$: 561.28, found 561.2828.

1,6-Di-*O*-acetyl-2,3,4-tri-*O*-benzyl-D-glucopyranoside (7). Concentrated sulfuric acid (1 mL) was added dropwise to a stirred solution of **6** (5.4651 g, 9.8529 mmol) in acetic acid: acetic anhydride (1:1, 50 mL) at 0 °C. After an hour, thin layer chromatography (72:25 hexanes/ethyl acetate) indicated complete consumption of the starting material. The reaction mixture was washed with 50 mL of sat. aq. $NaHCO_3$ and 50 mL of ice water. The aqueous phase was extracted with DCM (3x75 mL) and the

combined organic layers were washed with brine, dried with $MgSO_4$, filtered and concentrated in *vacuo*. The residue was purified by column chromatography over silica gel (gradient 100% hexanes to 70:30 hexanes/ethyl acetate) to afford the diacetate, **7**, (3.3131 g, 1:0.3, α:β, 62.3%) as a pale yellow oil.

*1,6-Di-O-acetyl-2,3,4-tri-O-benzyl-α-D-glucopyranoside (**7α**)* ^{1}H NMR (500 MHz, $CDCl_3$) δ 7.38-7.25 (m, 15H, Ar), 6.32-6.31 (d, $J_{1\text{-}2}$ = 3.5 Hz, 1H, H1), 5.00-4.98 (d, J = 10.8 Hz, 1H, -OCH_2Ar), 4.90-4.88 (d, J = 10.7 Hz, 1H, -OCH_2Ar), 4.84-4.82 (d, J = 10.8 Hz, 1H, -OCH_2Ar), 4.72-4.70 (d, J = 11.4 Hz, 1H, -OCH_2Ar), 4.65-4.63 (d, J = 11.4 Hz, 1H, -OCH_2Ar), 4.58-4.56 (d, J = 10.7 Hz, 1H, -OCH_2Ar), 4.32-4.26 (dd, $J_{6a\text{-}6b}$ = 12.2 Hz, $J_{6a\text{-}5}$ = 3.7 Hz, 1H, H6a), 4.26-4.21 (dd, $J_{6b\text{-}6z}$ = 12.2 Hz, $J_{6b\text{-}5}$ = 2.3 Hz, 1H, H6b), 4.01-3.95 (dd, $J_{3\text{-}2}$ = 9.6 Hz, $J_{3\text{-}4}$ = 9.0 Hz, 1H, H3), 3.96-3.91 (ddd, $J_{5\text{-}4}$ = 10.0 Hz, $J_{5\text{-}6a}$ = 3.7 Hz, $J_{5\text{-}6b}$ = 2.3 Hz, 1H, H5), 3.69-3.65 (dd, $J_{2\text{-}3}$ = 9.6 Hz, $J_{2\text{-}1}$ = 3.6 Hz, 1H, H2) 3.60-3.54 (dd, $J_{4\text{-}5}$ = 10.0 Hz, $J_{4\text{-}3}$ = 9.0 Hz, 1H, H3), 2.15 (s, 3H, -COOCH_3), 2.03 (s, 3H, -COOCH_3) ppm; ^{13}C NMR (125 MHz, $CDCl_3$): δ 170.8, 169.45 (-*C*OOCH$_3$), 138.5, 137.7, 137.6 (Ar$_{ipso}$), 128.7, 128.6, 128.5, 128.3, 128.2, 128.2, 128.1, 128.0, 127.9 (Ar), 89.8 (C1), 81.7 (C3), 78.9 (C2), 76.7 (C4), 75.9, 75.4, 73.3 (-O*C*H$_2$Ar), 71.2 (C5), 62.8 (C6), 21.2, 21.0 (-COO*C*H$_3$) ppm; FTIR (ATR) υ_{max} (neat, cm^{-1}): 3088, 3062, 3030, 2914, 2873, 1741, 1496, 1454, 1361, 1226, 1151, 1070, 1008, 933, 912, 734, 696; HRMS (+ESI) m/z calc'd for $C_{31}H_{34}O_8$ $[M+Li]^+$: 541.24, found 541.2414.

*1,6-Di-O-acetyl-2,3,4-tri-O-benzyl-β-D-glucopyranoside (**7β**)* ^{1}H NMR (500 MHz, $CDCl_3$) δ 7.38-7.25 (m, 15H, Ar), 5.61-5.60 (d, $J_{1\text{-}2}$ = 8.2 Hz, 1H, H1), 5.00-4.98 (d, J = 10.8 Hz, 1H, -OCH_2Ar), 4.90-4.88 (d, J = 10.7 Hz, 1H, -OCH_2Ar), 4.84-4.82 (d,

J = 10.8 Hz, 1H, -OC*H*$_2$Ar), 4.72-4.70 (d, *J* = 11.4 Hz, 1H, -OC*H*$_2$Ar), 4.65-4.63 (d, *J* = 11.4 Hz, 1H, -OC*H*$_2$Ar), 4.58-4.56 (d, *J* = 10.7 Hz, 1H, -OC*H*$_2$Ar), 4.32-4.26 (dd, $J_{6a\text{-}6b}$ = 12.2 Hz, $J_{6a\text{-}5}$ = 3.7 Hz, 1H, H6a), 4.26-4.21 (dd, $J_{6b\text{-}6a}$ = 12.2 Hz, $J_{6b\text{-}5}$ = 2.9 Hz, 1H, H6b), 4.01-3.95 (dd, $J_{3\text{-}2}$ = 9.6 Hz, $J_{3\text{-}4}$ = 9.0 Hz, 1H, H3), 3.96-3.91 (ddd, $J_{5\text{-}4}$ = 10.0 Hz, $J_{5\text{-}6a}$ = 3.7 Hz, $J_{5\text{-}6b}$ = 2.9 Hz, 1H, H5), 3.78-3.72 (dd, $J_{2\text{-}3}$ = 9.6 Hz, $J_{2\text{-}1}$ = 8.2 Hz, 1H, H2) 3.60-3.54 (dd, $J_{4\text{-}5}$ = 10.0 Hz, $J_{4\text{-}3}$ = 9.0 Hz, 1H, H4), 2.15 (s, 3H, -COOC*H*$_3$), 2.03 (s, 3H, -COOC*H*$_3$) ppm; ^{13}C NMR (125 MHz, $CDCl_3$): δ 170.8, 169.45 (-*C*OOCH$_3$), 138.5, 137.7, 137.6 (Ar$_{ipso}$), 128.7, 128.6, 128.5, 128.3, 128.2, 128.2, 128.1, 128.0, 127.9 (Ar), 89.8 (C1), 81.7 (C3), 78.9 (C2), 76.7 (C4), 75.9, 75.4, 73.3 (-O*C*H$_2$Ar), 71.2 (C5), 62.8 (C6), 21.2, 21.0 (-COO*C*H$_3$) ppm; FTIR (ATR) υ_{max} (neat, cm^{-1}): 3088, 3062, 3030, 2914, 2873, 1741, 1496, 1454, 1361, 1226, 1151, 1070, 1008, 933, 912, 734, 696; HRMS (+ESI) m/z calc'd for $C_{31}H_{34}O_8$ $[M+Li]^+$: 541.24, found 541.2414.

2,3,4-Tri-*O*-benzyl-ᴅ-glucopyranoside (8). To a stirred solution of 1,6-di-*O*-acetyl-2,3,4-tri-*O*-benzyl-β-ᴅ-glucopyranoside, **7**, (1.9940 g, 3.7299 mmol) in anhydrous methanol/THF (3:1, 32 mL) was added sodium methoxide (25% in methanol, 1.5 mL) at O °C for 30 min. Upon consumption of the starting material, the reaction was neutralized with 1 M $NaHSO_4$ solution. The reaction mixture was diluted with 100 mL of ethyl acetate, washed with 75 mL of distilled water and brine, dried with $MgSO_4$, filtered and concentrated in *vacuo*. Crude was purified by column chromatography (SiO_2, 1:1 hexanes/ethyl acetate) to afford 1.6465 g of 2,3,4-tri-*O*-benzyl-ᴅ-glucopyranoside (**8**), as a white solid (98%, 1:1 α:β).

*2,3,4-Tri-O-benzyl-α-D-glucopyranoside (**8α**).* ^{1}H NMR (500 MHz, $CDCl_3$) δ 7.36-7.26 (m, 15H, Ar), 5.19-5.18 (d, $J_{1\text{-}2}$ = 3.6 Hz, 1H, H1α), 4.97-4.62 (m, 6H, -OC*H*$_2$Ar), 4.02-3.98 (t, $J_{3\text{-}2} = J_{3\text{-}4}$ = 9.3 Hz, 1H, H3), 3.97-3.93 (ddd, $J_{5\text{-}4}$ = 10.0 Hz, $J_{5\text{-}6b}$ = 4.4 Hz, $J_{5\text{-}6a}$ = 2.3 Hz, 1H, H5), 3.82-3.79 (dd, $J_{6a\text{-}6b}$ = 12.1 Hz, $J_{6a\text{-}5}$ = 2.3 Hz, 1H, H6a), 3.69-3.65 (dd, $J_{6b\text{-}6a}$ = 12.1 Hz, $J_{6b\text{-}5}$ = 4.4, 1H, H6b), 3.56-3.49 (dd, $J_{2\text{-}3}$ = 9.3 Hz, $J_{2\text{-}1}$ = 3.6 Hz, 1H, H2), 3.56-3.49 (dd, $J_{4\text{-}5}$ = 10.0 Hz, $J_{4\text{-}3}$ = 9.3 Hz, 1H, H4) 3.00 (s, 1H, OH-1), 1.66 (s, 1H, OH-6) ppm; ^{13}C NMR (125 MHz, $CDCl_3$): δ 138.7, 138.5, 138.4 (Ar$_{ipso}$), 128.9, 128.6, 128.6, 128.5, 128.3, 128.2, 128.1, 128.0, 127.9, 127.8 (Ar), 91.3 (C1), 81.7 (C3), 80.2 (C2), 77.6 (C4), 75.8 (-O*C*H$_2$Ar), 75.2 (-O*C*H$_2$Ar), 73.4 (-O*C*H$_2$Ar), 71.1 (C5), 62.0 (C6) ppm; FTIR (ATR) υ_{max} (neat, cm^{-1}): 3433, 3307, 3088, 3062, 3028, 2916, 2900, 2872, 1496, 1452, 1359, 1319, 1234, 1215, 1147, 1109, 1085, 1060, 1028, 1016, 987, 748, 731; HRMS (+ESI) m/z calc'd for $C_{27}H_{30}O_6$ $[M+Li]^+$: 457.22, found 457.2214.

*2,3,4-Tri-O-benzyl-β-D-glucopyranoside (**8β**).* ^{1}H NMR (500 MHz, $CDCl_3$) δ 7.36-7.26 (m, 15H, Ar), 4.97-4.62 (m, 6H, -O*C*H$_2$Ar), 4.73-4.71 (d, $J_{1\text{-}2}$ = 7.8 Hz, 1H, H1β), 3.87-3.84 (dd, $J_{6a\text{-}6b}$ = 12.1 Hz, $J_{6a\text{-}5}$ = 2.3 Hz, 1H, H6a), 3.70-3.64 (dd, $J_{6b\text{-}6a}$ = 12.1 Hz, $J_{6b\text{-}5}$ = 4.4 Hz, 1H, H6b), 3.53-3.49 (t, $J_{3\text{-}2} = J_{3\text{-}4}$ = 9.3 Hz, 1H, H3), 3.56-3.49 (dd, $J_{4\text{-}5}$ = 9.9 Hz, $J_{4\text{-}3}$ = 9.3 Hz, 1H, H4) 3.43-3.39 (ddd, $J_{5\text{-}4}$ = 9.9 Hz, $J_{5\text{-}6b}$ = 4.4 Hz, $J_{5\text{-}6a}$ = 2.3 Hz, 1H, H5) 3.39-3.35 (dd, $J_{2\text{-}3}$ = 9.3 Hz, $J_{2\text{-}1}$ = 7.8 Hz, 1H, H2), 3.27 (s, 1H, OH-1), 1.95 (s, 1H, OH-6) ppm; ^{13}C NMR (125 MHz, $CDCl_3$): δ 138.1, 138.0, 137.9 (Ar$_{ipso}$), 128.9, 128.6, 128.6, 128.5, 128.3, 128.2, 128.1, 128.0, 127.9, 127.8 (Ar), 97.4 (C1), 84.6 (C3), 83.3 (C2), 77.7 (C4), 75.9 (-O*C*H$_2$Ar), 75.5 (C5), 75.2 (-O*C*H$_2$Ar), 75.0

(-OCH_2Ar), 62.0 (C6) ppm; FTIR (ATR) υ_{max} (neat, cm^{-1}): 3433, 3307, 3088, 3062, 3028, 2916, 2900, 2872, 1496, 1452, 1359, 1319, 1234, 1215, 1147, 1109, 1085, 1060, 1028, 1016, 987, 748, 731; HRMS (+ESI) m/z calc'd for $C_{27}H_{30}O_6$ $[M+Li]^+$: 457.22, found 457.2214.

Synthesis of Monomers 11 and 12

Methyl 3-*O*-benzyl-4,6-*O*-benzylidene-α-D-glucopyranoside (9) and **methyl 2-*O*-benzyl-4,6-*O*-benzylidene-α-D-glucopyranoside (10)**. Methyl-4,6-*O*-benzylidene glucopyranoside, **1**, (10.2 g, 36.1 mmol), benzyl bromide (10.5 g, 61.4 mmol), and tetrabutylammonium hydrogensulfate (2.53 g, 7.44 mmol) were dissolved in 600 mL of DCM. To this solution, 50 mL of 5% NaOH (aq.) solution was added and the mixture was heated to reflux and left for 26 hours. The mixture was separated and the aqueous layer was extracted with 50 mL of DCM. The organic layers were combined, dried with $MgSO_4$, filtered and concentrated under reduced pressure. The resulting residue was purified by column chromatography (SiO_2, gradient hexane to ethyl acetate) to afford methyl 2-O-benzyl-4,6-O-benzylidene-α-D-glucopyranoside **9** (7.61 g, 57%) and methyl 3-O-benzyl-4,6-O-benzylidene-α-D-glucopyranoside **10** (5.42 g, 40%) as white solids.

*Methyl 3-O-benzyl-4,6-O-benzylidene-α-D-glucopyranoside (**9**).* ^{1}H NMR (500 MHz, $CDCl_3$) δ 7.50-7.25 (m, 10H, Ar), 5.57 (s, 1H, -OC*H*Ar), 4.98-4.95 (d, J = 11.8 Hz, 1H, -OCH_2Ar), 4.82 (d, $J_{1\text{-}2}$ = 3.3 Hz, 1H, H1), 4.80-4.78 (d, J = 11.8 Hz, 1H, -OCH_2Ar), 4.31-4.28 (dd, $J_{6eq\text{-}5}$ = 9.9 Hz, $J_{6eq\text{-}6ax}$ = 4.6 Hz, 1H, $H6_{eq}$), 3.85-3.81 (td, $J_{5\text{-}4}$ = $J_{5\text{-}6ax}$ = 9.9 Hz, $J_{5\text{-}6eq}$ = 4.5 Hz, 1H, H5), 3.85-3.81 (t, $J_{3\text{-}2}$ = $J_{3\text{-}4}$ = 9.9 Hz, 1H, H3), 3.78-

3.74 (t, $J_{6ax\text{-}5} = J_{6ax\text{-}6eq}$ = 9.9 Hz, 1H, $H6_{eq}$), 3.75-3.71 (ddd, $J_{2\text{-}3}$ = 9.9 Hz, $J_{2\text{-}OH}$ = 6.9 Hz, $J_{2\text{-}1}$ = 3.3 Hz, 1H, H2), 3.67-3.63 (t, $J_{4\text{-}3} = J_{4\text{-}5}$ = 9.9 Hz, 1H, H4), 3.45 (s, 3H, -OCH_3), 2.31-2.30 (d, $J_{OH\text{-}2}$ = 6.9 Hz, 1H, $H_{OH\text{-}2}$) ppm; ^{13}C NMR (125 MHz, $CDCl_3$): δ 138.4, 137.3 (Ar_{ipso}), 129.0, 128.4, 128.2, 128.0, 127.7, 126.0 (Ar), 101.3 (-O*C*HAr), 99.9 (C1), 81.9 (C4), 78.4 (C3), 74.8 (-O*C*H_2Ar), 72.4 (C2), 69.0 (C6), 62.6 (C5), 55.4 (-O*C*H_3) ppm; FTIR (ATR) υ_{max} (neat, cm $^{-1}$): 3302 (broad), 3032, 2924, 2870, 1450, 1365, 1280, 1064, 987; HRMS (+ESI) m/z calc'd for $C_{21}H_{24}O_6$ $[M+H]^+$: 372.16; observed 373.1614.

*Methyl 2-O-benzyl-4,6-O-benzylidene-α-D-glucopyranoside (**10**).* ^{1}H NMR (500 MHz, $CDCl_3$) δ 7.50-7.30 (m, 10H), 5.52 (s, 1H, -OC*H*Ar), 4.80-4.78 (d, *J* = 11.9 Hz, 1H, -OCH_2Ar), 4.72-4.70 (d, *J* = 11.9 Hz, 1H, -OCH_2Ar), 4.62-4.61 (d, $J_{1\text{-}2}$ = 3.8 Hz, 1H, H1), 4.28-4.25 (dd, $J_{6eq\text{-}6ax}$ = 9.5 Hz, $J_{6eq\text{-}5}$ = 4.6 Hz, 1H, $H6_{eq}$), 4.18-4.13 (td, $J_{3\text{-}2} = J_{3\text{-}4}$ = 9.5 Hz, $J_{3\text{-}OH}$ = 2.1 Hz, 1H, H3), 3.84-3.79 (td, $J_{5\text{-}4} = J_{5\text{-}6ax}$ = 9.5 Hz, $J_{5\text{-}6eq}$ = 4.7 Hz, 1H, H5), 3.73-3.68 (t, $J_{6ax\text{-}5} = J_{6ax\text{-}6eq}$ = 9.5 Hz, 1H, $H6_{ax}$), 3.52-3.48 (t, $J_{4\text{-}3} = J_{4\text{-}5}$ = 9.5 Hz, 1H, H4), 3.48-3.46 (dd, $J_{2\text{-}3}$ = 9.5 Hz, $J_{2\text{-}1}$ = 3.8 Hz, 1H, H2), 3.38 (s, 3H, -OCH_3), 2.53-2.52 (d, $J_{OH\text{-}3}$ = 2.1 Hz, 1H, $H_{OH\text{-}3}$) ppm; ^{13}C NMR (125 MHz, $CDCl_3$): δ 137.9, 137.1 (Ar_{ipso}), 129.2, 128.6, 128.3, 128.1, 126.3 (Ar), 102.0 (-O*C*HAr), 98.6 (C1), 81.2 (C4), 79.5 (C2), 73.4 (-O*C*H_2Ar), 70.3 (C3), 70.0 (C6), 62.0 (C5), 55.4 (-O*C*H_3) ppm; FTIR (ATR) υ_{max} (neat, cm^{-1}): 3456 (broad), 2924, 2846, 1458, 1357, 1334, 1080, 1026, 972, 918, 856; HRMS (+ESI) m/z calc'd for $C_{21}H_{24}O_6$ $[M+Li]^+$: 379.17; found 379.1675.

Methyl 3,4-di-*O*-benzyl-α-D-glucopyranoside (11). To a solution of **7** (0.824 g, 2.21 mmol) in 22 mL of dry DCM, in a flame dried round bottom schlenk flask with 3Å

molecular sieves, was added borane-tetrahydrofuran complex (1M in THF, 11 mL) and trimethylsilyl trifluoromethanesulfonate (0.100 mL, 0.250 mmol) under N_2 nitrogen. After 90 min the reaction was quenched by addition of 10 mL of methanol and 1.5 mL of triethylamine. The solution was filtered, concentrated, co-evaporated with 50 mL of methanol 3 times and then purified by column chromatography (SiO_2, 1:0 to 5:5 Hex/EtOAc) to yield 1.7306 g (84%) of a white solid.

*Methyl 3,4-di-O-benzyl-α-D-glucopyranoside (**11**).* ^{1}H NMR (500 MHz, $CDCl_3$) δ 7.39-7.26 (m, 10H), 4.93-4.91 (d, J = 11.2 Hz, 1H, -OCH_2Ar), 4.90-4.87 (d, J = 11.0 Hz, 1H, -OCH_2Ar), 4.88-4.86 (d, J = 11.0 Hz, 1H, -OCH_2Ar), 4.77-4.76 (d, $J_{1\text{-}2}$ = 3.8 Hz, 1H, H1), 4.67-4.65 (d, J = 11.0 Hz, 1H, -OCH_2Ar), 3.84-3.80 (dd, $J_{6a\text{-}6b}$ = 11.2 Hz, $J_{6a\text{-}5}$ = 5.3 Hz, 1H, H6$_a$), 3.80-3.77 (t, $J_{3\text{-}2}$ = $J_{3\text{-}4}$ = 8.9 Hz, 1H, H3), 3.76-3.72 (dd, $J_{6b\text{-}6a}$ = 11.2 Hz, $J_{6b\text{-}5}$ = 5.3 Hz, 1H, H6b), 3.69-3.65 (dt, $J_{2\text{-}3}$ = $J_{2\text{-}OH}$ = 8.4 Hz, $J_{2\text{-}1}$ = 3.8 Hz, 1H, H2), 3.68-3.65 (dd, $J_{5\text{-}4}$ = 9.8 Hz, $J_{5\text{-}6}$ = 5.3 Hz, 1H, H5), 3.56-3.52 (dd, $J_{4\text{-}5}$ = 9.8 Hz, $J_{4\text{-}3}$ = 8.4 Hz, 1H, H4), 3.42 (s, 3H, -OCH_3), 2.14-2.13 (d, $J_{OH\text{-}2}$ = 8.4 Hz, 1H, H$_{OH\text{-}2}$), 1.73 (s, 1H, H$_{OH\text{-}6}$) ppm; ^{13}C NMR (125 MHz, $CDCl_3$): δ 138.7, 138.2 (Ar$_{ipso}$), 128.6, 128.6, 128.1, 128.0, 127.9 (Ar), 99.5 (C1), 83.2 (C3), 77.4 (C4), 75.5, 75.1 (-OCH$_2$Ar), 73.1 (C2), 71.1 (C5), 61.9 (C6), 55.4 (-OCH$_3$) ppm; FTIR (ATR) υ_{max} (neat, cm $^{-1}$): 3525–3225, 3100–3000, 2950–2775, 1500, 1452, 1358, 1329, 1206, 1142, 1093, 1059, 1026, 901, 760, 731, 692; +ESI MS: calculated [M + Li]$^+$ for $C_{21}H_{26}O_6$: 381.1889, found: 381.1898.

Methyl 2,4-di-*O*-benzyl-α-D-glucopyranoside (12). To a solution of **2** (05 g, 5.50 mmol) in 60 mL of DCM , in a flame dried round bottom schlenk flask with 3Å

molecular sieves, was added borane-tetrahydrofuran complex (1M in THF, 28 mL) and trimethylsilyl trifluoromethanesulfonate (0.25 mL, 1.4 mmol) under N_2 nitrogen. After 90 min the reaction was quenched by addition of 30 mL of methanol and 3 mL of triethylamine. The solution was filtered, concentrated, coevaporated with 75 mL of methanol three times and then purified by column chromatography (SiO_2, a gradient of 1:0 to 5:5 Hex:EtOAc) to yield **12** as a white solid (1.73 g, 84%).

*Methyl 2,4-di-O-benzyl-α-D-glucopyranoside (**12**).* ^{1}H NMR (500 MHz, $CDCl_3$, 25 °C) δ 7.38-7.27 (m, 10H, Ar), 4.92-4.89 (d, J = 11.2 Hz, 1H, -OCH_2Ar), 4.73-4.70 (d, J = 12.3 Hz, 1H, -OCH_2Ar), 4.71-4.69 (d, J = 11.2 Hz, 1H, -OCH_2Ar), 4.69-4.66 (d, J = 12.3 Hz, 1H, -OCH_2Ar), 4.60-4.59 (d, $J_{1\text{-}2}$ = 3.8 Hz, 1H, H1), 4.12-4.08 (dt, $J_{3\text{-}2}$ = $J_{3\text{-}2}$ = 9.8 Hz, $J_{3\text{-}OH}$ = 1.9 Hz, 1H, H3), 3.81-3.77 (ddd, $J_{6a\text{-}6b}$ = 12.0 Hz, $J_{6a\text{-}OH}$ = 6.9 Hz, $J_{6a\text{-}5}$ = 3.8 Hz, 1H, H6a), 3.74-3.70 (ddd, $J_{6b\text{-}6a}$ = 12.0 Hz, $J_{6b\text{-}OH}$ = 6.9 Hz, $J_{6b\text{-}5}$ = 3.8 Hz, 1H, H6b), 3.64-3.61 (td, $J_{5\text{-}4}$ = 9.7 Hz, $J_{5\text{-}6a}$ = $J_{5\text{-}6b}$ = 3.7 Hz, 1H, H5), 3.46 (t, $J_{4\text{-}3}$ = $J_{4\text{-}5}$ = 9.8 Hz, 1H, H4), 3.36-3.33 (dd, $J_{2\text{-}3}$ = 9.8 Hz, $J_{2\text{-}1}$ = 3.5 Hz, 1H, H2), 3.32 (s, 3H, -OCH_3), 2.47 (d, $J_{OH\text{-}1}$ = 1.9 Hz, 1H, $H_{OH\text{-}1}$), 1.66 (t, $J_{OH\text{-}6}$ = 6.9 Hz, 1H, $H_{OH\text{-}6}$) ppm; ^{13}C NMR (125 MHz, $CDCl_3$) δ 138.40, 138.02 (Ar_{ipso}), 128.2, 128.3, 128.3, 128.2, 128.2, 128.0 (Ar), 97.6 (C1), 79.8 (C2), 77.3 (C4), 74.69 (-OCH$_2$Ar), 73.6 (-OCH$_2$Ar), 73.2 (C3), 70.4 (C5), 62.1 (C6), 55.3 (-OCH$_3$) ppm; FTIR (ATR) υ_{max} (neat, cm $^{-1}$): 3400–3150, 3100–3000, 2975–2775, 1454, 1367, 1192, 1101, 1065, 1028, 993, 301, 841, 732, 694, 636; +ESI MS: calculated [M + Li]+ for $C_{21}H_{26}O_6$: 381.1889, found: 381.1881.

General Procedures for initial screening of polymerization conditions by Plackett-Burman experiment plane with diol 4.

Triphosgene was added to a cold solution (0 °C) of the appropriate diol in anhydrous pyridine at a concentration of 400mg/mL under N_2. The reaction was allowed to stir for 5 min. and then warmed to r.t. and allowed to react for 48 hours. The reaction was then quenched with a saturated solution of sodium bicarbonate (*ca*. 2 mL) until no further evolution of carbon dioxide was observed. The residue was diluted with dichloromethane; the organic layer was washed with 10% aq. HCl and then dried with $MgSO_4$, filtered and concentrated under reduced pressure.

General Procedures of the Copolymerization between Diols 3, 6, 8, 10 and Triphosgene in DCM and pyridine.

Triphosgene, dissolved in dry DCM, was added dropwise to solution of the appropriate diol in DCM and anhydrous pyridine at a concentration of 0.12 M to 1.0 M under N_2 atmosphere. The reaction was allowed to stir for 1 to 48 h. The reaction was then quenched with a saturated solution of Na_2CO_3 (*ca*. 2 mL) until no further evolution of carbon dioxide was observed. The residue was diluted with dichloromethane; the organic layer was washed with 10% aq. HCl and then dried over $MgSO_4$, filtered, and concentrated under reduced pressure.

Procedure for Polycondensation of diol 8 with diphosgene in dioxane.

Diol **8** and diphosgene were dissolved in dry dioxane and a solution of anhydrous pyridine in dry dioxane was added dropwise. After stirring for 24 hr at 25 °C, the reaction mixture was poured into cold methanol and precipitate was filtered and dried in *vacuo*. Analogous experiments were conducted with a slight excess of diphosgene.

Poly(*2,3,6-tri-O-benzyl-ᴅ-glucopyranoside)carbonate (13)*. ^{1}H NMR (300 MHz, $CDCl_3$, 25 °C) δ 7.40-7.05 (m, 15H, Ar), 6.23-5.95 (m, 0.55, H1α), 5.53-5.45 (m, 0.45, H1β), 5.13-3.90 (m, 8H, -OCH_2Ar and H6), 3.81-3.32 (m, 4H); FTIR (ATR) υ_{max} (neat, cm $^{-1}$): 3100–3000, 3000–2800, 1755, 1454, 1356, 1248, 1070, 1026, 1001, 735, 696;

*Polymer **13a***. GPC: M_p = 9.0 g/mol; DSC T_g = 44 °C. TGA in Ar: $(T_d)_{onset}$ = 137 °C, $(T_d)_{50}$ = 315 °C, 137-354 °C, 91% mass loss, 9% mass remaining at 500 °C.

*Polymer **13b***. GPC: M_w = 6800 g/mol, M_n = 6100 g/mol, PDI = 1.10; DSC: T_g not observable by DSC; TGA: $(T_d)_{onset}$ = 179 °C, $(T_d)_{50}$ = 315 °C, 179-345 °C, 77% mass loss, 23% mass remaining at 500 °C.

*Polymer **13j***. GPC: M_w = 5500 g/mol, M_n = 5000 g/mol, PDI = 1.13; DSC: $T_{g,}$ = 33 °C. TGA in Ar: $(T_d)_{onset}$ = 171 °C, $(T_d)_{50}$ = 317 °C, 267 °C, 15% mass loss; 345 °C, 74% mass loss; 26% mass remaining above 345 °C.

Poly(*2,3,4-tri-O-benzyl-ᴅ-glucopyranoside)carbonate (14)*. ^{1}H NMR (300 MHz, $CDCl_3$, 25 °C) δ 7.42-7.13 (m, 15H, Ar), 6.11 (m, 0.4, H1α), 5.49 (m, 0.6, H1β), 5.01-4.52 (m, 6H, -OCH_2Ar), 4.52-4.25 (m, 2H, H6), 4.13-4.08 (m, 1H), 4.03-3.95 (m, 1H),

3.80-3.36); FTIR (ATR) υ_{max} (neat, cm $^{-1}$): 3100–3000, 3000–2800, 1747, 1454, 1361, 1338, 1246, 1126, 1047, 1001, 785, 735, 696.

*Polymer **14d***. GPC: M_w = 21000 g/mol, M_n = 15000 g/mol, PDI = 1.40; DSC: T_g = 63 °C; TGA in Ar: 379 °C, 82% mass loss; 18% mass remaining above 379 °C.

*Polymer **14i***. GPC: M_w = 4800 g/mol, M_n = 4400 g/mol, PDI = 1.09; DSC: T_g = 63 °C; $(T_d)_{onset}$ = 230 °C, $(T_d)_{50}$ = 310 °C, 230-364 °C, 94% mass loss, 6% mass remaining at 500 °C.

Poly(methyl-3,4-di-O-benzyl-ᴅ-glucopyranoside)carbonate (15). ^{1}H NMR (500 MHz, $CDCl_3$) δ 7.34-7.21 (m, 10H, Ar), 4.89-4.68 (m, 5H, -OC*H*$_2$Ar, H2), 4.59-4.54 (m, 1H, -OC*H*$_2$Ar), 4.38-4.26 (m, 2H, H6), 4.03 (s, 1H, H3), 3.82 (s, 1H, H5), 3.58-3.52 (m, 1H, H4), 3.31-3.12 (m, 3H, -OC*H*$_3$) ppm; ^{13}C NMR (125 MHz, $CDCl_3$): δ 155.1, 154.7, 154.3 (carbonate), 138.4, 138.2, 137.7 (Ar$_{ipso}$), 128.6, 128.5, 128.2, 128.1, 128.0, 127.9, 127.8, 127.6, 127.6 (Ar), 96.9 (C1), 80.1 (C3), 80.0 (C2), 77.1 (C4), 75.7, 75.5 (-O*C*H$_2$Ar), 68.8 (C5), 66.6 (C6), 55.3 (-O*C*H$_3$) ppm; FTIR (ATR) υ_{max} (neat, cm^{-1}): FTIR (ATR): 3100–3000, 3000–2800, 1747, 1454, 1361, 1338, 1246, 1126, 1047, 1001, 785, 735, 696;

*Polymer **15d***: GPC: M_w = 32100 g/mol, M_n = 19200 g/mol, PDI = 1.67; DSC: T_g = 85 °C; TGA in Ar: 397 °C, 82% mass loss; 18% mass remaining at 500 °C.

*Polymer **15k***: GPC: M_w = 11600 g/mol, M_n = 10000 g/mol, PDI = 1.16; DSC: T_g = 70 °C; $(T_d)_{onset}$ = 325, $(T_d)_{50}$ = 359, 325-406 °C, 86% mass loss, 14% remaining at 500 °C

Poly(methyl-3,4-di-O-benzyl-ᴅ-glucopyranoside)carbonate (16). ^{1}H NMR (500 MHz, $CDCl_3$) δ 7.35-7.09 (m, 10H, Ar), 5.50-5.31 (m, 1H, H3), 4.70-4.22 (m, 6H, -OCH_2Ar, H1, H6), 4.18-4.06 (m, 1H, H6), 3.89-3.76 (m, 1H, H5), 3.55-3.43 (m, 2H, H2,H4), 3.31-3.10 (m, 3H, -OCH_3) ppm; ^{13}C NMR (125 MHz, $CDCl_3$): δ 154.9, 154.6, 154.3 (carbonate), 137.9, 137.2 (Ar_{ipso}), 128.8, 128.6, 128.6, 128.5, 128.5, 128.3, 128.2, 128.2, 128.2, 128.1, 128.0, 128.0, 127.9 (Ar), 97.7 (C1), 79.0 (C3), 75.6 (C2), 74.7 (C4), 74.1, 72.9 (-OCH_2Ar), 68.3 (C5), 66.5 (C6), 55.3 (-OCH_3) ppm; FTIR (ATR) υ_{max} (neat, cm^{-1}): 3100–2800, 1753, 1454, 1369, 1238, 1070, 1041, 1028, 999, 905, 781, 736, 696, 605. *Polymer **16b***: GPC: M_w = 21000 g/mol, M_n = 15000 g/mol, PDI = 1.40; DSC: $T_{g,midpoint}$ = 83 °C. TGA in Ar: 379 °C, 82% mass loss; 18% mass remaining above 379 °C. *Polymer **16e***: GPC: M_w = 10800 g/mol, M_n = 9800 g/mol, PDI = 1.10; DSC: T_g = 71 °C; $(T_d)_{onset}$ = 336 °C, $(T_d)_{50}$ = 361 °C, 85% mass loss, 15% mass remaining at 500 °C.

2.5 Results and Discussion

Based upon our overall goal of producing engineering types of polymers that are derived from glucose and modeled from cellulose, yet capable of undergoing hydrolytic degradation without the requirement of cellulase enzymes, we initially designed a *1,4*-diol monomer of glucose, and then expanded the scope to other regioisomeric glucose diol analogs. It was hypothesized that a series of glucose-derived diols could be copolymerized with a carbonylation agent to afford a series of regioisomeric polycarbonates. The series of poly(ᴅ-glucose carbonate)s were designed to mimic

certain aspects of cellulose and also glycogen. The 1→4-β-D-glycosidic linkages of cellulose facilitate chain packing to create crystallinity and provide for appropriate mechanical properties. The crystallinity also contributes to the relative hydrolytic stability and its need of enzymatic catalysis for degradation.[130] Unlike glucose, glycogen, connected by linear α-*1,4*- and *1,6*-repeat units as well as branching *1,4,6*-repeat units, does not share the same hydrolytic stability and mechanical strength. In contrast to the relative stability of the *1,4*-glycosidic linkages of cellulose, *1,4*-carbonate connectivity of the glucose repeat units was expected to reduce hydrolytic and thermal stability, due to the carbonate linkage being through a hemiacetal functionality of the anomeric site. With proper understanding of structure-property relationships with regards to various regiochemistries of possible glucose monomers, a polymer system with the ability to fulfill a myriad of applications can be developed. Therefore, a series of monomers and corresponding polymers having *1,4*-, *1,6*-, *2,6*- and *3,6*-regiochemistries was investigated.

2.5.1 Monomer Synthesis

Starting from commercially available methyl-α-D-glucopyranoside and methyl-4,6-benzylidene-α-D-glucopyranoside, four different regioisomeric monomers having *1,4*- (**4**), *1,6*- (**8**), *2,6*- (**11**), and *3,6*- (**12**) diols were prepared by three different sequences (Scheme 2.1 and 2.2). The *1,4*- diol, **4**, methyl-4,6-benzylidene-α-D-glucopyranoside was prepared by protecting the alcohols at positions carbon 2 (C2) and

C3 positions with benzyl groups to afford the completely protected glucose derivative (**2**). Selective benzylidene ring opening, using $NaCNBH_3$ and $AlCl_3$, was then performed to give a free alcohol at C4 as the major product (84%). Demethylation under acidic conditions afforded the *1,4* diol in 35% yield after column chromatography, and the structure was confirmed by ^{1}H, ^{13}C, COSY, HSQC NMR and IR spectroscopies and high-resolution mass spectrometry.

For the preparation of monomers **11** and **12**, single benzylation of methyl-4,6-*O*-benzylidene-α-D-glucopyranoside (**1**) occurred in a biphasic system utilizing a bulky phase transfer agent, tetra-butyl ammonium hydride to afford two products, **9** and **10** in near 1:1 ratio. Electronically, the C3 alcohol is more reactive than the C2 alcohol and is protected first under various protection reactions. Moreover, initial protection with sodium hydride in DMF afforded only C3-benzylated compound as the major product. However, the use of a bulky phase transfer agents decreases electronic control on the reaction and favorability of the C3 alcohol, thus affording near equal quantities of each mono-benzylated product. Conversion to monomers **11** and **12**, respectively, was performed by selective benzylidene ring opening in high yields with trimethylsilyl trifluoromethanesulfonate and borane-THF complex.

Initial attempts to synthesize the *1,6* diol monomer **6** were *via* a similar strategy used for the synthesis of **4**. However, with isolation of a single product during the final demethylation step of methyl 2,3,4-tri-*O*-benzyl-α-D-glucopyranoside proving difficult, an alternate strategy was explored. Per-benzylation of methyl-α-D-glucopyranoside (**5**) was carried out by reaction with sodium hydride, benzyl bromide and a catalytic amount

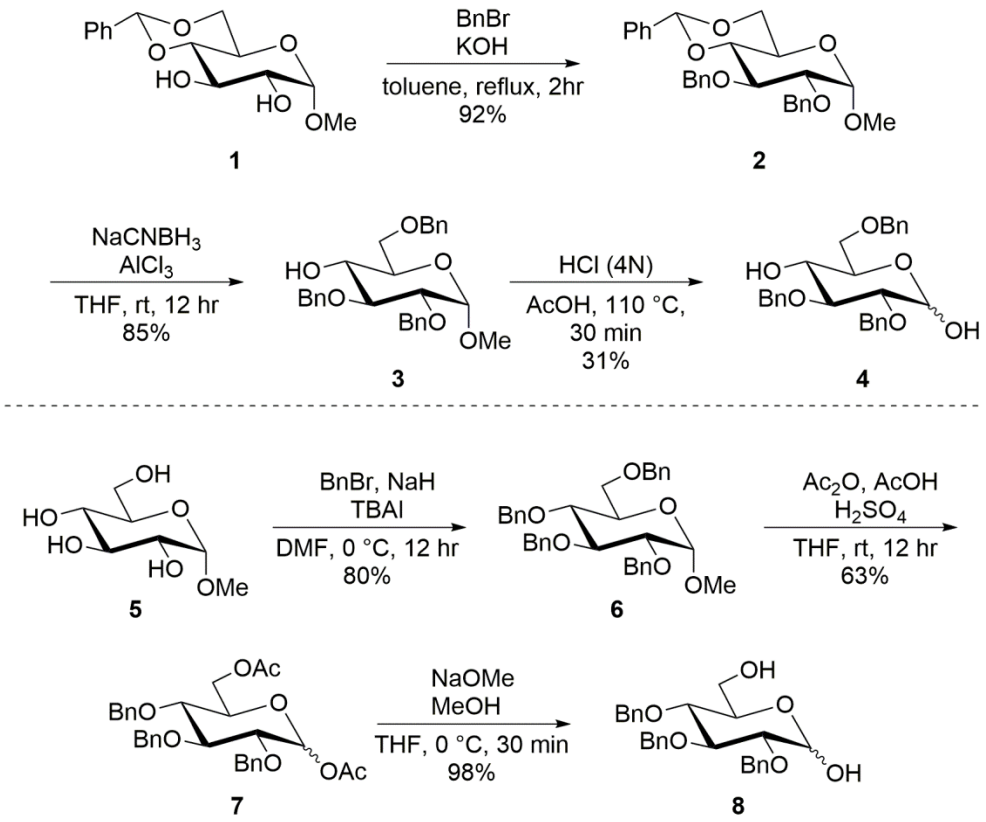

Scheme 2.1. Synthesis of *1,4*- and *1,6*- glucose-based diol monomers, **4** and **8** respectively.

of TBAI in dimethyl formamide (DMF) to give **4** in 80% yield. The removal of the methyl group at C1 and the benzyl group on C6 was performed by acid catalyzed acetolysis as described by Lam and Gervay-Hague[131] to afford the diacetate **7** (65%), which was subsequently converted to **8** in near quantitative yield by deprotection with sodium methoxide in methanol.

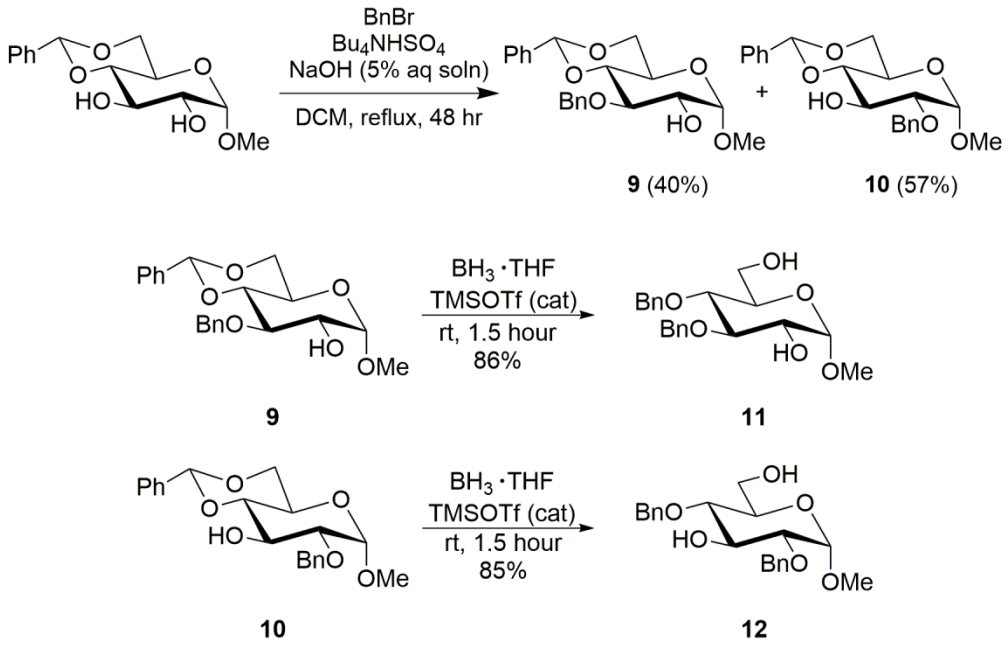

Scheme 2.2. Synthesis of *2,6*- and *3,6*- glucose-based diol monomers, **11** and **12** respectively.

*2.5.2 Initial screening of Polymerizations of diol **4**, with Phosgene, Diphosgene, and Triphosgene in Pyridine*

Testing for optimal polycondensation reaction conditions was performed using **4**, since, of the four monomers, it would generate a polycarbonate most analogous to cellulose, having *1,4*-backbone connectivity. In addition, since monomer **4** possesses a secondary alcohol and hemiacetal functionalities, as supposed to primary alcohols, it was predicted to be the most difficult to polymerize. Initial screening efforts were focused on employing alternative carbonylation reagents to phosgene, such as diphenyl, di-*p*-

nitrophenyl, dimethyl, and diethyl carbonates. While successful with commercially available diols, such as cylcohexanediol and cyclohexane dimethanol, it was observed that these conditions were either too harsh, causing degradation of the starting material, or not conducive to forming large molecular weight polymers, as monitored by NMR spectroscopy or GPC. As a result, testing of traditional polycarbonate reaction conditions utilizing phosgene, diphosgene, or triphosgene was pursued.

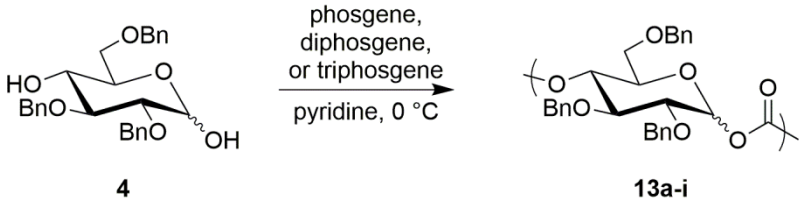

4 **13a-i**

Scheme 2.3. Synthesis of benzyl-protected *1,4*-poly(glucocarbonate)s.

Variations in reaction duration, monomer concentration, and the quantity of phosgene analogues, *i.e.*, phosgene, diphosgene, or triphosgene, were tested with a Plackett-Burman experimental design matrix. (matrix 4^3, where 4 is the number of factors and 3 is the number of levels tested for each factor).[132,133] Nine different experiments were carried out based on nine experimental conditions (Table 2.1, Experiments 1–9) conducted on scales of 150 mg of monomer in the volume of solvent needed to give the three desired monomer concentrations (combined pyridine and toluene (in the case of phosgene reagent)). Summary of the impact of each condition,

calculated with Equation 2.1., can be reviewed in Table 2.2 and Figure 2.2. To calculate the value of effectiveness for each factor, reactions sharing the same conditions, are averaged, and to this value, the average of all the experiments is subtracted. For example, experiments 3, 4, and 8 utilized triphosgene as a carbonylation agent. The resulting molecular weights of these three reactions average to 7.0 kDa. Subtracting the average of all the experiments (6.7 kDa) gives an effectiveness of value of 220. According to the survey, conditions with the larger (most positive) impact value are more effective at producing large molecular weight polymers.

This study of the effects of individual factors indicated that PGCs with the highest molecular weights could be produced under polymerization conditions that included a monomer concentration of 400 g/L, phosgene as the carbonylation agent at a stoichiometry of one molar equivalence, and a reaction time of 48 h (Table 2.2). Reaction conditions with a concentration of 400g/L (0.9 M) produced polymers with a M_p ranging from 5.6 to 8.8 kDa. Reactions lasting longer than 24 hours led to larger M_p, although reactions lasting 48 hours produced polymers with the largest M_p values. Since molecular weight is dependent on stoichiometric ratios of monomer during step-growth polymerizations, it is no surprise that reactions that exceeded one molar equivalent of

Table 2.1. Condition and results of the experimental design for the copolymerization between *1,4*-glucose diol, **4**, and phosgene in toluene/pyridine, diphosgene in pyridine, and triphosgene in pyridine.

Experiment	Polymer	Concentration (mg/mL)[a]	Duration (h)	Equivalents[b]	Carbonylation Agent	M_n[c] (kDa)
1	**13a**	200	48	1	Phosgene	9.0
2	**13b**	200	72	2	Diphosgene	5.5
3	**13c**	200	24	3	Triphosgene	5.6
4	**13d**	400	48	2	Triphosgene	8.7
5	**13e**	400	72	3	Phosgene	8.8
6	**13f**	400	24	1	Diphosgene	5.6
7	**13g**	600	48	3	Diphosgene	5.6
8	**13h**	600	72	1	Triphosgene	6.6
9	**13i**	600	24	2	Phosgene	5.6

[a]Concentration of 4 in anhydrous pyridine. [b]Number of equivalents of carbonylation agent. [c]Estimated by GPC (DMF, 0.05 M LiBr) calibrated with polystyrene standards.

$$\text{Effect} = \hat{y} - x$$

$\hat{y}$: average of each factor

x: average of all experiments

Equation 2.1. Plackett Burman equation.

Table 2.2. Results and analysis from Plackett-Burman experiment plane.

		Experiments	$\hat{Y}$ (kDa)	Effect ($\hat{y}$-x)
Concentration (g/L)	200	1,2,3	6.7	-82
	400	4,5,6	7.7	930
	600	7,8,9	5.9	-850
Duration (h)	24	3,6,9	5.6	-1200
	48	1,4,7	7.8	1000
	72	2,5,8	6.9	170
Equivalents of Carbonylation Agent	1	1,6,8	7.0	280
	2	2,4,9	6.6	-170
	3	3,5,7	6.7	-100
Carbonylation Agent	Phosgene	1,5,9	7.8	1000
	Diphosgene	2,6,7	5.5	-1200
	Triphosgene	3,4,8	7.0	220

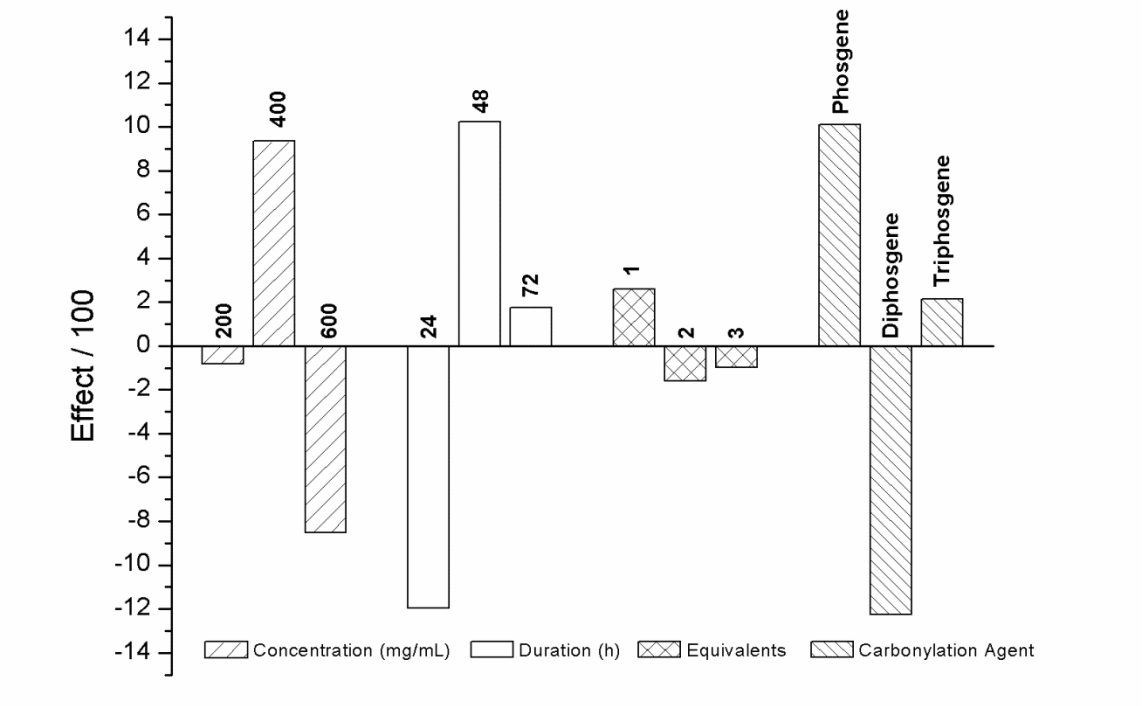

Figure 2.2. Effect of each factor evaluated during the experimental design.

phosgene, diphosgene, or triphosgene comonomer produced lower molecular weight polymers. Phosgene and triphosgene were more successful than diphosgene, which failed to produce polymers with molecular weights above 5.6 kDa. Although phosgene produced the highest molecular weight polymers, it was precluded from further study because of its instability and safety concerns associated with its use. Experiments with triphosgene, a more stable, solid alternative to phosgene, also provided PGCs with reasonably high molecular weights (M_n, of 8.7 kDa), and was also considered as a carbonylation agent later in this study.

The poly(glucose carbonate)s prepared with phosgene in pyridine were characterized by IR, ^{1}H and ^{13}C NMR spectroscopies. The characteristic carbonyl

vibration of the carbonate linkage was observed at 1759 cm^{-1} in the IR spectra. The copolymerizations of the diol with phosgene was demonstrated with ^{1}H NMR spectroscopy by observation of the downfield shifts for majority of the protons from the glucose ring and, in particular, the significant downfield shift of the protons on the carbons involved in the formation of the carbonate linkages; H1 and H6. With the amount of polymer isolated, 2D NMR techniques, such as COSY, proved difficult and thus could identify all signals in the ^{1}H NMR. However, synthetic analogues, phenylcarbonate-2,3,4,6-*O*-tetra-acetate-α-D-glucopyranoside and phenylcarbonate-2,3,4,6-*O*-tetra-acetate-β-D-glucopyranoside, allowed for the deduction of H1 signals. The H6 protons shifted slightly downfield 0.3 ppm (3.83 to 4.41 ppm) whereas the anomeric protons had much larger downfield shifts of 0.91 and 0.79 for $H1_{\alpha}$ and $H1_{\beta}$, respectively. The ^{1}H NMR spectra, however, did not reveal clearly detectable end group signals. The ^{13}C NMR spectra displayed three carbonate signals at 155 ppm having intensity ratios near 1:2:1, indicating a random sequence of head-to-head, head-to-tail, and tail-to-tail connected carbonate groups.

*2.5.3 Polymerization of Monomer **8** with Phosgene Generated in situ from Diphosgene in Pyridine and Dioxane.*

Concerned with the stability of the chloroformate in the presence of high concentrations of pyridine, changes were made to the reactions conditions determined tested previous. The second series of polycondensations was conducted in way that both

the *1,6* monomer, **8**, and diphosgene were dissolved in dioxane and a solution of pyridine was subsequently added, to limit the exposure of chloroformate to pyridine. Kricheldorf *et al.* previously reported that this procedure prevented an excess pyridine from decomposing diphosgene and chloroformate groups.[79] In their studies, side reactions between chloroformate chain ends and pyridine led to low molecular weight linear polymers (Scheme 2.4). It was rationalized that nucleophilic attack of chloroformates by pyridine was taking place, resulting in the degradation of chain ends to form alkoxide chain ends. As a result, polymerizations utilizing pyridine as a solvent needed an excess of phosgene in order to regenerate lost chloroformate chain ends. Loss of the chloroformate group through nucleophilic attack represents a unique challenge for monomers **4** and **8**, as the glucopyranoside anion can undergo ring-opening and lead to several different products (Scheme 2.4). The authors were able to reduce side reactions by modifying the polymerization conditions, in which lower amount of pyridine (near 1 equivalent) was added to the reaction mixture. Instead of adding phosgene/diphosgene/triphosgene solution to the diol monomer dissolved in pyridine, the authors dissolved a diol monomer and diphosgene in dioxane and subsequently added pyridine dropwise. With these reaction conditions, lower amounts of diphosgene was needed to afford linear polymers; maximum molecular weights, as measured by viscosity, were achieved when using between 0 and 0.2 mol % excess of phosgene generated *in situ* from diphosgene.

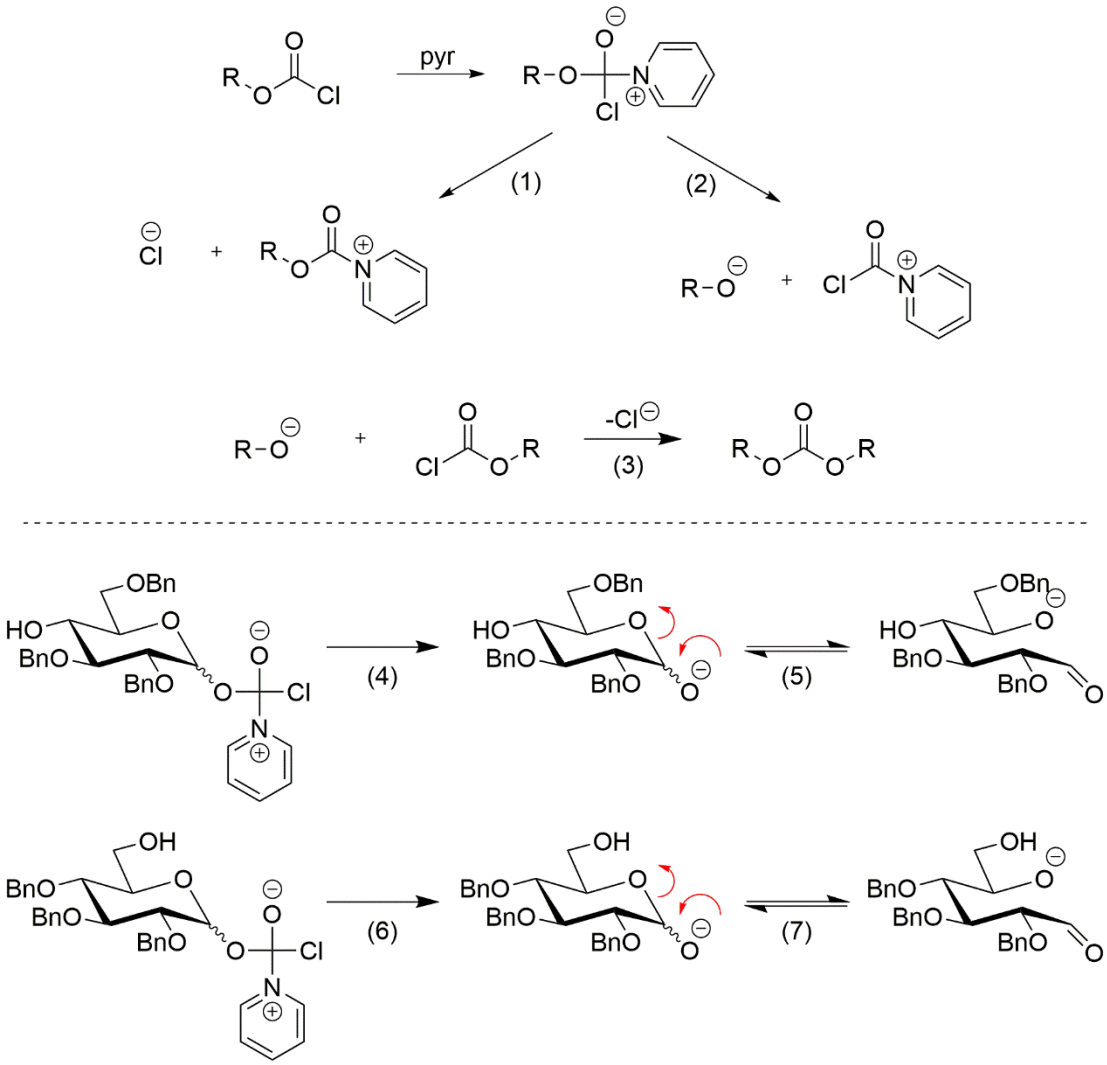

Scheme 2.4. High concentrations of pyridine may lead to decomposition of chloroformate chain ends due to nucleophilic attack by pyridine, as described by Kricheldorf *et al*. Complications may arise with monomers **4** and **8**, as ring opening of the glycosidic anion may lead to several side products.

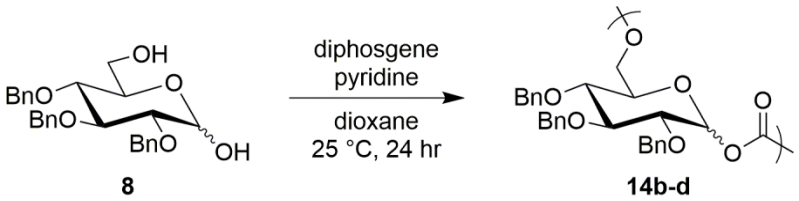

Scheme 2.5. Synthesis of benzyl-protected *1,6*-poly(glucose carbonate)s *via* polycondensation of monomer **8** with diphosgene in pyridine and dioxane.

Application of these conditions to the *1,6* monomer, **8**, saw a reduction in side reactions and polymers were formed, as demonstrated by the higher molecular weights (M_n = 10.6 kDa) observed by GPC (Table 2.3). In addition, the nature of the reaction was remarkably different for series of polymerizations. Previously, reactions in pyridine resulted in a dark brown gel, which may indicate the insolubility of products in pyridine. Reactions utilizing these new conditions ceased to produce a dark brown gel, but rather were clear with white precipitate, similar to other high molecular weight producing reactions experienced with monomers **11** and **12**, which will be discussed in the next section. These are promising conditions for the monomers bearing hemiacetal functionalities, however further investigations are needed to complete this study. Additional tests with higher amounts of diphosgene need to be performed to determine if higher molecular weights can be achieved. Also, it cannot be determined which factor was the primary cause for the success of these reactions as multiple factors (solvent and carbonylation agent and monomer) were changed to conduct this study. Upon further inquiry, optimized conditions can be used on the *1,4* diol, in attempts to synthesize a high molecular weight polycarbonate that resembles cellulose in structure.

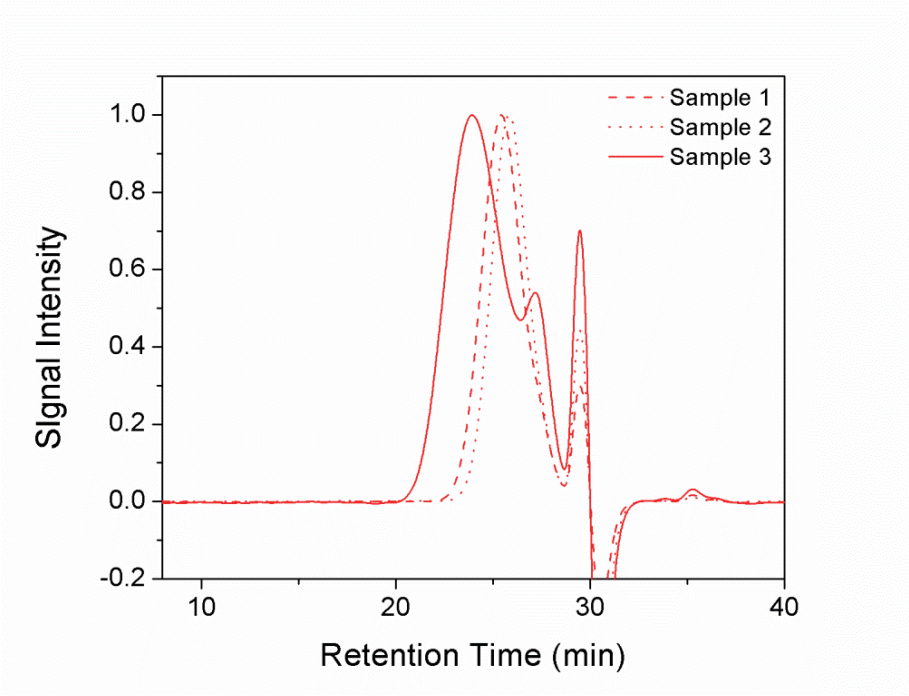

Figure 2.3. GPC traces of polycarbonates resulting from the copolymerization of the *1,6* diol, **8**, and diphosgene in dioxane.

Table 2.3. Summary of polymerization conditions with *1,6* diol, **8**, and diphosgene in dioxane.

Sample	Polymer	Diphosgene Equivalents	M_n (kDa)[a]	M_w (kDa)[a]	PDI[a]	% Yield[b]
1	**14b**	0.50	8.4	10.0	1.18	79
2	**14c**	0.55	7.5	8.6	1.15	82
3	**14d**	0.60	10.6	15.9	1.50	90

[a]Estimated by GPC (DMF, 0.05 M LiBr) calibrated with polystyrene standards. [b]Yield calculated from dried, filtered samples after precipitation in cold methanol.

*2.5.4 Polymerization of Four Regioisomeric Diols, **4**,**8**,**11**,and **12**, with Phosgene Generated in Situ from Triphosgene, as a Comonomer and Pyridine as a Base*

Triphosgene was reexamined as a possible carbonylation agent while employing lessons from previous polymerization attempts with favorable results. Using the conditions from the polymerization survey, four regioisomeric polymers **13**, **14**, **15**, and **16**, were synthesized from each diol monomer, **4**, **8**, **11**, and **12**, respectively (Scheme 2.6). In addition, with concerns of instability of chloroformate instability in the presence of high concentration of pyridine, dichloromethane was chosen as the primary solvent and the amount of pyridine was reduced, ranging from 2.0 to 4.7 mol percent. Since favorable results in previous attempts resulted from reaction conditions with a monomer concentration of 400 mg/mL (0.9 M), similar concentrations were tested. Polycarbonates are typically synthesized using an excess of the carbonyl donor (i.e. triphosgene), which hinders the control over final molecular weight due to step-growth polymerization's dependence on stoichiometry. Earlier we found that only one equivalent of phosgene and a slight excess of diphosgene was necessary for the production of high molecular weight polymers. Therefore, the *2,6* monomer, **11**, was initially copolymerization with 0.33 equivalent of triphosgene in DCM with 2 equivalents of pyridine at a monomer concentration of 0.5 M over 24 h (Table 2.4, Entry 13), affording polymers with M_n of 38.0 kDa. Increasing the amount of pyridine to 4 equivalents increased the molecular weight and led to the polymers with the highest

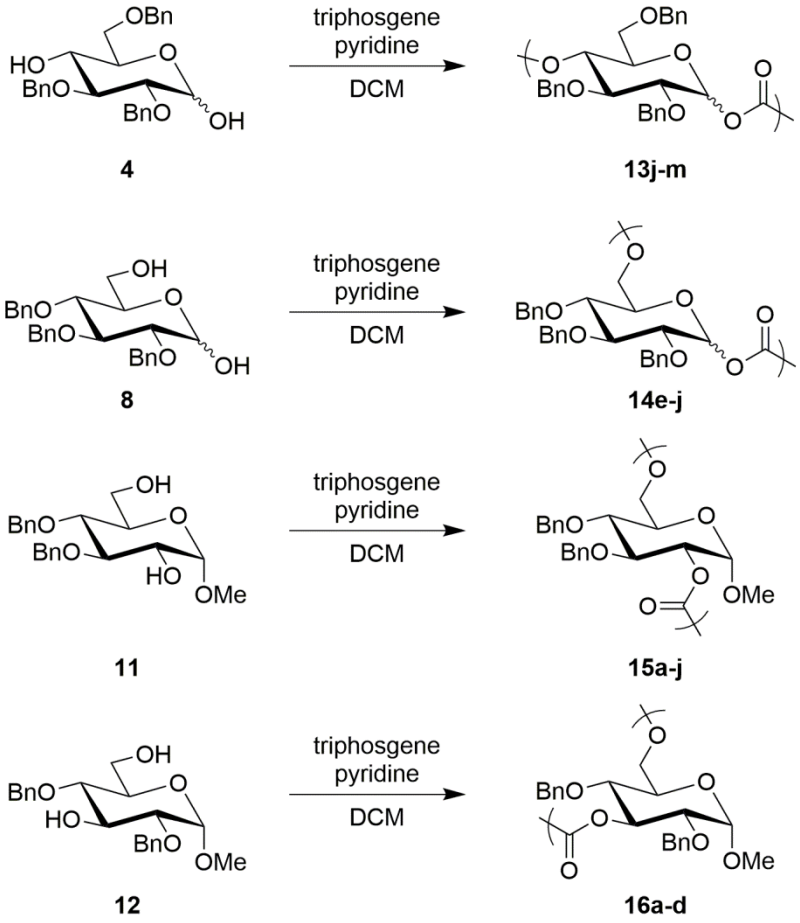

Scheme 2.6. Synthesis of four different regioisomeric polycarbonates from monomers **4**, **8**, **11**, and **12** with triphosgene in pyridine and dichloromethane.

Table 2.4. Summary of reaction conditions and resulting molecular weights of copolymerizations of monomers **4**, **8**, **11**, and **12** with triphosgene in DCM and pyridine.

Entry	Monomer	Polymer	Solvent	Duration (h)	Eq. of Triphosgene	Eq. of Pyridine	[M][a]	M_n[b] (kDa)	M_w[b] (kDa)	PDI[b]
1	*1,4* (**4**)	**13j**	DCM	1	0.40	2.5	0.56	5.0	5.5	1.13
2	*1,4* (**4**)	**13k**	DCM	5	0.40	4.2	0.57	6.2	6.7	1.08
3	*1,4* (**4**)	**13l**	DCM	24	0.40	4.7	0.26	7.8	8.5	1.09
4	*1,4* (**4**)	**13m**	DCM	24	0.33	4.0	1.0	no ppt		
5	*1,6* (**8**)	**14e**	DCM	1	0.40	3.8	0.12	5.7	6.6	1.16
6	*1,6* (**8**)	**14f**	DCM	24	0.33	2.0	1.0	5.9	7.0	1.20
7	*1,6* (**8**)	**14g**	DCM	24	0.33	4.0	0.50	7.1	8.2	1.16
8	*1,6* (**8**)	**14h**	DCM	24	0.33	4.0	0.50	11.2	11.7	1.04
9	*1,6* (**8**)	**14i**	DCM	24	0.33	4.0	1.0	4.4	4.8	1.09
10	*1,6* (**8**)	**14j**	Dioxane	24	0.33	4.0	1.0	5.1	5.3	1.03
11	*2,6* (**11**)	**15a**	DCM	24	0.33	4.0	0.50	334.0	557.0	1.67
12	*2,6* (**11**)	**15b**	DCM	24	0.33	4.0	0.50	93.0	134.3	1.44
13	*2,6* (**11**)	**15c**	DCM	24	0.33	2.0	0.50	38.0	52.0	1.37
14	*2,6* (**11**)	**15d**	DCM	24	0.33	4.0	0.50	19.2	32.1	1.67
15	*2,6* (**11**)	**15e**	DCM	1	0.33	4.0	0.50	12.4	15.1	1.22
16	*2,6* (**11**)	**15f**	DCM	12	0.33	4.0	0.50	15.5	19.4	1.25
17	*2,6* (**11**)	**15g**	DCM	24	0.33	4.0	0.50	31.4	38.4	1.22
18	*2,6* (**11**)	**15h**	DCM	48	0.33	4.0	0.50	25.0	30.1	1.20
19	*2,6* (**11**)	**15i**	DCM	24	0.5	4.0	0.50	42.0	57.0	1.36
20	*2,6* (**11**)	**15j**	DCM	24	0.5	2.0	0.50	17.0[c]	18.0[c]	1.06[c]
21	*3,6* (**12**)	**16a**	Bulk	24	0.50	4.0	-	28.4	38.0	1.34
22	*3,6* (**12**)	**16b**	DCM	24	0.33	4.0	0.50	15.0	21.0	1.40
23	*3,6* (**12**)	**16c**	DCM	24	0.33	4.0	0.50	34.2	41.6	1.21
24	*3,6* (**12**)	**16d**	DCM	72	0.33	4.0	0.50	21.2	25.3	1.19

[a]Molar concentration of monomer after addition of triphosgene solution. [b]Estimated by GPC (DMF, 0.05 M LiBr) calibrated with polystyrene standards. [c]Lower retention time segment of bimodal GPC trace.

molecular weights (334.0 kDa and 93.0 kDa). To confirm the need for stoichiometric balance, monomer **11** was copolymerized with 0.5 equivalents of triphosgene, leading to lower molecular weight polymers (Table 2.4, entries 19 and 20). Even though high molecular weights were already achieved, previous polymerization attempts needed longer durations to achieve high molecular weights, questioning the necessity to quench the reaction after 24 hours. The results of the experiments quenched after 1, 12, 24, and 48 h (Table 2.4, entries 15-18) showed that a 24 h duration was the optimal duration for polymerization of the *2,6* diol, **11**. Similar observations were made when the optimized experimental conditions for the polymerization of **11** were applied to the *3,6* monomer **12**. High molecular weights were observed after 24 h (34.2 kDa) whereas lower weight polymer was produced after 72 h (Table 2.4, entries 14 and 15).

The optimized experimental conditions for the polymerizations of **11** and **12**, were applied to the anomeric monomers **4** and **8**. These conditions led to polymers with M_n of 11.2 kDa, however in low yields (Table 2.4, entry 11). Increasing the monomer concentration to 1 M, closer to the concentration of earlier tests (400 mg/mL), led to an increase in in polymer yield, while changing the solvent to dioxane led to smaller M_n polymers (Table 2.4, entries 4 and 5). Applying these conditions to the 1,4 monomer, **4**, failed to produce any precipitate after 24 hours. The copolymerizations of the diol monomers **11** and **12**, with triphosgene to give polycarbonates **15** and **16**, were clearly demonstrated by ^{1}H NMR spectroscopy by observation of the downfield shifts for most of the protons from the glucose ring and, in particular, the significant downfield shift (1.0 to 1.2 ppm) of the protons on the carbons involved in the formation of the carbonate

linkages; H2 and H6 for **15**, H3 and H6 for **16**. The carbonate linkages were directly observed by the introduction of ^{13}C resonances *ca*. 155 ppm, with three sets of observed signals, arising to regiorandom ordering. Additionally, the presence of the carbonate was confirmed by the absorbance band at 1751 cm^{-1} in the IR spectra.

2.5.5 Differential Scanning Calorimetry

Thermal characterization by differential scanning calorimetry (DSC) showed a single glass transition for each polymer, dependent on the regiochemistry and M_w of each polymer system. All polymers exhibited amorphous properties with relatively high glass transition temperatures. The T_gs (Table 2.5) were considerably higher than typically observed for aliphatic polycarbonates such as poly(ethylene carbonate) (T_g = 5-20 °C) and poly(1,3-trimethylene carbonate) (T_g = -15 °C). In comparison, the more common polycarbonates based on aromatic bisphenol A monomer have T_gs *ca*. 150 °C and aromatic polycarbonate biomaterials based on tyrosine have T_gs between 50 °C and 90 °C, depending upon the particular structure. Presumably the ring structure of the monomers imparts a degree on chain rigidity and the benzyl side groups increase chain entanglement, leading to high T_g for aliphatic polycarbonates. In addition, the T_g appeared to be both dependent on molecular weight and regiochemistry of the polymer. The polymers that exhibited the highest glass transitions were those synthesized from *2,6* monomers (**11**) and *3,6* monomers (**12**), 83 and 85 °C, respectively. Despite having similar polymer connectivity (1,3 in respect to the six-membered ring), the *1,6* polymer

Table 2.5. Properties of protected poly(glucose carbonate)s.

Entry	Polymer	M_n (kDa)[a]	PDI[a]	T_g (°C)[b]	T_d^5 (°C)[c]	T_d^{50} (°C)[d]
1	**13a**	9.0[e]	-	44	137	315
2	**13b**	6.2	1.1	-	179	315
3	**13j**	5.0	1.13	33	171	317
4	**14d**	10.6	1.50	63	230	310
5	**14i**	4.4	1.09	33	163	331
6	**15d**	19.2	1.67	85	363	382
7	**15k**	10.0	1.16	70	325	359
8	**16b**	15.0	1.40	83	336	361
9	**16e**	9.8	1.10	71	321	353

[a]Estimated by GPC (DMF, 0.05 M LiBr) calibrated with polystyrene standards. [b]Glass transition temperature determined by DSC. [c]Temperature degradation onset (5% mass loss) observed by TGA. [d]Temperature at 50% mass loss observed by TGA. [e]M_p value from GPC

(**14d**) exhibited a T_g almost 10 °C lower than that of the *2,6* and *3,6* polymers (**15k** and **16e**) with similar M_n. This could be in part to the differences in monomer compositions. The *3,6* monomer was a single isomer, whereas the *1,6* monomer was a mixture of diastereomers (*ca*. 1:1 α/β), which could hinder the chain-chain packing in the final polymer. In addition, a transition was observed at 44 °C for the *1,4* polymer. The difference could also be attributed to the fact that *1,4* polymer was a mixture of α and β connectivities and was lower in molecular weight.

2.5.6 Thermogravimetric Analysis

Polymers with different regiochemistries exhibited significantly different properties in terms of thermal stability. Based on TGA data, the polymers can be separated into two classes, those that incorporate the anomeric carbon in the carbonate linkage (**13** and **14**) and those that do not (**15** and **16**). The non-anomeric *2,6* polymer, **15d**, exhibited thermal properties in agreement with other highly rigid polymers, by possessing high thermal stability and a sharp decomposition profile, with a T_d^{onset} at 363 °C and T_d^{50} at 382 °C. Other polymers in the same class (**15k**, **16b**, and **16e**) also demonstrated high thermal stabilities, with T_gs > 320 °C.

On the other hand, the polymers with the carbonate linkage running through the anomeric center of the glucose ring, which contained carbonates of acetals, were much thermally sensitive, having lower onset decompositions. Two versions of the *1,4* polymer, **13a** and **13b**, were formed under different polymerization and workup conditions. Polymer **13a** underwent an aqueous workup, which would have removed any residual chloroformate groups, leaving hydroxyl chain ends, whereas the reaction mixture containing polymer **13b**, as well as polymers **14**, **15** and **16**, was directly precipitated into methanol, which would have reacted with any residual chloroformate groups to form methylcarbonate chain ends. The different chain ends seemed to have an effect on the thermal stability of the polymers, as seen in Table 2.5 and Figure 2.4. Thermal degradation of polymer **13a** proceeded at lower temperatures (137-315 °C for initial to complete mass loss, Figure 2.4) than that of polymer **13b** (179-315 °C for

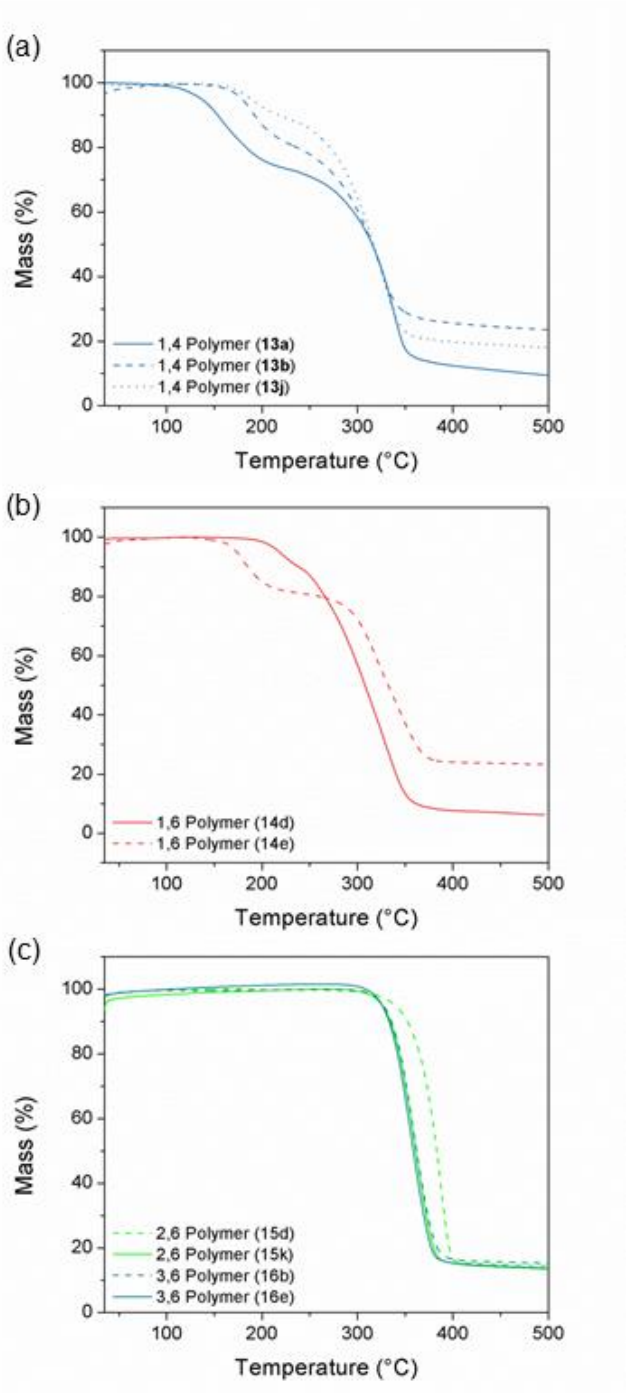

Figure 2.4. Thermogravimetric analysis of (a) *1,4*- PDGCs (**13a**, **13b**, **13j**), (b) *1,6*- PDGCs (**14d**, **14e**), (c) *2,6*- PDGCs (**15d**, **15k**), and *3,6*- PDGCs (**16b**, **16e**).

initial to complete mass loss, Figure 2.4) which could be attributed to the difference in chain ends. The *1,6* polymers, **14d** and **14e**, also exhibited low onset decomposition temperature with 5% mass loss an onset decomposition temperature at 230°C.

Initially, it was proposed that the endocyclic oxygen in the glucose ring was playing a role in the thermal degradation, similar to previously reported carbonate sugars,[134,135] accelerating the decomposition of the backbone. To test this hypothesis, the degradation products were analyzed by mass spectrometry. Tandem TGA-MS detected a release of ions with *m*/*z* of 44, which could be attributed to the loss of CO_2^+, during the initial degradation period, *ca*. 150–220 °C, which can be seen in Figure 2.5. While this finding supports our initial degradation mechanism, the mass loss that occurred during the first phase of degradation is too great to be attributed to the loss of only CO_2. In addition, peaks were also observed early in the decomposition of the polymer at increments of *m/z* 77, 91 and 92, as well as 105 and 106, which correspond to phenyl, toluyl, and benzoyl radicals, respectively (Figure 2.5). To account for these additional fragments, a more complicated mechanism must be occurring (Scheme 2.7). The *3,6* polymer was also analyzed by tandem TGA-MS. As hypothesized, no fragments were observed at lower temperatures (Figure 2.6). The difference in T_ds of the various regioisomers are an interesting finding, and adds to the tunability of this new class of polycarbonates, making these polymers attractive for a wide ranging of applications that require various thermal stabilities.

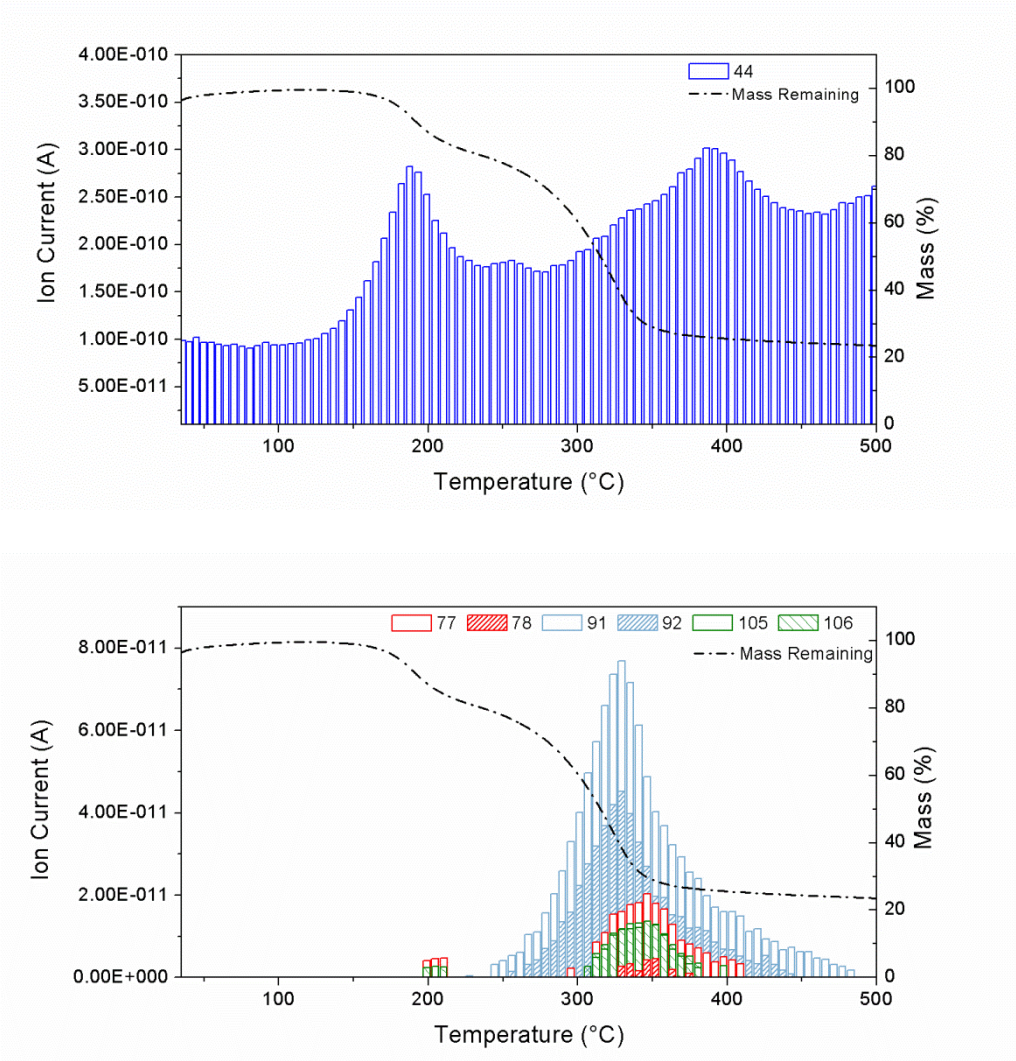

Figure 2.5. TGA-MS data of polymer **13**. During the initial stage of thermal decomposition (*ca*. 150 to 200 °C) fragments with the m/z of 44 were observed, corresponding to the release of CO_2. Additional fragments with m/z of 77/78, 91/92 and 105/106, corresponding to phenyl, toluyl, and benzoyl radicals, was also observed at low temperatures (*ca.* 200 °C).

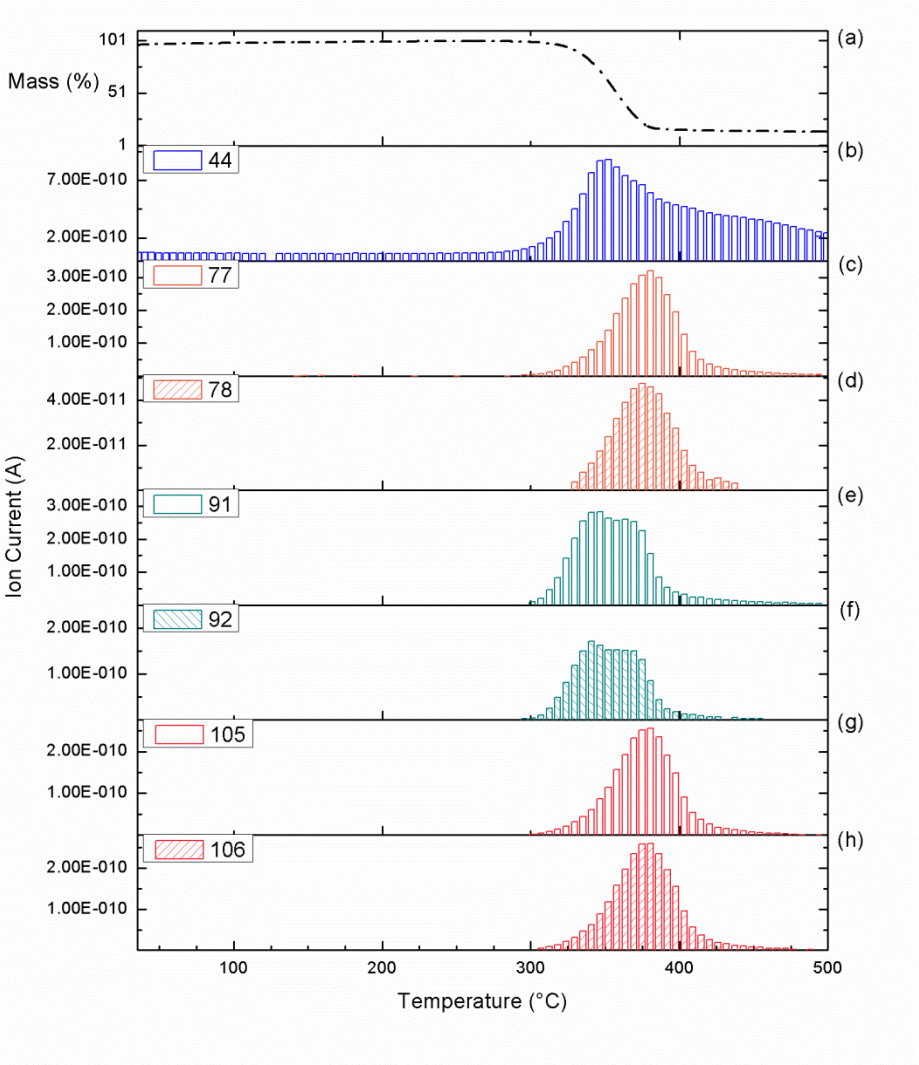

Figure 2.6. Thermal decomposition of polymer **15** as seen by TGA (a) and TGA-MS (b-h) data with respect to temperature for select ions. Unlike the *1,4* polymer, **13**, fragments from the loss of carbon dioxide and benzyl protecting groups were not observed during the thermolysis of **15** until higher temperatures were reached (*ca*. 300 °C).

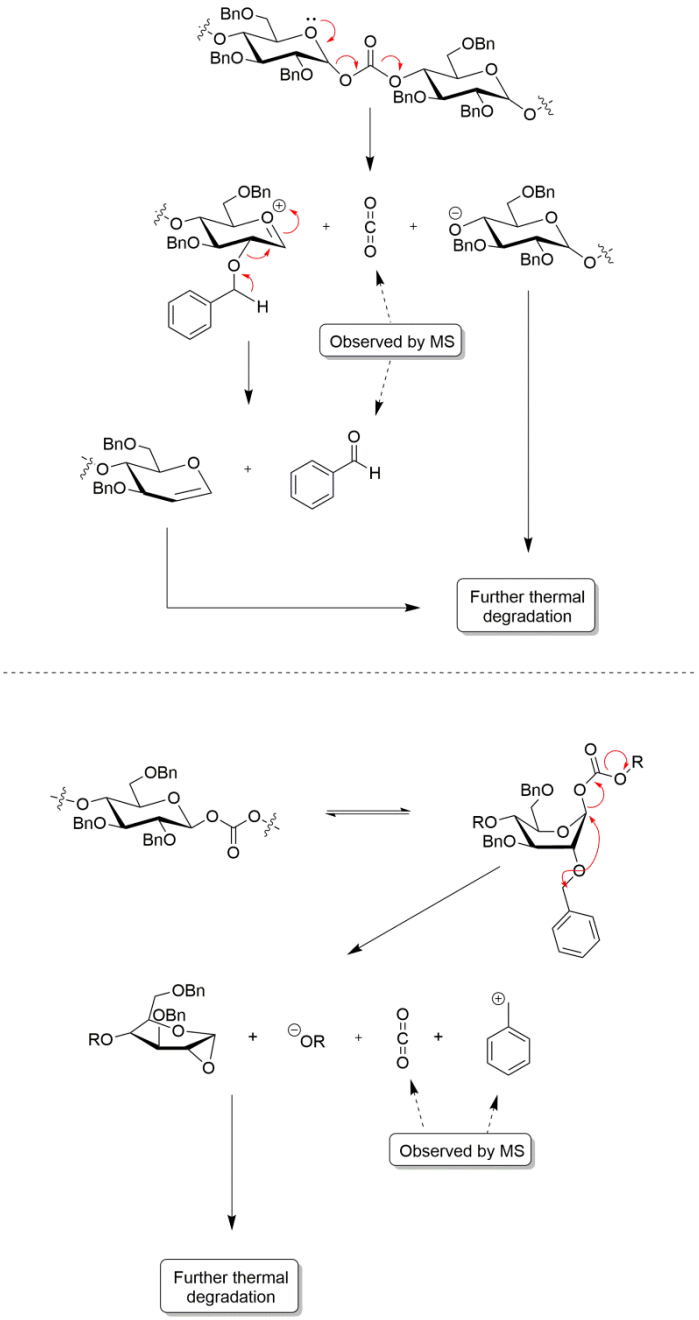

Figure 2.7. Proposed mechanisms for initial thermal degradation of *1,4*-benzyl protected poly(glucose-carbonate)s resulting in the liberation of carbon dioxide as well as benzoyl, toluyl, and phenyl fragments.

2.6 Conclusions

The synthesis of four different polycarbonates from a readily-available glucose starting material and their differences in physical properties are reported. Monomers exhibited different reactivities depending on its regiochemistry and functionality; monomers with hemiacetal functionalities afforded polycarbonates with lower molecular weights when exposed to phosgene, diphosgene, and triphosgene as compared to monomers bearing primary and secondary alcohols. The *1,4*- and *1,6*-monomers with anomeric centers proved difficult to polymerize, reaching M_ns near 10 kDa, whereas the *2,6*- and *3,6*-monomers, those with primary and secondary alcohols, were able to form polymers with molecular weights above 35 kDa, reaching over 300 kDa in certain instances. Different regiochemistry in the polymer backbone also had an effect on the resulting physical properties of each resulting polymer. The two polymers, **15** and **16**, not incorporating the anomeric position into the polymer backbone, behaved like rigid polymers, exhibiting high thermal stability and a sharp decomposition profile, with onset decomposition temperature, $T_{d,onset,}$ at 363 and 336 °C, respectively. Meanwhile, as predicted, polymers with the carbonate linkage connected through the anomeric center showed much lower thermal stabilities. For example, **13** had two different $T_{d,onset}$ values, with the first onset, $T_{d1,onset}$ appearing at 171 °C and the second, $T_{d2,onset}$ at 267 °C. Similarly, **14** had $T_{d1,onset}$ at 163 °C and $T_{d2,onset}$.at 294 °C. Initially it was hypothesized that the acetal carbonate linkage at the anomeric position plays a role in the thermal degradation and thus accelerates decomposition, however, further investigation of the

thermally sensitive of the *1*,*4*-polymer, **13**, by TGA-MS showed loss of CO^+, CO_2^+, phenyl, toluyl, and benzoyl ions, evidence that the carbonate linkage interacts with the primary benzyl protecting group during thermal degradation. These synthetic methodology developments are important steps towards the use of glucose as an effective and innovative feedstock for polycarbonate-based materials. Furthermore these findings show that a wide range of polycarbonates, with varying molecular weights, glass transitions, and thermal properties can be formed from these glucose monomers, making this monomer system attractive for a wide range of potential applications. In addition, simple modifications to the monomer protection chemistry that may influence the polymer properties could be established to further increase the tunability of these glucose-based polycarbonates. Further studies on the mechanical characterization of deprotected polymers are currently being investigated. This study represents the first step in the development of viable glucose-based biomedical materials.

CHAPTER III

SYNTHESIS OF REGIOREGULAR POLYCARBONATES DERIVED FROM AA'A'A GLUCOSE DIOL MONOMERS

3.1 Overview

Strategies for the preparation of high molecular weight, bio-sourced polycarbonates were developed using protected polyhydroxyl monomer repeat units, derived from glucose. The design and synthesis of regioselectively methyl- (Me) and benzyl- (Bn) protected *2,2'*-glucopyranosyl-glucopyranoside and *3,3'*-glucopyranosyl-glucopyranoside monomers was followed by the copolymerization with phosgene, generated *in situ* from trichloromethyl chloroformate, to yield protected poly(*6,2-2',6'*-glucose carbonate) and poly(*6,3-3',6'*-glucose carbonate). The molecular weights (M_w) reached over 100 kDa, corresponding to degrees of polymerization of *ca*. 50, with polydispersities ranging from 1.5 to 1.9, as measured by gel permeation chromatography (GPC) using tetrahydrofuran as the eluent and with polystyrene calibration standards. Due to the regioregularity and high molecular weights of the polymers, each regioisomeric poly(glucose carbonate) exhibited relatively high glass-transition temperatures for aliphatic polycarbonates, 92 °C for poly(*6,2-2',6'*-glucose carbonate) and 101 °C for poly(*6,3-3',6'*-glucose carbonate). The polymers also exhibited relatively high thermal stability, with onset decomposition temperatures (T_d^5) near 300 °C, as revealed by thermogravimetric analysis (TGA).

3.2 Introduction

Polymers derived from natural resources have gained interest not only to form commodity plastics and high performing engineering polymers, which decrease the dependence on petroleum based products, but also to form materials with biocompatible degradation products. Degradable polymers have been used in various biomedical applications, where issues of biocompatibility and biodegradability are paramount. For this purpose, the polymers used are typically polyesters, capable of hydrolytically degrading to afford products that contain carboxylic acid and alcohol functional groups, which in turn can be metabolized or expelled from the body. However, the inherent nature of the polyester backbone can pose significant issues in the application of these materials. The process in which hydrolytic degradation occurs and nature of degradation products creates acidic microenvironments that can lead to local aseptic inflammation.[30,136,137] In addition, polyesters have been used in drug-delivery systems for delivering pH sensitive materials with limited success.[138-140]

Recently the Wooley lab has have expanded the field of polycarbonates by using natural products such as ferulic acid,[141] quinic acid,[142] and glucose[104,105] to develop compatible biodegradable materials. In Chapter II, we explored the synthesis of polycarbonates from four different monomers, exhibiting different regiochemistries. The different regiochemistries had a significant effect on the monomer reactivity and the resulting polymer physical properties. Despite the polymerization technique used, certain monomers did not readily form high molecular weight (>10kDa) polymers in

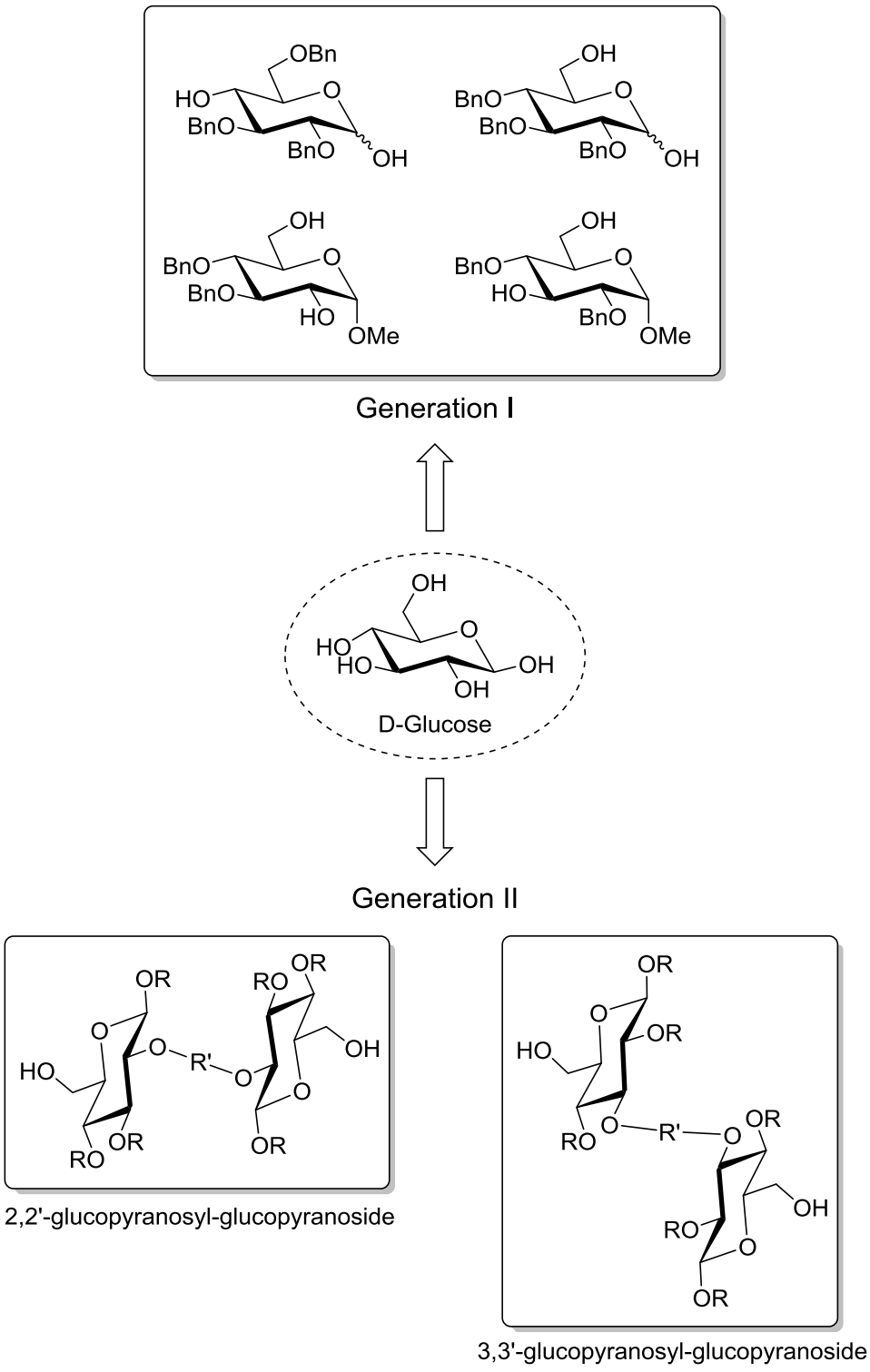

Figure 3.1. Development of second generation glucose diol monomers, symmetrical AA'A'A dimers.

high yields, while other monomers, possessing primary alcohols, formed much higher molecular weight polymers in higher yields. By adjusting the design of the monomer, changing reactive chain ends from secondary to primary alcohols, it could be possible to form high molecular weights polymers in high yields, regardless of the polymerization conditions. A monomer with two primary alcohols can be achieved, without changing the chemical composition of the polymer, by initially forming a carbonate-linked dimer. The addition of a single synthetic step can also add increased flexibility and tunability to the resulting polymers as a variety of linkages could be utilized, allowing for the incorporation of additional functionalities and greater control over chemical and physical properties. This chapter reports the design, synthesis, and characterization of polycarbonates from 2,2'- and 3,3'-glucose dimers, and comparisons to previously synthesized regiorandom glucose polycarbonates with similar functionalities and regiochemistries.

3.3 Experimental

3.3.1 Materials

Unless otherwise noted, all reagents were used as received. Dichloromethane (DCM) was purified by passage through a solvent purification system (J.C. Meyer Solvent Systems) and used as a dried solvent. Anhydrous pyridine was used as received from Sigma Aldrich. Monomers **4**, **11**, **12**, **18**, and **20** were dried under reduced pressure, over P_2O_5 and stored under Ar environment. Column chromatography was performed on a combiflash Rf4x (Teledyne ISCO) with RediSep Rf Columns (Teledyne ISCO).

3.3.2 Characterization

The ^{1}H NMR (500 MHz) and ^{13}C NMR (125 MHz) spectra were obtained on an Inova 500 MHz spectrometer using the solvent as an internal reference. IR spectra were recorded on an IR Prestige 21 system (Shimadzu Corp., Japan), equipped with an ATR accessory, and analyzed using IRsolution v. 1.40 software. High resolution mass spectrometry analyses were conducted on an Applied Biosystems PE SCIEX QSTAR instrument by Texas A&M University Laboratory for Biological Mass Spectrometry. Glass transition (T_g) temperatures were measured by differential scanning calorimetry on a Mettler Toledo DSC822e apparatus (Mettler Toledo, Columbus, OH) with a heating

rate of 10 °C/min. The measurements were analyzed using Mettler-Toledo Star[e] v. 10.00 software, and the T_g was taken as the midpoint of the inflection tangent, upon the third heating scan. Thermogravimetric analysis (TGA) was performed under an Ar atmosphere using a Mettler Toledo model TGA/SDTA851[e] apparatus with a heating rate of 10 °C/min.

Gel permeation chromatography (GPC) was conducted two Waters systems using THF and DMF eluents. The THF system was composed of a Waters 1515 HPLC (Waters Chromatography, Inc.) equipped with a Waters 2414 differential refractometer, a PD2026 dual-angle (15 and 90º) light scattering detector (Precision Detectors, Inc.), and a three column series PLgel 5 μm Mixed C, 500 Å, and 10^4 Å, 300 × 7.5 mm columns (Polymer Laboratories, Inc.). The system was equilibrated at 35 ºC in anhydrous THF, which served as the polymer solvent and eluent with a flow rate of 1.0 mL/min. Polymer solutions were prepared at a known concentration (*ca.* 3 mg/mL) and an injection volume of 200 μL was used. Data collection and analysis were performed, respectively, with Precision Acquire software and Discovery 32 software (Precision Detectors, Inc.). Interdetector delay volume and the light scattering detector calibration constant were determined by calibration using a nearly monodispersed polystyrene standard (Pressure Chemical Co., M_p = 90 kDa, M_w/M_n < 1.04). The differential refractometer was calibrated with standard polystyrene reference material (SRM 706 NIST), of known specific refractive index increment d*n*/d*c* (0.184 mL/g). The d*n*/d*c* values of the analyzed polymers were then determined from the differential refractometer response.

The DMF GPC was equipped with an model 1515 isocratic pump, a model 2414 differential refractometer, and a three-column set of Polymer Laboratories (Amherst, MA) Styragel columns (PL_{gel} 5 μm Mixed C, 500 Å, and 104 Å, 300 x 7.5 mm columns) for the THF system equilibrated at 35 °C, or a four-column set of 5 μm Guard (50 × 7.5 mm), Styragel HR 4 5 μm DMF (300 × 7.5 mm), Styragel HR 4E 5 μm DMF (300 × 7.5 mm), and Styragel HR 2 5 μm DMF (300 × 7.5 mm) equilibrated at 70 °C. Polymer solutions were prepared at a known concentration (*ca.* 3 mg/mL), and an injection volume of 200 μL was used. Data collection and analyses were performed with Precision Acquire software. The differential refractometer was calibrated with standard polystyrene materials (SRM 706 NIST) of known specific refractive index increment d*n*/d*c* (0.184 mL/g). The d*n*/d*c* values of the analyzed polymers were then determined from the differential refractometer response.

3.3.3 Synthesis

Methyl 2-*O*-benzyl-4,6-*O*-benzylidene-α-D-glucopyranoside (9) and **methyl 3-*O*-benzyl-4,6-*O*-benzylidene-α-D-glucopyranoside (10)** Methyl-4,6-*O*-benzylidene glucopyranoside, (10.2 g, 36.1 mmol), benzyl bromide (10.5 g, 61.4 mmol), and tetrabutylammonium hydrogensulfate (2.53 g, 7.44 mmol) were dissolved in 600 mL of DCM. To this solution, 50 mL of 5% NaOH (aq.) solution was added and the mixture was heated to reflux and left for 26 hours. The mixture was separated and the aqueous layer was extracted with 50 mL of DCM. The organic layers were combined, dried with

$MgSO_4$, filtered and concentrated under reduced pressure. The resulting residue was purified by column chromatography (SiO_2, gradient hexane/ethyl acetate) to afford methyl 3-*O*-benzyl-4,6-*O*-benzylidene-α-D-glucopyranoside **9** (5.42 g, 40%) and methyl 2-*O*-benzyl-4,6-*O*-benzylidene-α-D-glucopyranoside **10** (7.61 g, 57%) as white solids.

*Methyl 3-O-benzyl-4,6-O-benzylidene-α-D-glucopyranoside (**9**).* ^{1}H NMR (500 MHz, $CDCl_3$) δ 7.50-7.25 (m, 10H, Ar), 5.57 (s, 1H, -OC*H*Ar), 4.98-4.95 (d, J = 11.8 Hz, 1H, -OCH_2Ar), 4.82 (d, $J_{1\text{-}2}$ = 3.3 Hz, 1H, H1), 4.80-4.78 (d, J = 11.8 Hz, 1H, -OCH_2Ar), 4.31-4.28 (dd, $J_{6eq\text{-}5}$ = 9.9 Hz, $J_{6eq\text{-}6ax}$ = 4.6 Hz,1H, H6$_{eq}$), 3.85-3.81 (td, $J_{5\text{-}4}$ = $J_{5\text{-}6ax}$ = 9.9 Hz, $J_{5\text{-}6eq}$ = 4.5 Hz, 1H, H5), 3.85-3.81 (t, $J_{3\text{-}2}$ = $J_{3\text{-}4}$ = 9.9 Hz, 1H, H3), 3.78-3.74 (t, $J_{6ax\text{-}5}$ = $J_{6ax\text{-}6eq}$ = 9.9 Hz, 1H, H6$_{eq}$), 3.75-3.71 (ddd, $J_{2\text{-}3}$ = 9.9 Hz, $J_{2\text{-}OH}$ = 6.9 Hz, $J_{2\text{-}1}$ = 3.3 Hz, 1H, H2), 3.67-3.63 (t, $J_{4\text{-}3}$ = $J_{4\text{-}5}$ = 9.9 Hz, 1H, H4), 3.45 (s, 3H, -OCH_3), 2.31-2.30 (d, $J_{OH\text{-}2}$ = 6.9 Hz, 1H, H$_{OH\text{-}2}$) ppm; ^{13}C NMR (125 MHz, $CDCl_3$): δ 138.4, 137.3 (Ar$_{ipso}$), 129.0, 128.4, 128.2, 128.0, 127.7, 126.0 (Ar), 101.3 (-O*C*HAr), 99.9 (C1), 81.9 (C4), 78.4 (C3), 74.8 (-O*C*H$_2$Ar), 72.4 (C2), 69.0 (C6), 62.6 (C5), 55.4 (-O*C*H$_3$) ppm; FTIR (ATR) υ_{max} (neat, cm $^{-1}$): 3302 (broad), 3032, 2924, 2870, 1450, 1365, 1280, 1064, 987; HRMS (+ESI) m/z calc'd for $C_{21}H_{24}O_6$ $[M+H]^+$: 372.16; observed 373.1614.

*Methyl 2-O-benzyl-4,6-O-benzylidene-α-D-glucopyranoside (**10**).* ^{1}H NMR (500 MHz, $CDCl_3$) δ 7.50-7.30 (m, 10H), 5.52 (s, 1H, -OC*H*Ar), 4.80-4.78 (d, J = 11.9 Hz, 1H, -OCH_2Ar), 4.72-4.70 (d, J = 11.9 Hz, 1H, -OCH_2Ar), 4.62-4.61 (d, $J_{1\text{-}2}$ = 3.8 Hz, 1H, H1), 4.28-4.25 (dd, $J_{6eq\text{-}6ax}$ = 9.5 Hz, $J_{6eq\text{-}5}$ = 4.6 Hz, 1H, H6$_{eq}$), 4.18-4.13 (td, $J_{3\text{-}2}$ = $J_{3\text{-}4}$ = 9.5 Hz, $J_{3\text{-}OH}$ = 2.1 Hz, 1H, H3), 3.84-3.79 (td, $J_{5\text{-}4}$ = $J_{5\text{-}6ax}$ = 9.5 Hz, $J_{5\text{-}6eq}$ = 4.7 Hz, 1H, H5), 3.73-3.68 (t, $J_{6ax\text{-}5}$ = $J_{6ax\text{-}6eq}$ = 9.5 Hz, 1H, H6$_{ax}$), 3.52-3.48 (t, $J_{4\text{-}3}$ = $J_{4\text{-}5}$ =

9.5 Hz, 1H, H4), 3.48-3.46 (dd, $J_{2\text{-}3}$ = 9.5 Hz, $J_{2\text{-}1}$ = 3.8 Hz, 1H, H2), 3.38 (s, 3H, -OCH_3), 2.53-2.52 (d, $J_{OH\text{-}3}$ = 2.1 Hz, 1H, $H_{OH\text{-}3}$) ppm; ^{13}C NMR (125 MHz, $CDCl_3$): δ 137.9, 137.1 (Ar_{ipso}), 129.2, 128.6, 128.3, 128.1, 126.3 (Ar), 102.0 (-O*C*HAr), 98.6 (C1), 81.2 (C4), 79.5 (C2), 73.4 (-O*C*H_2Ar), 70.3 (C3), 70.0 (C6), 62.0 (C5), 55.4 (-O*C*H_3) ppm; FTIR (ATR) υ_{max} (neat, cm^{-1}): 3456 (broad), 2924, 2846, 1458, 1357, 1334, 1080, 1026, 972, 918, 856; HRMS (+ESI) m/z calc'd for $C_{21}H_{24}O_6$ $[M+Li]^+$: 379.17; found 379.1675.

Synthesis of 6,2-2',6'-Glucose Monomer

Methyl-2-*O*-[(1-*O*-methyl-3-*O*-benzyl-4,6-*O*-benzylidene-α-D-glucopyanoside)carbonyloxy]-3-*O*-benzyl-4,6-*O*-benzylidene-α-D-glucopyranoside (17). To a 25 mL flame dried schlenk flask, **9** (5.6189 g, 15.128 mmol) was added under N_2 and dissolved in dry toluene (12 mL) and anhydrous pyridine (2 mL). The reaction mixture was cooled to 0 °C, and triphosgene (0.7600 g, 0.169 mmol) in 6 mL of toluene was added dropwise over an hour. The reaction was allowed to warm to room temperature and stir for an additional six hours. The reaction mixture was diluted with 50 mL of DCM and washed with 50 mL sat. $NaHCO_3$ solution, 50 mL 0.5 HCl (2x), and 50 mL of brine. Organic layer was dried with $MgSO_4$, filtered and concentrated in *vacuo* to afford a white foam. The crude sample was purified by column chromatography (3:1 Hex/EtOAc) yielding 7.4631 g of **17** as a white solid (64%).

*Methyl-2-O-[(1-O-methyl-3-O-benzyl-4,6-O-benzylidene-α-D-glucopyanoside)carbonyloxy]-3-O-benzyl-4,6-O-benzylidene-α-D-glucopyranoside (**17**).*

^{1}H NMR (500 MHz, $CDCl_3$) δ 7.50-7.24 (m, 20H, Ar), 5.59 (s, 2H, -OC*H*Ar), 4.92-4.90 (d, J = 11.8 Hz, 2H, -OCH_2Ar), 4.88-4.87 (d, $J_{1\text{-}2}$ = 3.7 Hz, 2H, H1), 4.84-4.82 (dd, $J_{2\text{-}3}$ = 9.6 Hz, $J_{2\text{-}1}$ = 3.7 Hz, 2H, 2H), 4.79-4.76 (d, J = 11.8 Hz, 2H, -OCH_2Ar), 4.32-4.29 (dd, $J_{6eq\text{-}6ax}$ = 9.6 Hz, $J_{6eq\text{-}5}$ = 4.7 Hz, 2H, H6$_{eq}$), 4.10 (t, $J_{3\text{-}2}$ = $J_{3\text{-}4}$ = 9.6 Hz, 2H, H3), 3.90-3.85 (dt, $J_{5\text{-}4}$ = $J_{5\text{-}6ax}$ = 9.5 Hz, $J_{5\text{-}6eq}$ = 4.7 Hz, 2H, H5), 3.79 (t, $J_{6ax\text{-}5}$ = $J_{6ax\text{-}6ax}$ = 9.6 Hz, 2H, H6$_{eq}$), 3.72 (t, $J_{4\text{-}3}$ = $J_{4\text{-}5}$ = 9.6 Hz, 2H, H4), 3.28 (s, 6H, -OCH_3) ppm; ^{13}C NMR(125 MHz, $CDCl_3$): δ 154.4 (C=O), 138.4, 137.2 (Ar$_{ipso}$), 129.0, 128.2, 127.6, 127.5, 126.0 (Ar), 101.3 (-O*C*HAr), 97.7 (C1), 82.0 (C3), 76.5 (C2), 76.0 (C4), 74.7 (-O*C*H$_2$Ar), 68.9 (C5), 62.3 (C6), 55.3 (-O*C*H$_3$) ppm,; FTIR (ATR) (neat, cm^{-1}) 3034, 2928, 2908, 2839, 1774 (C=O), 1745 (C=O), 1452, 1371, 1307, 1240, 1055, 1043, 974. 748, 696; HRMS (+ESI) m/z calc'd for $C_{43}H_{46}O_{13}$ $[M+Li]^+$: 777.31, found 777.3071.

Methyl-2-*O*-[(1-*O*-methyl-3,4-*O*-benzyl-α-D-glucopyanoside)carbonyloxy]-3,4-*O*-benzyl-α-D-glucopyranoside (18). To a solution of **7** (0.8580 g, 1.113 mmol) in dry DCM (20 mL), a 1 M solution of BH_3THF (11 mL, 11 mmol) was added, followed by the dropwise addition of TMSOTf (0.1 mL, 0.5 mmol). The solution was stirred under N_2 at room temperature for 3 hours. The reaction was quenched by the addition of Et_3N (1 mL), followed by the careful addition of MeOH (>0.5 mL) until the evolution of H_2 ceased. The mixture was concentrated and the residue was coevaporated with MeOH (3x50 mL). Purification by column chromatography (7:3 Hex/EtOAc) afforded **18** (0.7676 g) as white solid in an 89% yield.

*Methyl-2-O-[(1-O-methyl-3,4-O-benzyl-α-D-glucopyanoside)carbonyloxy]-3,4-O-benzyl-α-D-glucopyranoside (**18**).* ^{1}H NMR (500 MHz, $CDCl_3$) δ 7.35-7.25 (m, 20H

Ar), 4.86-4.84 (d, J = 11.1 Hz, 4H, -OCH_2Ar), 4.81-4.79 (d, J = 11.1 Hz, 2H, -OCH_2Ar), 4.80-4.79 (d, $J_{1\text{-}2}$ = 3.6 Hz, 2H, H1), 4.76-4.73 (dd, $J_{2\text{-}3}$ = 9.9 Hz, $J_{2\text{-}1}$ = 3.6 Hz, 2H, H2), 4.66-4.63 (d, J = 11.1 Hz, 2H, -OCH_2Ar),4.08-4.05 (dd, $J_{3\text{-}2}$ = 9.9 Hz, $J_{3\text{-}4}$ = 8.7 Hz, 2H, H3), 3.83-3.79 (ddd, $J_{6\text{-}6'}$ = 11.8 Hz, $J_{6\text{-}OH}$ = 5.3 Hz, $J_{6\text{-}5}$ = 2.6 Hz, 2H, H6) 3.75-3.70 (ddd, $J_{6'\text{-}6}$ = 11.8 Hz, $J_{6'\text{-}OH}$ = 7.6 Hz, $J_{6'\text{-}5}$ = 3.8 Hz, 2H, H6'), 3.69-3.66 (ddd, $J_{5\text{-}4}$ = 9.8 Hz, $J_{5\text{-}6'}$ = 3.8 Hz, $J_{5\text{-}6}$ = 2.6 Hz, 2H, H5) 3.64-3.60 (dd, $J_{4\text{-}5}$ = 9.8 Hz, $J_{4\text{-}3}$ = 8.7 Hz, 2H, H4), 3.20 (s, 6H, -OCH_3), 1.69-1.66 (dd, $J_{OH\text{-}6'}$= 7.6 Hz, $J_{OH\text{-}6}$ = 8.7 Hz, 2H, OH) ppm; ^{13}C NMR(125 MHz, $CDCl_3$): δ 154.5 (C=O), 138.5, 138.0 (Ar$_{ipso}$), 128.6, 128.5, 128.2, 128.1, 127.8, 127.7 (Ar), 97.1 (C1), 79.9 (C3), 77.4 (C2), 77.3 (C4), 75.5 (-OCH_2Ar), 75.2 (-OCH_2Ar), 71.0 (C5), 61.8 (C6), 55.2 (-OCH_3) ppm; FTIR (ATR) (neat, cm^{-1}) 3516 (br), 2991 2937 2872, 1753 (C=O), 1496, 1454 1361, 1310, 1246, 1120, 1089, 1043, 1026, 1018, 898, 738, 696; HRMS (+ESI) m/z calc'd for $C_{43}H_{50}O_{13}$ $[M+Li]^+$: 781.34, found 781.3411.

Synthesis of 6,3-3',6'-Glucose Monomer

Methyl-3-*O*-[(1-*O*-methyl-2-*O*-benzyl-4,6-*O*-benzylidene-α-D-glucopyanoside)carbonyloxy]-2-*O*-benzyl-4,6-*O*-benzylidene-α-D-glucopyranoside (19). To a 25 mL flame dried schlenk flask, **10** (3.3454 g, 8.9831 mmol) was added under N_2 and dissolved in dry toluene (5.5 mL) and anhydrous pyridine (0.8 mL). The solution was cooled to 0 °C, and triphosgene (0.4412 g, 0.1655 mmol) dissolved in toluene (2.5 mL) was added dropwise over an hour. The reaction was allowed to warm to room temperature and stir for an additional four hours. The reaction mixture was

diluted with 50 mL of DCM and washed with 50 mL sat. $NaHCO_3$ solution, 50 mL 0.5 HCl (2x), and 50 mL brine. Organic layer was dried with $MgSO_4$, filtered and concentrated in *vacuo* to afford a white foam. Crude was recrystallized in hexanes/Et_2O to give the desired di-3-glucopyranoside carbonate as colorless crystals in 70% yield.

Methyl-3-O-[(1-O-methyl-2-O-benzyl-4,6-O-benzylidene-α-D-glucopyanoside)carbonyloxy]-2-O-benzyl-4,6-O-benzylidene-α-D-glucopyranoside ***(19)****.* ^{1}H NMR (500 MHz, $CDCl_3$) δ 7.33-7.11 (m, 20H Ar), 5.42 (t, $J_{3-2} = J_{3-4}$ = 9.9 Hz, 2H, H3), 5.38 (s, 2H, -OC*H*Ar), 4.48-4.28 (d, J_{1-2} = 3.7 Hz, 2H, H1), 4.44-4.42 (d, J = 12.6 Hz, 2H, -OCH_2Ar), 4.30-4.28 (d, J = 12.6 Hz, 2H, -OCH_2Ar), 4.25-4.22 (dd, $J_{6eq-6ax}$ = 9.9 Hz, J_{6eq-5} = 4.8 Hz, 2H, $H6_{eq}$), 3.90-3.85 (td, $J_{5-4} = J_{5-6ax}$ = 9.9 Hz, J_{5-6eq} = 4.8 Hz, 2H, H5), 3.67 (t, $J_{6ax-5} = J_{6ax-6eq}$ = 9.9 Hz, 2H, $H6_{ax}$), 3.60 (t, $J_{4-3} = J_{4-5}$ = 9.9 Hz, 2H, H4), 3.55-3.52 (dd, J_{2-3} = 9.9 Hz, J_{2-1} = 3.7 Hz, 2H, H2), 3.35 (s, 6H, -OCH_3) ppm; ^{13}C NMR(125 MHz, $CDCl_3$): δ 153.7 (C=O), 137.8, 136.9 (Ar_{ipso}), 129.1, 128.4, 128.3, 128.2, 128.0, 126.2 (Ar), 101.8 (-O*C*HAr), 99.2 (C1), 79.3 (C4), 76.8 (C2), 75.7 (C3), 73.1 (-O*C*H_2Ar), 69.1 (C6), 62.3 (C5), 55.6 (-O*C*H_3) ppm; FTIR (ATR) (neat, cm^{-1}) 3064, 3034, 2929, 2907, 2839, 1774, 1745, 1454, 1371, 1309, 1238, 1213, 1091, 1043, 975. 748; HRMS (+ESI) m/z calc'd for $C_{43}H_{46}O_{13}$ $[M+H]^+$: 771.30, found 770.3017.

Methyl-3-*O*-[(1-*O*-methyl-2,4-*O*-benzyl-α-D-glucopyanoside)carbonyloxy]-2,4-*O*-benzyl-α-D-glucopyranoside (20). To a solution of **19** (5.0020 g, 6.4891 mmol) in dry DCM (60 mL), a 1 M solution of BH_3THF (40 mL, 40 mmol) was added, followed by the dropwise addition of TMSOTf (0.18 mL, 0.99 mmol). The solution was stirred under N_2 at room temperature for 2.5 hours. The reaction was quenched by the

addition of Et_3N (8 mL), followed by the carful addition of MeOH (>2 mL) until the evolution of H_2 ceased. The mixture was concentrated and the residue was coevaporated with MeOH (3x200 mL). Purification by column chromatography (7:3 Hex/EtOAc) afforded **20** as white solid in 86% yield.

*Methyl-3-O-[(1-O-methyl-2,4-O-benzyl-α-D-glucopyanoside)carbonyloxy]-2,4-O-benzyl-α-D-glucopyranoside (**20**).* ^{1}H NMR (500 MHz, $CDCl_3$) δ 7.27-7.21 (m, 20H Ar), 5.50-5.47 (dd, $J_{3\text{-}2}$ = 9.9 Hz, $J_{3\text{-}4}$ = 8.3 Hz, 2H, H3), 4.73-4.71 (d, J = 11.4 Hz, 2H, -OCH_2Ar), 4.54-4.51 (d, J = 12.8 Hz, 2H, -OCH_2Ar), 4.46-4.44 (d, J = 11.4 Hz, 2H, -OCH_2Ar) 4.40-4.39 (d, $J_{1\text{-}2}$ = 3.6 Hz, 2H, H1), 4.37-4.35 (d, J = 12.8 Hz, 2H, -OCH_2Ar), 3.68-3.55 (m, 6H, H4+H5+H6), 3.60-3.55 (ddd, $J_{6'\text{-}5}$ = 8.5 Hz, $J_{6'\text{-}OH}$ = 7.8 Hz, $J_{6'\text{-}6}$ = 3.2 Hz, 2H, H6'), 3.54-3.51 (dd, $J_{2\text{-}3}$ = 9.9 Hz, $J_{2\text{-}1}$ = 3.6 Hz, 2H, H2), 3.35 (s, 6H, -OCH_3) 1.41-1.39 (dd, $J_{OH\text{-}6'}$ = 7.8 Hz, $J_{OH\text{-}6}$ = 5.1 Hz, 2H, OH) ppm; ^{13}C NMR(125 MHz, $CDCl_3$): δ 154.3 (C=O), 138.0, 137.6 (Ar_{ipso}), 128.6, 128.6, 128.5, 128.4, 128.1, 128.0 (Ar), 97.9 (C1), 79.1 (-O*C*H_2Ar), 77.4 (C3), 75.4 (C2), 74.15 (C5), 72.9 (-O*C*H_2Ar), 70.2 (C4), 61.6 (C6), 55.23(-O*C*H_3) ppm; FTIR (ATR) (neat, cm^{-1}) 3435 (br), 2950, 2917, 1774, 1745, 1437, 1332, 1309, 1238, 1213, 1091, 1043, 975. 748; HRMS (+ESI) m/z calc'd for $C_{43}H_{50}O_{13}$ $[M+Li]^+$: 781.34, found 781.3411.

General Polycondensation Protocol. The following protocol was used to synthesize 0.25 g of poly(1,4-cyclohexane)carbonate (Table 3.1, Entry 2). The same protocol was used to synthesize polymers **13n**, **15k**, **16e**, **21** and **22**. Alterations to the protocol (duration of triphosgene addition) and the effect on molecular weight are outlined in

Table 3.1. To a solution of 1,4-cyclohexane diol (0.275 g, 2.367 mmol) in pyridine (0.712 g, 9.00 mmol) and 3 mL of DCM at room temperature was added dropwise a solution of triphosgene (0.279 g, 0.940 mmol) in 0.6 mL of DCM over 1 hour. After complete addition, the mixture was allowed to stir for an additional hour, followed by the direct precipitation into methanol. The resulting white fibrous solid was collected by filtration, dissolved in DCM and precipitated into methanol two additional times. Polymer was dried under vacuum and characterized.

Poly(6,2-2',6'-glucose)carbonate (21). ^{1}H NMR (500 MHz, $CDCl_3$) δ 7.36-7.20 (m, 10H, Ar), 4.89-4.73 (m, 5H, -OCH_2Ar+H1+H2), 4.60-4.54 (d, J = 11.2 Hz, 1H, -OCH_2Ar), 4.40-4.23 (m, 2H, $H6_{RP}$), 3.86-3.77 (t, $J_{3\text{-}2} = J_{3\text{-}4}$ = 9.5 Hz, 1H, H3), 3.73-3.64 (m, 0.22H, $H6_{CE}$), 3.60-3.50 (t, $J_{4\text{-}3} = J_{4\text{-}5}$ = 9.5 Hz, 1H, H4), 3.18 (s, 6H, OCH_3) ppm; ^{13}C NMR(125 MHz, $CDCl_3$): δ 154.9 (2,2' carbonate), 154.1 (6,6' carbonate), 138.2, 137.6 (Ar_{ipso}), 128.5, 128.4, 128.1, 128.0, 127.9, 127.7, 127.5, 127.4 (Ar), 96.8 (C1), 79.9 (C3), 72.2 (C4), 76.9 (C2), 75.4 (-OCH$_2$Ar), 75.1 (-OCH$_2$Ar), 68.6 (C5), 66.5 (C6), 55.1 (-OCH$_3$) ppm; FTIR (ATR) (neat, cm^{-1}) 3031, 2910, 2839, 1753 (C=O), 1497, 1456, 1380, 1239, 1196, 1161, 1072, 1043, 1028; M_n (NMR) 12000 g/mol; M_n (GPC) 15000 g/mol; PDI = 1.53; T_g = 92 °C; TGA in Ar: $T_d^{5\%}$ = 280 °C, $T_d^{50\%}$ = 364 °C.

Poly(6,3-3',6'-glucose)carbonate (22). ^{1}H NMR (500 MHz, $CDCl_3$) δ 7.38-7.18 (m, 10H, Ar), 5.49 (t, $J_{3\text{-}2} = J_{3\text{-}4}$ = 9.4 Hz, 1H, H3), 4.72-4.69 (d, J = 10.7 Hz, 1H, -OCH_2Ar), 4.54-4.52 (d, J = 12.7 Hz, 1H, -OCH_2Ar), 4.41-4.40 (d, $J_{1\text{-}2}$ = 3.3 Hz, 1H, H1), 4.39-4.36

(d, J = 10.7 Hz, 1H, -OCH_2Ar), 4.37-4.34 (d, J = 10.7 Hz, 1H, -OCH_2Ar), 4.20-4.14 (m, 2H, $H6_{RP}$), 3.88-3.84 (m, 1H, H5), 3.71-3.68 (m, 0.04H, $H6_{CE}$), 3.59-3.55 (t, $J_{4\text{-}3}$ = $J_{4\text{-}5}$ = 9.4 Hz, 1H, H4), 3.57-3.55 (dd, $J_{2\text{-}3}$ = 9.4 Hz, $J_{2\text{-}1}$ = 3.3 Hz, 1H, H2), 3.23 (s, -OCH_3) ppm; ^{13}C NMR(125 MHz, $CDCl_3$): δ 154.7 (3,3' carbonate), 154.2 (6,6' carbonate), 137.8, 137.0 (Ar_{ipso}), 128.5, 128.4, 128.3, 128.0, 127.9, 127.8 (Ar), 97.6, (C1), 78.9 (C3), 77.1 (C4), 75.4 (C2), 74.0 (-OCH$_2$Ar), 72.8 (-OCH$_2$Ar), 68.0 (C5), 66.4 (C6), 55.2 (-OCH$_3$) ppm; FTIR (ATR) (neat, cm^{-1}) 3062, 3030, 2908, 2839, 1753 (C=O), 1497, 1454, 1371, 1238, 1161, 1072, 1043; M_n (NMR) 41600 g/mol; M_n (GPC) 56600 g/mol; PDI = 1.86; T_g = 101 °C; TGA in Ar: $T_d^{5\%}$ = 311 °C, $T_d^{50\%}$ = 348 °C.

3.4 Results and Discussion

Since the utility of a material can be expense-limited, we set out to design a straightforward and high yielding synthetic route to make polycarbonates by using the fewest number of synthetic steps from an abundant renewable compound. Previously, four different diol monomers were synthesized in two to four steps (Chapter 2, Schemes 2.1 and 2.2) and copolymerized with phosgene, diphosgene, or triphosgene in DCM and pyridine to afford low molecular weight polycarbonates. Initially, we experienced difficulties in achieving polycarbonates with molecular weights above 10 kDa in high yields, leading to weak materials too difficult to mechanically characterize by traditional methods. Due to this, different methods were explored to achieve polymers with

molecular weights that are consistent with other prominent polymeric materials used for biomedical applications.

Polycarbonates are typically synthesized using an excess of the carbonyl donor (i.e. phosgene), which complicates the control over the final molecular weight by stoichiometric imbalances. In a study performed by Zelikin and Putnam,[143] control of molecular weight and yield was achieved by using the rate of triphosgene addition as a variable parameter. Polycarbonates were synthesized from the diol, dihydroxyacetone (DHA), an intermediate in glucose metabolism, with molecular weights ranging from *ca.* 37 kDa (56% yield) to 43 kDa (76% yield), by varying the rate of triphosgene addition. These conditions seemed attractive, as they utilized triphosgene, a solid phosgene analogue with fewer safety issues than phosgene, and led to high molecular weight poly-

Table 3.1. Polymerization testing with *1,4*-cylcohexanediol and *1,4*-cyclohexane dimethanol, *via* polycondensation with triphosgene in DCM and pyridine.

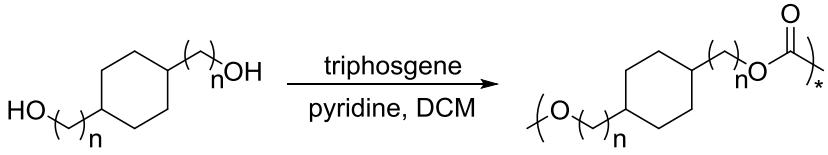

Entry	n	Triphosgene Addition Duration	M_n (Da)[a]	M_w (Da)[a]	PDI[a]	Yield (%)[b]
1	0	5	11600	13900	1.20	54.3
2	0	60	21500	32700	1.52	73.2
3	1	60	42700	84400	1.98	80.1

[a]Estimated by GPC (DMF, 0.05 M LiBr) calibrated with polystyrene standards. [b]Yield calculated from dried, filtered samples after precipitation in methanol three times.

mers from monomers sharing a similar chemical structure to the AA' glucose diols. Results from the testing of similar conditions with two model compounds, *1,4*-cyclohexanediol and *1,4*-cyclohexane dimethanol are shown in Table 3.1. In agreement with previously reported, slowing the rate of addition of triphosgene led to a slight

Table 3.2. GPC results of polymerization conditions applied to Generation I monomers.

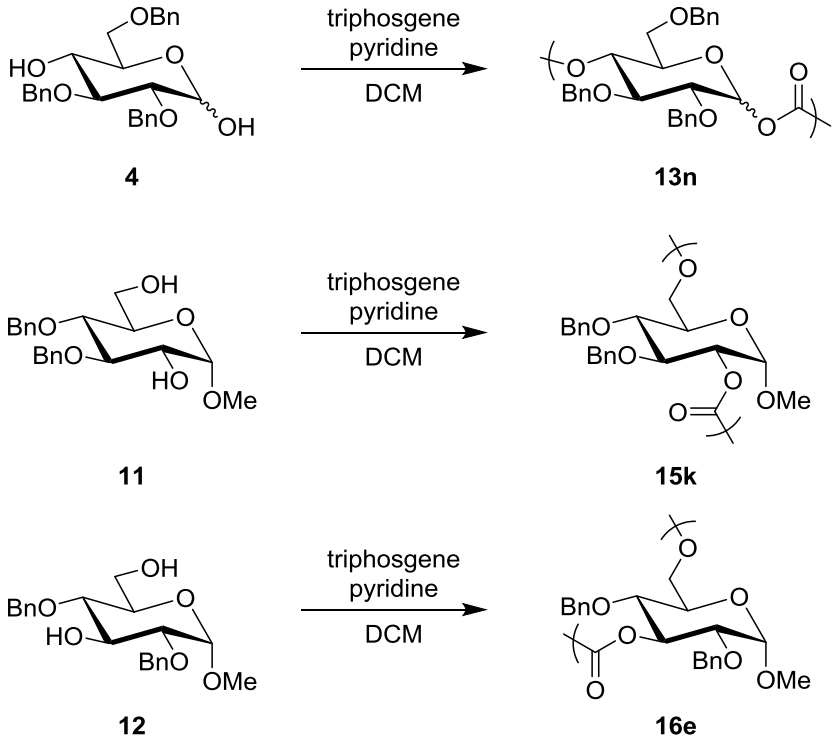

Sample	Polymer	M_n (Da)[a]	M_w (Da)[a]	PDI[a]	Yield (%)[b]
1	*1,4* (**13n)**	6200	6700	1.08	5.1
2	*2,6* (**15k)**	10000	11600	1.16	46.2
3	*3,6* (**16e)**	9800	10800	1.10	53.0

[a]Estimated by GPC (DMF, 0.05 M LiBr) calibrated with polystyrene standards. [b]Yield calculated from dried, filtered samples after precipitation in methanol three times.

increase in M_n, from 11.6 kDa to 21.5 kDa (Table 3.1, entries 1 and 2) and increased yields by nearly 20%. Polymers with a M_n above 40 kDa were achieved when these conditions were applied to a monomer with two primary alcohols, *1,4*-cyclohexane dimethanol (Table 3.1, entry 3).

After successful results were achieved with the model compounds, similar conditions were applied to previously synthesized glucose monomers, **4, 11** and **12** (Table 3.2). Unfortunately, number average molecular weights above 10 kDa were not achieved with these monomers. The *2,6* diol, **3**, resulted in M_n of 9800 Da in a 53% yield, whereas the *1,4* diol, **1**, gave a lower M_n polymer in much lower yields (5.1 %). Differences in yields and molecular weights can be explained by the different chemical compositions of each monomer; in accord with findings in Chapter 2; monomers with hemiacetals formed lower molecular weights, with M_ns ranging from 5.0 to 11.2 kDa. Since higher molecular weights were obtained with monomers containing a more nucleophilic and less sterically hindered alcohol, we sought to design a new glucose-based monomer containing two primary alcohols.

3.4.1 Monomer Synthesis

The existing monomer design (Chapter 2, Scheme 2.1 and 2.2) can be adapted to synthesize glucose-based AA'A'A bis-adduct monomers (where A represents a primary alcohol functionality and A' represents a secondary alcohol functionality) in three steps in high yields (Scheme 3.1) from the same starting material, initially used to synthesize

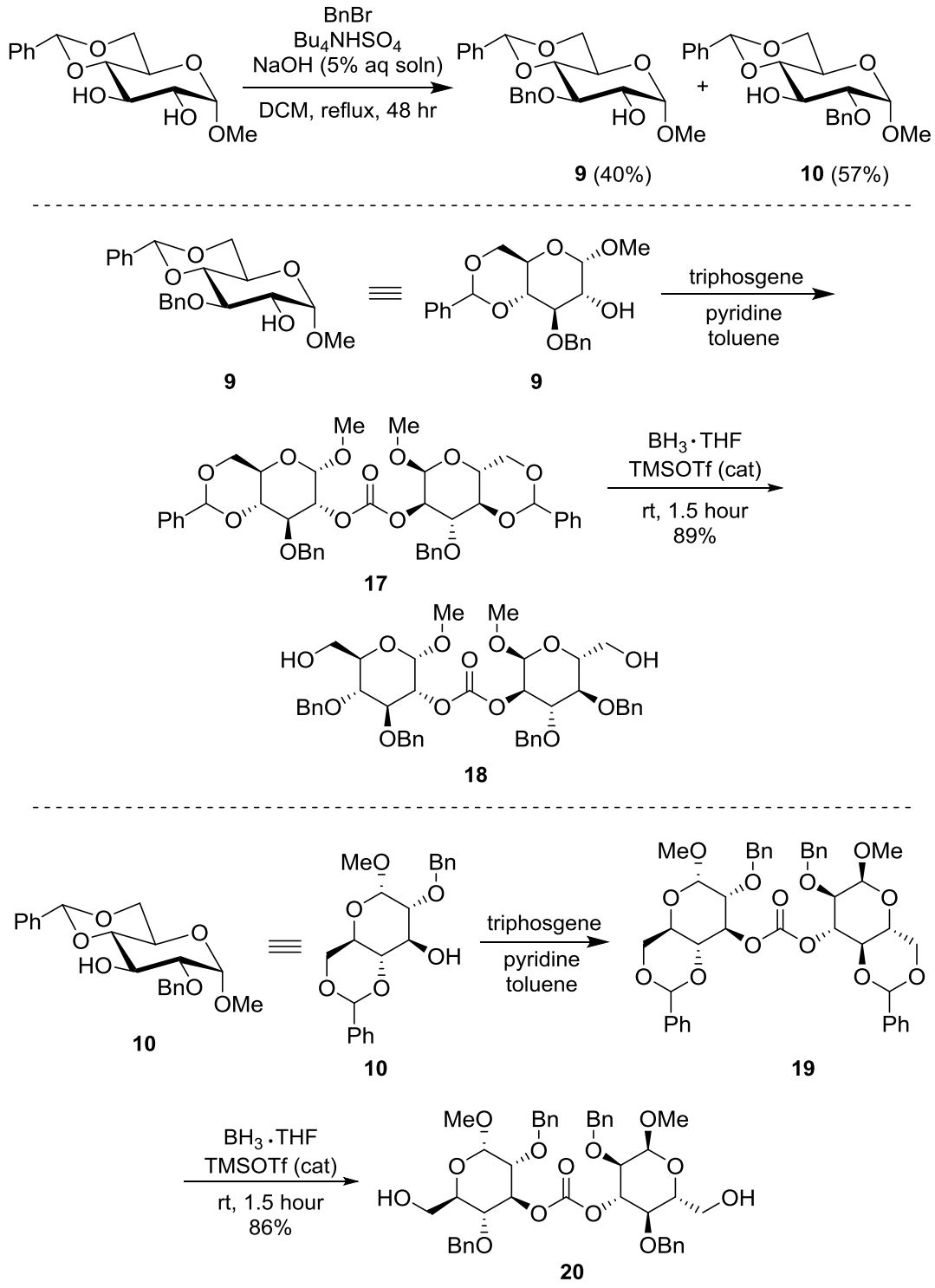

Scheme 3.1. Synthetic route for AA'A'A diol monomers, **18** and **20**, based on dimers of protected glucopyranosides.

monomers **4**, **11**, and **12**. Monobenzylation of commercially available, methyl-4,6-benzylidene-α-D-glucosyl pyranoside, in near equal quantities was performed in the presence of benzyl bromide, aqueous sodium hydroxide, and a bulky phase-transfer agent, to afford the corresponding 2-*O*-benzyl ether, **9**, and the 3-*O*-benzyl ether, **10**, in 40% and 57% yields, respectively. An additional step was added at this point to form benzylidene protected glucose-based dimers, which could subsequently be ring-opened to selectively afford primary alcohols. A number of linkages could be used to make various dimers, however a carbonate functional group was chosen in order to produce polymers with similar chemical compositions as previously synthesized glucose polycarbonates. When compared to previously synthesized monomers, these monomers will only form head-to-head/tail-to-tail connections and since all chemical compositions will remain the same, structure-property relationships due to regioregularity can be determined.

Compounds **9** and **10** were dimerized with a carbonate linkage by reaction with triphosgene in toluene and pyridine, to afford bis-adducts **17** and **19** in 64% and 70% yields, respectively. Addition of the carbonate group was evident by IR and NMR spectroscopies. In the IR spectrum, disappearance of broad OH stretches around 3500 cm^{-1} and the addition of a strong absorbance at 1754 cm^{-1}, characteristic of carbonyl stretching, were observed. The emergence of a single peak at *ca*. 155 ppm in the ^{13}C NMR spectrum, with no ^{1}H coupling (determined by HSQC) in both products, **17** and **19** was also observed. A large downfield shift of the proton on C2, from *ca*. 3.8 to 4.8 ppm for the 2,2'-bis-adduct could be observed and the proton on C3 shifted from 4.15 to 5.5

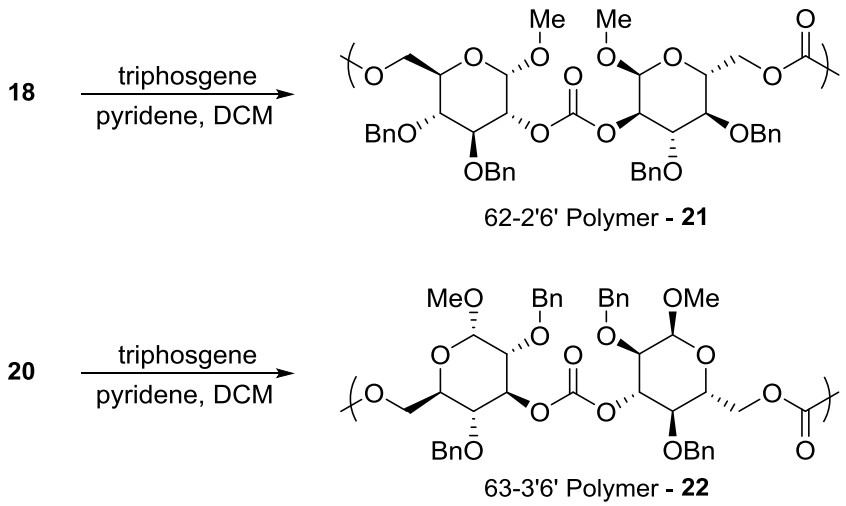

Scheme 3.2. Polymerization of bis-adduct monomers, **18** and **20**, to afford polymers **21** and **22**, respectively.

ppm for the 3,3'-bis-adduct. An increase in mass that corresponded to the expected dimer was also observed by ESI HRMS; a m/z of 771.3017 [M+H] for **17** and 777.3071 [M+Li] for **19**. Both benzylidene cyclic acetals underwent reductive ring opening using BH_3·THF and a catalytic amount of TMSOTf at room temperature to afford, **18** and **20** in 89% and 86% yields, respectively. With the ring opening, two H6 protons could no longer be differentiated by their axial or equatorial positions by ^{1}H NMR, with a 0.7 ppm upfield shift for the $H6_{eq}$ signals and no observed axial-axial coupling constants. Loss of a benzylidene ^{1}H and ^{13}C signals and addition of hydroxyl signals in IR and ^{1}H NMR spectra further demonstrate successful synthesis of AA'A'A dimer monomers.

3.4.2 Polymer Synthesis

The copolymerization between the dimer monomers, **18** and **20**, and triphosgene were conducted as previously described; triphosgene (1.2 eq) dissolved in DCM was added dropwise over an hour to a solution of diol dissolved in DCM and dry pyridine, which was precipitated directly into methanol after stirring for an additional hour. Using this method gave higher molecular weights and much higher yields (Table 3.3), up to 88% yield and a number average molecular weight of 56.6 kDa., as estimated by THF GPC using a polystyrene standard. Attempts to copolymerize the *6,2-2',6'* diol (**18**) with allyl alcohol (0.1 eq), in order to produce polymers with alkene functionalized chain ends, ultimately led to polymers with a lower M_n of 15 kDa and, unfortunately, without noticeable allyl functional groups by ^{1}H NMR spectroscopy.

Table 3.3. Molecular weights of polycarbonates, **21** and **22**, formed from glucopyranoside dimers, **18** and **20**, respectively.

		NMR	THF GPC						DMF GPC		
Polymer	Yield[a] (%)	M_n[b]	M_n[c] (Da)	M_w[c] (Da)	PDI[c]	M_n[d] (Da)	M_w[d] (Da)	PDI[d]	M_n[e]	M_w[e]	PDI[e]
21	78	12000	15000	23000	1.53	16800	22000	1.31	35400	46000	1.30
22	88	41600	56600	105200	1.86	-	-	-	76500	210200	2.75

[a]Yield calculated from dried, filtered samples after precipitation in methanol three times. [b]Estimated by ^{1}H NMR spectroscopy. [c]Estimated by GPC (THF) calibrated with polystyrene standards. [d]Estimated by GPC (THF) using a light-scattering detector. [e]Estimated by GPC (DMF, 0.05 M LiBr) calibrated with polystyrene standards.

The structure of polycarbonate was confirmed by IR, ^{1}H NMR and ^{13}C NMR spectroscopies. The assignments of the ^{1}H and ^{13}C NMR spectra were carried out by COSY and HSQC NMR analyses. The characteristic carbonyl vibration of the carbonate linkage was observed at 1754 cm^{-1} in the IR spectra. The copolymerizations of the diol monomers **18** and **20** with triphosgene to give poly(*6,2-2,'6'*-glucose)carbonate, **21**, and poly(*6,3-3',6'*-glucose)carbonate, **22**, were demonstrated by ^{1}H NMR spectroscopy by observation of significant downfield shifts (0.7 ppm) of the H6 protons, similar to the other protons which are involved in the carbonate linkages. As a result, the molecular weight could also be estimated by the ratio of the integral for the methylene H6 protons

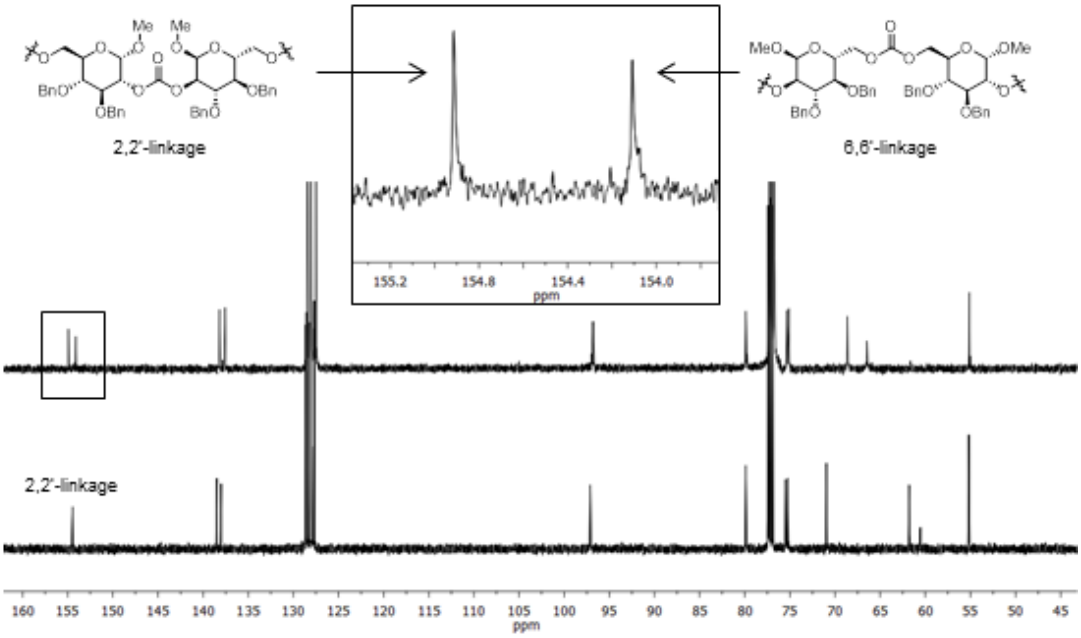

Figure 3.2. ^{13}C NMR spectra of *6,2-2',6'* monomer (**18**, below) and *6,2-2',6'* polymer (**21**, above).

of the chain ends (3.65 to 3.70 ppm) to that of the methylene H6 protons in the repeat unit (4.45 to 4.15 ppm for poly(*622'6*-glucose)carbonate, **21**, and 4.25-4.10 for poly(*633'6*-glucose)carbonate, **22**), which were in close accord with GPC-estimated values. Slight downfield shifts of the C6 signals, from 61 to 66 ppm, were also observed in the ^{13}C NMR spectra. The carbonate linkages were observed by the introduction of ^{13}C NMR resonances at 154 ppm, in addition to the already present head-to-head signals (Figure 3.4 and Figure 3.5). As expected, there are two clear and distinct carbonate linkages, which correspond to the head-to-head (2-2' and 3-3') and tail-to-tail (6-6') connections, indicating a regioregular order.

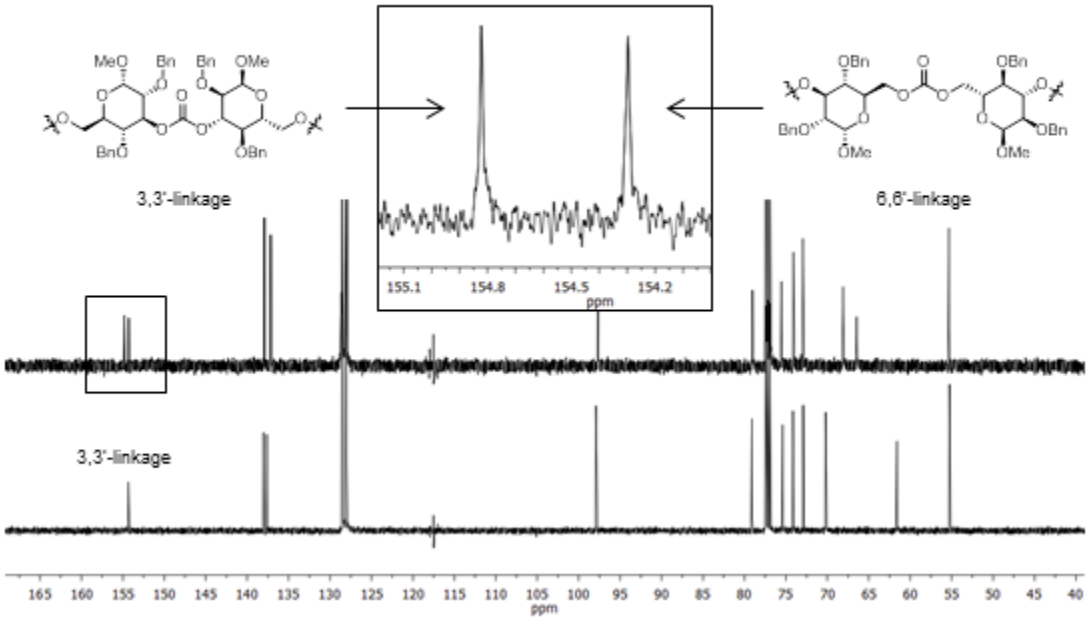

Figure 3.3. ^{13}C NMR spectra of *6,3-3',6'* monomer (**20**, below) and *6,3-3',6'* polymer (**22**, above).

3.4.3 Thermal Analysis

The thermal properties of the glucose polycarbonates were evaluated by thermogravimetric analysis (TGA) and differential scanning calorimetry (DSC) under inert atmosphere (Figure 3.7). Both regioregular polymers exhibited similar decomposition profiles as the regiorandom *2,6* and *3,6* regiorandom glucose polycarbonates with onset thermal decomposition temperatures (T_d^5) at high temperatures, greater than or equal to 280 °C. The *6,2-2',6'* polycarbonate, **21**, had an

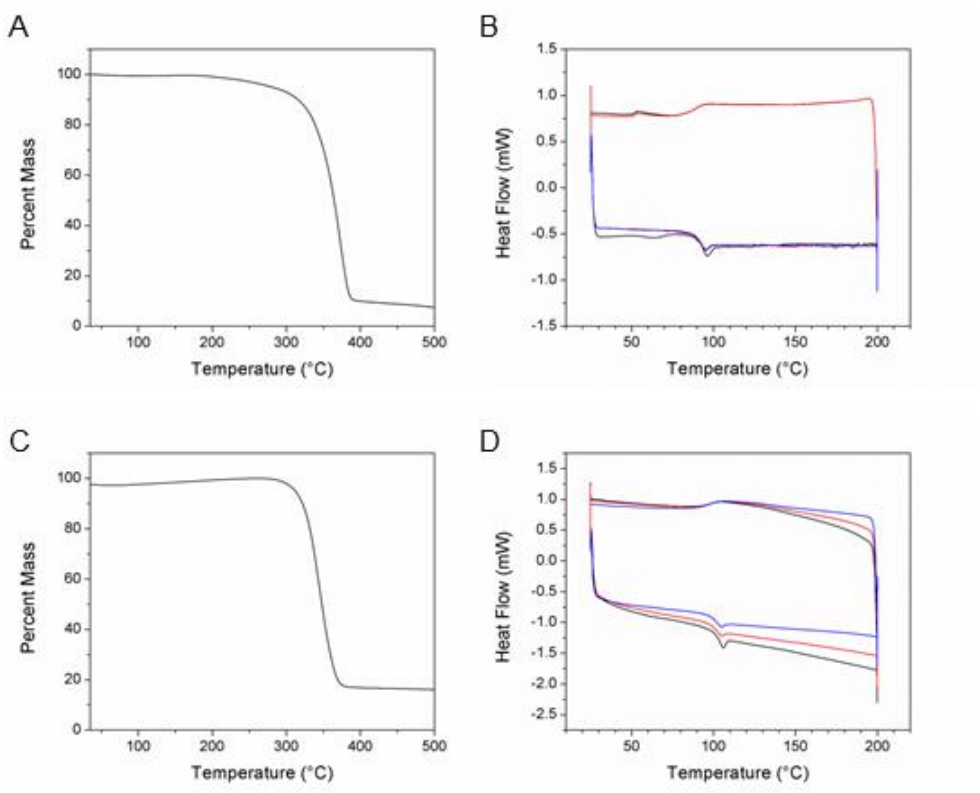

Figure 3.4. TGA characterization of *6,2-2',6'* polymer (a) and *6,3-3',6'* polymer (c); DSC characterization of *6,2-2',6'* polymer (b) and *6,3-3',6'* polymer (d).

initial 5% mass loss at 280 °C and 50% mass loss at 364 °C whereas, the *6,3-3',6'* polycarbonate, **22**, had a slightly higher onset decomposition temperature, with 5% mass loss at 311 °C and lost 50% mass at 348 °C. It cannot be concluded, though, that the regioregularity, had the only effect on the glass transitions of the resulting materials, as this generation of polymers were much larger than the previously synthesized regiorandom *2,6* and *3,6* polymers. Polycarbonate **21** exhibited a T_g almost 15 °C higher than the regiorandom polymer **15d**, however, the polymer had a larger molecular weight. Polycarbonate **22** also had an elevated T_g at 101 °C, however, as mentioned previously, some of the increase could be attributed to the larger molecular weight rather than the different regiochemistries.

Table 3.4. Thermal properties of glucose-based polycarbonates with various regiochemistries and regioregularities.

Monomer	Polymer	M_n (kDa)[a]	T_g (°C)[b]	T_d^5 (°C)[c]	T_d^{50}(°C)[c]
1,4 (**4**)	**13n**	6.2	-[d]	179	315
1,6 (**8**)	**14d**	10.6	62	218	308
2,6 (**11**)	**15d**	19.2	85	339	382
3,6 (**12**)	**16b**	15.0	83	327	361
6,2-2',6' (**18**)	**21**	35.4	92	280	364
6,3-3',6' (**20**)	**22**	76.5	101	311	348

[a]Estimated by GPC (DMF, 0.05 M LiBr) calibrated with polystyrene standards. [b]Determined by DSC. [c]Determined by TGA, T_d^5 = 5% mass loss and T_d^{50} = 50% mass loss. [d]T_g not observed.

3.5 Conclusions

The design and synthesis of high molecular weight polycarbonates based on glucose, a widely available renewable and biocompatible resource has been reported. After difficulties in producing polycarbonates above 10 kDa from glucose based AA' diol monomers, changes in the synthetic design were made to afford AA'A'A monomers bearing to primary alcohols with expectations that more nucleophilic and less hindered hydroxyl groups would lead to higher molecular weight polymers. Benzylidene protected glucosyl pyranosides were coupled *via* a carbonate link and subsequently ring-opened to afford symmetrical dimers with two primary alcohols. In contrast to previously synthesized regiorandom glucose polycarbonates, dimerized monomers afforded high molecular regioregular polymers in high yields. A good overall control over of the regioselectivity of the resulting monomers was achieved by careful design of the monomers and led to the synthesis of poly(glucose carbonate)s, possessing head-to-head and tail-to-tail sequences exclusively. Although thermal degradation of the poly(glucose carbonate)s were similar between polymers of similar regioisomers, the glass transitions differed significantly, most likely due to regioselectivity and chain length. Regioregular polymers with similar and greater molecular weights exhibited an increased T_g of *ca*. 20 °C and 30 °C, respectively. Glucose-based polycarbonates with high molecular weights and high T_g with respect to common aliphatic polycarbonates are attractive for a broad range of potential applications. Moreover, modifications to the polymer protection chemistry can influence the polymer properties, introducing another

variable for modification and tunability. For example, removal of benzyl protecting groups will afford polymers with free hydroxyl groups, which may lead to hydrogen-bonded materials with enhanced mechanical properties. It is envisioned that bio-based polycarbonates derived from glucose could potentially undergo hydrolytic breakdown and lead to biologically beneficial byproducts and carbon dioxide. Further studies to investigate the degradation and mechanical properties will need to be performed in order to assess the efficacy of these polymers to fulfill roles as engineering plastics, biomedical materials, and other applications where mechanical strength and degradation are both desired.

CHAPTER IV

RING-OPENING POLYMERIZATION OF GLUCAL-DERIVED CYCLIC CARBONATES VIA AN ORGANOCATALYTIC APPROACH: A NOVEL PLATFORM FOR TUNABLE, MULTIFUNCTIONAL BIOMATERIALS

4.1 Original Publication Information*

This chapter contains excerpts from the article *Functional Polycarbonate of D-Glucal-Derived Bicyclic Carbonates via an Organocatalytic Ring-Opening Polymerization.* Modifications to the original document are cosmetic and used only to conform to the format of this document or provide uniformity of enumeration. Contents found in the supporting information, which was originally a separate document, has been included in the chapter, and schemes and figures have been renumbered to the style of this document.

4.2 Overview

Herein we demonstrated the synthesis of a glycal-based cyclic carbonate monomer in three steps and its controlled ROP *via* organocatalysis with initiation by 4-

---

*Reprinted with permission from "A Functional Polycarbonate of a D-Glucal-Derived Bicyclic Carbonate *via* Organocatalytic Ring-Opening Polymerization", by Alexander T. Lonnecker, Young H. Lim and Karen L. Wooley, **2017**, *ACS Macro Lett.*, *6*, 748-753, DOI: 10.1021/acsmacrolett.7b00362), Copyright 2017 by The American Chemical Society.

methylbenzyl alcohol. The ROP was studied as a function of time, catalyst type, and catalyst concentration by gel permeation chromatography (GPC) and ^{1}H NMR. Using a 1,5,7-triazabicyclo[4.40]dec-5-ene (TBD) catalyst (1 mol %) a polymer with a molecular weight of 9900 g/mol and a unimodal polydispersity (PDI) of 1.21 whereas a 1,8-diazabicyclo[5.4.0]undec-7-ene/1-(3,5-bis(trifluoromethyl)phenyl)-3-cyclohexyl-2-thiourea (DBU/TU) catalyst system (2 mol%) afforded a polymer with a molecular weight of 5000 g/mol and a unimodal polydispersity of 1.20. Both catalyst systems reached full conversion in dichloromethane under argon at 30 °C in fewer than ten minutes. Glucal-based polycarbonates analyzed by differential scanning calorimetry (DSC) and thermogravimetric analysis (TGA) exhibited an amorphous character with a high glass transition temperature (T_g) at 65 °C and an onset decomposition temperature (T_d) at 200 °C. This new polymer represents a functional architecture that can be rapidly transformed into a diverse variety of polymers through thiol-ene "click chemistry" along the polycarbonate backbone or through the addition of pendant functionalities to the monomer for further post-polymerization modification.

4.3 Introduction

Polycarbonates, polymers with backbones containing repeating carbonate linkages, can be categorized into two families based on their structural composition: aromatic polycarbonates and aliphatic polycarbonates (APCs). The former has been widely utilized as an engineering and commodity plastic for over 60 years, owing to

attractive processing and unique physical properties, including, in particular, mechanical strength, temperature and impact resistance, as well as optical transparency. These properties make aromatic polycarbonates, in particular poly(bisphenol-A-carbonate)s, desirable not only for use in everyday materials but also for engineering plastics used in automotive industry, aircraft components, as electronics, for data storage, in construction, and as biomedical materials.

Despite their discovery in the 1930s by Carothers[42], APCs were largely overlooked until well into the 1990s. Their comparatively poor thermal stability and susceptibility to hydrolysis were considered inferior to properties displayed by other polymers [*e.g.*, polyesters, polyamide, poly(methyl methacrylate)] developed at the time for fiber applications.[144] Although aliphatic polycarbonates have been proposed as alternative materials for films, packaging and rigid plastics applications, the current industrial applications are still limited as low-molecular weight macromonomers for the production of polyurethanes and other copolymers.

Since the 1990s, APCs have gained a renewed interest, particularly as soft materials for biomedical applications, for the same reasons that were deemed inferior in decades past. An increasing demand for more versatile degradable materials have led scientists to utilize APCs alongside aliphatic polyesters, since they possess important properties such as biocompatibility, biodegradability, low glass transitions and elasticity, which are important to a number of applications including, medical devices, drug delivery systems and engineered tissues.[44,45] For medical applications, the hydrolytic instability of APCs is actually an attractive advantage from the perspectives of safety

concerns and biofunctional requirements. For example, biodegradable polymeric materials do not require removal after implantation, thereby avoiding a second surgical procedure that would otherwise be necessary for removal of a permanent device.

So far, aliphatic polyesters are predominantly used in the development of synthetic degradable polymers for many applications in the vast field of biomedical and pharmaceutical sciences. However, the inherent nature of the polyester backbone can pose significant issues in the application of these materials. The process in which hydrolytic degradation occurs and nature of degradation products creates acidic microenvironments that can lead to local aseptic inflammation.[30,136,137] In addition, polyesters have been used in drug-delivery systems for delivering pH sensitive materials with limited success. In previous work, inactivation of proteins and plasmid DNA encapsulated in poly(lactic-*co*-glycolic acid)(PLGA) particles was observed in the course of polymer degradation.[138-140] In comparison, the advantage of APCs is embodied in the absence of acidic compounds during *in vivo* degradation.[145-147] In addition, the degradation rate of polycarbonates is generally slower than polyesters, which is desirable for applications in need of relatively long-term durability in the body.[148,149]

Early study of APCs has focused on the improvement of the mechanical properties and thermal stability of poly(trimethylene carbonate) (PTMC) or on the improvement of existing materials. Copolymers of polycarbonates such as PTMC with other polymers such as PLA or PGA have already found application in sutures and fixation devices and in other biomedical fields such as drug delivery. While this field

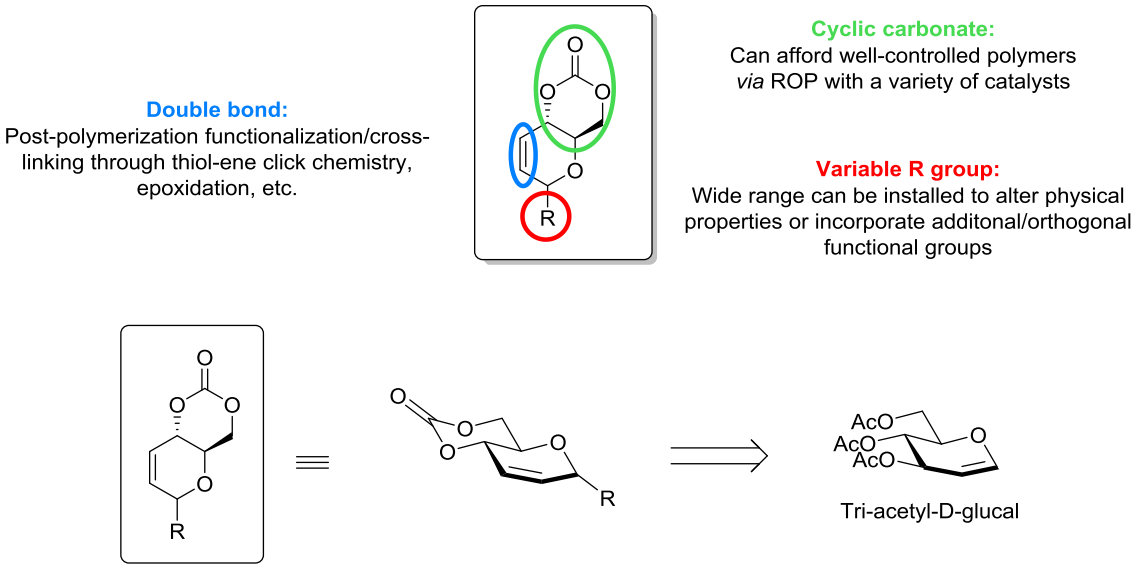

Figure 4.1. Platform design rational for glucal-based cyclic carbonate monomer for the synthesis of multifunctional polycarbonates.

continues to grow, it heavily relies on materials studied for more than 40 years. To create the next generation of materials, with improved biodegradation characteristics and biocompatibility, the expansion of feedstocks to include the use of natural products has become a significant focus. The preparation and application of polysaccharide or sugar-based polymers is one of the most attractive research subjects the biomedical field due, apart from being sourced from an abundant natural product, to their anticipated biocompatibility. The Wooley lab recently developed a novel glucose-based bicyclic carbonate monomer that undergoes ring-opening polymerization with catalysis by an organic base, TBD, to yield an amorphous poly(D-glucose carbonate) (PDGC).[104,105] PDGC is particularly attractive, as its hydrolytic degradation is expected to produce

carbon dioxide plus the (protected) monosaccharide. A similar approach can be applied to other types of saccharide feedstocks to develop degradable polycarbonates with a wide range of functionalities. Herein, we report the synthesis of a glucal-based bicyclic carbonate monomer, **4**, and it's controlled ROP with an organocatalytic system. We wanted to build from previous glucose-based polycarbonates and expand to make a flexible platform that can be easily modified to apply towards a broad range of applications. In order to achieve this goal, we sought to incorporate four goals when synthesizing the monomer:

1) Design a streamlined synthetic strategy that utilizes a glucose-based feedstock
2) Monomer must possess a six-membered cyclic carbonate functional group
3) Demonstrate facile ROP *via* organocatalyst to afford well-defined polymers
4) Increase the utility of the polymer platform by allowing the possibility of multiple functional groups in the final monomer to increase the ability for orthogonal post-polymerization modifications

4.4 Experimental

4.4.1 Materials

Reagents were available from Sigma Aldrich and used as received unless otherwise noted. TU was prepared as previously reported;[150] TU, 4-methylbenzyl alcohol (99%) and 1,5,7-triazabicyclo[4.4.0]dec-5-ene (TBD; 98%) were dried by stirring in dry THF with CaH_2, filtering and removing solvent in *vacuo*; 1,8-diazabicyclo[5.4.0]undec-7-ene (DBU, 98%) was stirred over CaH_2, vacuum distilled, then stored over molecular sieves (3 Å). Dichloromethane (DCM) was purified by passage through a solvent purification system (J.C. Meyer Solvent Systems) and used as a dried solvent. Monomer **4**, was dried under reduced pressure, over P_2O_5 and stored under an Ar environment. Column chromatography was performed on a combiflash Rf4x (Teledyne ISCO) with RediSep Rf Columns (Teledyne ISCO).

4.4.2 Characterization

The ^{1}H NMR (500 MHz) and ^{13}C NMR (125 MHz) spectra were obtained on an Inova 500 MHz spectrometer using the solvent as an internal reference. Glass transition (T_g) temperatures were measured by differential scanning calorimetry on a Mettler Toledo DSC822e apparatus (Mettler Toledo, Columbus, OH) with a heating rate of 10 °C/min. The measurements were analyzed using Mettler-Toledo Star^{e} v. 10.00

software. The T_g was taken as the midpoint of the inflection tangent, upon the third heating scan. Thermogravimetric analysis (TGA) was performed under an Ar atmosphere using a Mettler Toledo model TGA/SDTA851^e apparatus with a heating rate of 10 °C/min. Gel permeation chromatography (GPC) was conducted on two Waters Chromatography, Inc. (Milford, MA) systems eluted with either tetrahydrofuran (THF) or dimethylformamide (DMF) at a flow rate of 1.00 mL/min. Both GPC instruments were equipped with an model 1515 isocratic pump, a model 2414 differential refractometer, and a three-column set of Polymer Laboratories (Amherst, MA) Styragel columns (PL_{gel} 5 μm Mixed C, 500 Å, and 104 Å, 300 x 7.5 mm columns) for the THF system equilibrated at 35 °C, or a four-column set of 5 μm Guard (50 × 7.5 mm), Styragel HR 4 5 μm DMF (300 × 7.5 mm), Styragel HR 4E 5 μm DMF (300 × 7.5 mm), and Styragel HR 2 5 μm DMF (300 × 7.5 mm) columns equilibrated at 70 °C. Polymer solutions were prepared at a known concentration (*ca.* 3 mg/mL), and an injection volume of 200 μL was used. Data collection and analyses were performed with Precision Acquire software and Discovery 32 software, respectively (Precision Detectors, Inc.). The differential refractometer was calibrated with standard polystyrene materials (SRM 706 NIST) for the THF system and poly(ethylene glycol) for the DMF system. IR spectra were recorded on an IR Prestige 21 system (Shimadzu Corp., Japan), equipped with an ATR accessory, and analyzed using IRsolution v. 1.40 software.

4.4.3 Synthesis

Isopropyl 4,6-di-*O*-acetyl-2,3-dideoxy-α-D-*erythro*-hex-2-enopyranoside (1). Tri-*O*-acetyl D- glucal (12.0997, 44.443 mmol) was added to a 150 mL flamed dried schlenk flask under nitrogen and dissolved in 100 mL of anhydrous dichloromethane and 4.20 mL of isopropyl alcohol (54.9 mmol). After cooling to 0 °C, boron trifluoride diethyl etherate (2.2 mL, 18 mmol) was added dropwise. The reaction mixture was removed from the ice bath allowed to stir for an additional 30 min, or until the solution turned a deep purple color. The reaction was quenched by the addition of 150 mL saturated solution of $NaHCO_3$, at which point the color of the solution was discharged. The aqueous layer was extracted with dichloromethane (100 mL) and the combined organic layers were dried with $MgSO_4$ and the solvent was removed under reduced pressure, resulting in a light amber syrup. The crude was purified by column chromatography (SiO_2; 9:1 hexanes/ethyl acetate), resulting in 10.8427 g (89.6%) of **1** (9:1, α/β) as a colorless syrup.

*Isopropyl 4,6-di-O-acetyl-2,3-dideoxy-α-D-erythro-hex-2-enopyranoside (**1α**).* ^{1}H NMR (500 MHz, $CDCl_3$) δ 5.88-5.86 (ddd, $J_{3\text{-}2}$ = 10.2 Hz, $J_{3\text{-}4}$ = 1.7 Hz, $J_{3\text{-}1}$ = 1.5 Hz, 1H, H3), 5.82-5.79 (ddd, $J_{2\text{-}3}$ = 10.2 Hz, $J_{2\text{-}1}$ = 2.8 Hz, $J_{2\text{-}4}$ = 1.9 Hz, 1H, H2), 5.31-5.28 (ddd, $J_{4\text{-}5}$ = 9.6 Hz, $J_{4\text{-}2}$ = 1.9 Hz, $J_{4\text{-}3}$ = 1.7 Hz, 1H, H4), 5.14-5.12 (dd, $J_{1\text{-}2}$ = 2.8 Hz, $J_{1\text{-}3}$ = 1.5 Hz, 1H, H1), 4.25-4.22 (dd, $J_{6\text{-}6'}$ = 11.6 Hz, $J_{6\text{-}5}$ = 5.6 Hz, 1H, H6), 4.19-4.16 (dd, $J_{6'\text{-}6}$ = 11.6 Hz, $J_{6'\text{-}5}$ = 2.5 Hz, 1H, H6'), 4.17-4.13 (ddd, $J_{5\text{-}4}$ = 9.6 Hz, $J_{5\text{-}6}$ = 5.6 Hz, $J_{5\text{-}6'}$ = 2.5 Hz, 1H, H5), 4.02-3.95 (septet, J = 6.2 Hz, 1H, C*H*(CH_3)(CH_3)), 2.09 (s, 3H,

OAc), 2.08 (s, 3H, OAc), 1.26-1.25 (d, J = 6.6, 3H, -CH(CH_3)(CH$_3$)), 1.19-1.18 (d, J = 6.6, 3H, -CH(CH$_3$)(CH_3)) ppm; ^{13}C NMR (125 MHz, CDCl$_3$): δ 170.9 (O*C*OCH$_3$), 170.5 (O*C*OCH$_3$), 128.9 (C=C), 128.6 (C=C), 92.9 (C1), 70.9 (*C*H(CH$_3$)(CH$_3$)), 66.9 (C5), 65.5 (C4), 63.2 (C6), 23.6 (OCO*C*H$_3$), 22.1 (OCO*C*H$_3$), 21.1 (CH(*C*H$_3$)(CH$_3$)), 20.9 (CH(CH$_3$)(*C*H$_3$)); FTIR (ATR) υ_{max} (cm^{-1}) 2972, 2931, 1739, 1369, 1222, 1099, 1028, 981. ESI MS: calculated [M + Li] for $C_{13}H_{20}O_6$, 279.2345; found, 279.1138.

Isopropyl 4,6-di-O-acetyl-2,3-dideoxy-β-D-erythro-hex-2-enopyranoside ***(1β)***. ^{1}H NMR (500 MHz, CDCl$_3$) δ 5.97-5.93 (ddd, $J_{3\text{-}2}$ = 10.3 Hz, $J_{3\text{-}4}$ = 3.7 Hz, $J_{3\text{-}1}$ = 1.8 Hz, 1H, H3), 5.91-5.88 (ddd, $J_{2\text{-}3}$ = 10.3 Hz, $J_{2\text{-}4}$ = 1.5 Hz, $J_{2\text{-}1}$ = 1.0 Hz, 1H, H2), 5.22-5.20 (ddd, $J_{4\text{-}5}$ = 7.8 Hz, $J_{4\text{-}3}$ = 2.5 Hz, $J_{4\text{-}2}$ = 1.5 Hz, 1H, H4), 5.21 – 5.20 (dd, $J_{1\text{-}3}$ = 1.8 Hz, $J_{1\text{-}2}$ = 1.0 Hz, 1H, H1), 4.29-4.25 (dd, $J_{6\text{-}6'}$ = 11.6 Hz, $J_{6\text{-}5}$ = 6.0 Hz, 1H, H6), 4.19-4.16 (dd, $J_{6'\text{-}6}$ = 11.6 Hz, $J_{6'\text{-}5}$ = 2.5 Hz, 1H, H6'), 4.17-4.13 (ddd, $J_{5\text{-}4}$ = 7.8 Hz, $J_{5\text{-}6}$ = 6.0 Hz, $J_{5\text{-}6'}$ = 2.5 Hz, 1H, H5), 4.10-4.02 (septet, J = 6.3 Hz, 1H, C*H*(CH$_3$)(CH$_3$)), 2.09 (s, 3H, OAc), 2.08 (s, 3H, OAc), 1.24-1.23 (d, J = 6.1 Hz, 3H, -CH(CH_3)(CH$_3$)), 1.18-1.17 (d, J = 6.0 Hz, 3H, -CH(CH$_3$)(CH_3)) ppm; ^{13}C NMR (125 MHz, CDCl$_3$): δ 170.9 (O*C*OCH$_3$), 170.5 (O*C*OCH$_3$), 131.0 (C=C), 125.8 (C=C), 93.2 (C1), 72.7 (C5), 70.2 (*C*H(CH$_3$)(CH$_3$)), 64.5 (C4), 63.5 (C6), 23.6 (OCO*C*H$_3$), 22.1 (OCO*C*H$_3$), 21.1 (CH(*C*H$_3$)(CH$_3$)), 20.9 (CH(CH$_3$)(*C*H$_3$)); FTIR (ATR) υ_{max} (cm^{-1}) 2972, 2931, 1739, 1369, 1222, 1099, 1028, 981. ESI MS: calculated [M + Li] for $C_{13}H_{20}O_6$, 279.2345; found, 279.1138.

Isopropyl-2,3-dideoxy-α-D-*erythro*-hex-2-enopyranoside (2). A solution of **1** (10.5 g, 58.6 mmol) in 180 mL of dry methanol under nitrogen at room temperature was treated with a solution of sodium methoxide in methanol (0.80 mL, 4.37 M, 3.5 mmol); the reaction mixture was stirred at room temperature for 45 min. Solid NH_4Cl (0.5 g) was added, and the mixture was stirred 15 min and then diluted with 200 mL of acetone. The solids were removed by filtration, and the filtrate was concentrated in *vacuo* to afford **2** (7.26 g, 9:1 α/β) in quantitative yields, which was used directly in the next reaction.

*Isopropyl-2,3-dideoxy-a-D-erythro-hex-2-enopyranoside (**2α**).* ^{1}H NMR (500 MHz, $CDCl_3$) δ 5.96-5.94 (dt, $J_{3\text{-}2}$ = 10.2 Hz, $J_{3\text{-}1}$ = $J_{3\text{-}4}$ = 1.2 Hz, 1H, H3), 5.75-5.72 (ddd, $J_{2\text{-}3}$ = 10.2 Hz, $J_{2\text{-}4}$ = 3.0 Hz, $J_{2\text{-}1}$ = 2.1 Hz, 1H, H2), 5.10-5.08 (dd, $J_{1\text{-}2}$ = 2.1 Hz, $J_{1\text{-}3}$ = 1.2 Hz, 1H, H1), 4.24-4.19 (dddd, $J_{4\text{-}5}$ = 9.2 Hz, $J_{4\text{-}OH}$ = 8.5 Hz, $J_{4\text{-}2}$ = 3.0 Hz, $J_{4\text{-}3}$ = 1.7 Hz, 1H, H4), 4.01-3.93 (septet, J = 6.3 Hz, 1H, C*H*(CH_3)(CH_3)), 3.91-3.84 (m, 2H, H6+H6'), 3.77-3.74 (dt, $J_{5\text{-}4}$ = 9.2 Hz, $J_{5\text{-}6}$ = $J_{5\text{-}6'}$ = 4.6 Hz, 1H, H5), 1.97-1.93 (t, $J_{OH\text{-}6}$ = $J_{OH\text{-}6'}$ =7.5 Hz, 1H, OH), 1.84-1.81 (d, $J_{OH\text{-}4}$ = 8.5 Hz, 1H, OH), 1.25-1.24 (d, J = 6.2 Hz, 3H, -CH(C*H*$_3$)(CH_3)), 1.19-1.17 (d, J = 6.2 Hz, 3H, -CH(CH_3)(C*H*$_3$)) ppm; ^{13}C NMR (125 MHz, $CDCl_3$): δ 133.3 (C=C), 126.9 (C=C), 92.7 (C1), 71.39 (C5), 70.60 (*C*H(CH_3)(CH_3)), 64.4 (C4), 62.8 (C6), 23.8 (CH(*C*H$_3$)(CH_3)), 22.1 (CH(CH_3)(*C*H$_3$)); FTIR (ATR) υ_{max} (cm^{-1}) 3500-3150 (br), 2968, 2933, 2877, 1384, 1037, 945. ESI MS: calculated [M + Li] for $C_9H_{16}O_4$, 195.1209; found, 195.1201.

*Isopropyl-2,3-dideoxy-β-D-erythro-hex-2-enopyranoside (**2β**).* ^{1}H NMR (500 MHz, $CDCl_3$) δ 6.04-6.01 (ddd, $J_{3\text{-}2}$ = 10.3 Hz, $J_{3\text{-}1}$ = 3.4 Hz, $J_{3\text{-}4}$ = 1.7 Hz, 1H, H3),

5.78-5.75 (dt, $J_{2\text{-}3}$ = 10.3 Hz, $J_{2\text{-}1}$ = $J_{2\text{-}4}$ = 1.7 Hz, 1H, H2), 5.22-5.21 (dd, $J_{1\text{-}3}$ = 3.4 Hz, $J_{1\text{-}2}$ = 1.7 Hz, 1H, H1), 4.20-4.16 (m, 1H, H4), 4.07 (septet, J = 6.3 Hz, 1H, C*H*(CH_3)(CH_3)), 3.91-3.82 (m, 2H, H6+H6'), 3.77-3.74 (dt, $J_{5\text{-}4}$ = 9.2 Hz, $J_{5\text{-}6}$ = $J_{5\text{-}6'}$ = 4.6 Hz, 1H, H5), 2.54-2.51 (t, $J_{OH\text{-}6}$ = $J_{OH\text{-}6'}$ = 6.7 Hz, 1H, OH), 1.84-1.81 (d, $J_{OH\text{-}4}$ = 8.5 Hz, 1H, OH), 1.25-1.24 (d, J = 6.2 Hz, 3H, -CH(C*H*$_3$)(CH_3)), 1.19-1.17 (d, J = 6.2 Hz, 3H, -CH(CH_3)(C*H*$_3$)) ppm; ^{13}C NMR(125 MHz, $CDCl_3$): δ 131.2 (C=C), 128.7 (C=C), 94.23 (C1), 71.4 (C5), 70.6 (*C*H(CH_3)(CH_3)), 64.4 (C4), 63.3 (C6), 23.8 (CH(*C*H$_3$)(CH_3)), 22.1 (CH(CH_3)(*C*H$_3$)); FTIR (ATR) υ_{max} (cm^{-1}) 3500-3150 (br), 2968, 2933, 2877, 1384, 1037, 945; ESI MS: calculated [M + Li] for $C_9H_{16}O_4$, 195.1209; found, 195.1201.

Isopropyl 4,6-carbonate-2,3-dideoxy-α-D-*erythro*-hex-2-enopyranoside (3). The diol, **2**, (2.4089 g, 14.923 mmol) was dissolved in dry dichloromethane (600 mL) and anhydrous pyridine (3.6 mL, 45 mmol). Triphosgene (2.2166 g, 7.4696 mmol) dissolved in 25 mL of dry dichloromethane was added dropwise over 10 min and the reaction mixture was allowed to stir at room temperature for 3.5 hours. After quenching with 25 mL of saturated $NaHCO_3$, the organic layer was washed with saturated NH_4Cl solution (25 mL) and brine (25 mL), dried with $MgSO_4$, and concentrated in *vacuo*. The crude was purified by column chromatography (SiO_2; 1/1 hexane/ethyl acetate) and recrystallized (ether/hexanes) to afford **3** (1.2788 g, 40.0%, 1:0 α/β) as white needle-like crystals. The monomer was dried in a desiccator over P_2O_5, for three days and stored in a glovebox.

*Isopropyl 4,6-carbonate-2,3-dideoxy-a-D-erythro-hex-2-enopyranoside (**3**).* ^{1}H NMR (500 MHz, $CDCl_3$): δ 6.12-6.10 (ddd, $J_{3\text{-}2}$ = 10.0 Hz, $J_{3\text{-}4}$ = 2.7 Hz, $J_{3\text{-}1}$ = 1.4 Hz, 1H, H3), 5.86-5.83 (dt, $J_{2\text{-}3}$ = 10.0 Hz, $J_{2\text{-}1}$ = $J_{2\text{-}4}$ =2.5 Hz, 1H, H2), 5.20-5.18 (dd, $J_{1\text{-}2}$ = 2.5 Hz, $J_{1\text{-}3}$ = 1.4 Hz, 1H, H1), 4.66-4.63 (ddd, $J_{4\text{-}5}$ = 9.1 Hz, $J_{4\text{-}3}$ = 2.7 Hz, $J_{4\text{-}2}$ = 2.5 Hz, 1H, H4), 4.53-4.50 (dd, $J_{6eq\text{-}6ax}$ = 9.7 Hz, $J_{6eq\text{-}5}$ = 6.0 Hz, 1H, $H6_{eq}$), 4.32-4.28 (dd, $J_{6ax\text{-}5}$ = 10.4 Hz, $J_{6ax\text{-}6eq}$ = 9.7 Hz, 1H, $H6_{ax}$), 4.20-4.15 (ddd, $J_{5\text{-}6ax}$ = 10.4 Hz, $J_{5\text{-}4}$ = 9.1 Hz, $J_{5\text{-}6eq}$ = 6.0 Hz, 1H, H5), 3.96 (septet, J = 6.0 Hz, 1H, C*H*(CH_3)(CH_3)), 1.26-1.25 (d, J = 6.2 Hz, 3H, -CH(C*H*$_3$)(CH_3)), 1.22-1.21 (d, J = 6.2 Hz, 3H, -CH(C*H*$_3$)(CH_3)); ^{13}C NMR(125 MHz, $CDCl_3$): δ 148.0 (carbonate), 129.4 (C=C), 126.83 (C=C), 93.6 (C1), 72.6 (C4), 71.5 (*C*H(CH_3)(CH_3)), 70.3 (C6), 60.9 (C5), 23.8 (CH(*C*H$_3$)(CH_3)), 22.0 (CH(CH_3)(*C*H$_3$)); FTIR (ATR) υ_{max} (cm^{-1}) 2976, 2907, 1755 (carbonate), 1396, 1267, 1238, 1183, 1130, 1120, 1010, 952, 933. ESI MS: calculated [M + H] for $C_{10}H_{14}O_5$, 215.0919; found, 215.0917.

General procedure for polymerization of 3 using TBD (polymers 4 and 5). Solutions of the initiator, 4-methylbenzyl alcohol and catalyst, TBD, in dry DCM with a concentration of 10 mg/mL were prepared prior to polymerization. In a 5 mL vial containing a magnetic stir bar in the glovebox, **3** (0.100 g, 0.467 mmol, 1 eq) and 4-methylbenzyl alcohol (228 μL, 0.0187 mmol, 0.04 eq) were dissolved in DCM (974 μL). DBU (355 μL, 0.0234 mmol, 0.05 eq) was then added to initiate polymerization. The reaction was allowed to stir at 30 °C and aliquots of samples were taken to monitor the monomer conversion and evolution of ^{1}H NMR spectroscopy and GPC. After 10 min,

the reaction mixture was quenched by addition of Amberlyst 15 H resin (20-50 mg). The product was precipitated from DCM to methanol and dried in a falcon tube under reduced pressure, yielding a white powder.

General procedure for polymerization of 3 using DBU (polymers 6, 8, and 10). Solutions of the initiator, 4-methylbenzyl alcohol and catalyst, DBU, in dry DCM with a concentration of 10 mg/mL were prepared prior to polymerization. In a 5 mL vial containing a magnetic stir bar in the glovebox, **3** (0.100 g, 0.467 mmol, 1 eq) and 4-methylbenzyl alcohol (228 μL, 0.0187 mmol, 0.04 eq) were dissolved in DCM (974 μL). DBU (355 μL, 0.0234 mmol, 0.05 eq) was then added to initiate polymerization. The reaction was allowed to stir at 30 °C and aliquots of samples were taken to monitor the monomer conversion and evolution of ^{1}H NMR spectroscopy and GPC. After 10 min, the reaction mixture was quenched by addition of Amberlyst 15 H resin (20-50 mg). The product was precipitated from DCM to methanol and dried in a falcon tube under reduced pressure, yielding a white powder.

General procedure for polymerization of 3 using DBU+TU (polymers 7 and 9). Solutions of the initiator, 4-methylbenzyl alcohol and catalysts, DBU and TU, in dry DCM with a concentration of 10 mg/mL were prepared prior to polymerization. In a 5 mL vial containing a magnetic stir bar in the glovebox, **3** (0.117 g, 0.546 mmol, 1 eq), 4-methylbenzyl alcohol (267 μL, 0.0218 mmol, 0.04 eq), and TU (1011 μL, 0.0273, 0.05 eq) were dissolved in DCM (126 μL). DBU (416 μL, 0.0273 mmol, 0.05 eq) was then

added to initiate polymerization. The reaction was allowed to stir at 30 °C and aliquots of samples were taken to monitor the monomer conversion and evolution of ^{1}H NMR spectroscopy and GPC. After 10 min, the reaction mixture was quenched by addition of Amberlyst 15 H resin (20-50 mg). The product was precipitated from DCM to methanol and dried in a falcon tube under reduced pressure, yielding a white powder.

*Poly(hex-2-enopyranoside)carbonate (**4**).* ^{1}H NMR (500 MHz, CD_2Cl_2) δ 7.27-7.26 (d, Ar), 7.19-7.17 (d, Ar), 5.96-5.91 (m, H3), 5.85-5.79 (m, H2), 5.16-5.08 (m, H4+H1), 4.43-4.23 (m, H6), 4.18-4.10 (m, H5), 3.99-3.90 (septet, -C*H*(CH_3)(CH_3)), 2.34 (s, -OC*H*$_3$Ar), 1.21-1.20 (d, -CH(C*H*$_3$)(CH_3)), 1.16-1.14, (d, -CH(CH_3)(C*H*$_3$)) ppm; ^{13}C NMR(125 MHz, CD_2Cl_2): δ 155.5-154.6 (carbonate), 129.7 (C=C), 128.2 (C=C), 93.2 (C1), 71.3 (C4), 68.4 (-*C*H(CH_3)(CH_3)), 67.1 (C6), 66.9 (C5), 23.9 (-CH(*C*H$_3$)(CH_3)), 22.2 (-CH(CH_3)(*C*H$_3$)); FTIR (ATR) υ_{max} (cm^{-1}) 2968, 2933, 2877, 1751, 1384, 1037, 945; M_n (NMR) 11800 g/mol; M_n (GPC) 9800 g/mol; PDI = 1.31; Tg = 65 °C; TGA in Ar: $T_d^{5\%}$ = 190 °C, $T_d^{50\%}$ = 296 °C.

4.5 Results and Discussion

Expanding from previous glucose-based polycarbonates, we sought to create a flexible platform that can be easily modified to apply towards a broad range of applications. In order to achieve this goal, we designed a streamlined synthetic strategy that utilizes a glucose-based feedstock, tri-*O*-acetyl-D-glucal, to create a monomer possessing a six-membered cyclic carbonate that can be easily polymerized *via* ROP

with an organocatalyst, affording well-defined polymers. Glycals are used extensively as a chiral feedstock in organic chemistry for the preparation of non-carbohydrate natural products as well as biologically important complex carbohydrates and glycoconjugates. Tri-*O*-acetyl D-glucal, is decorated with fewer alcohol than glucose, leading to fewer protection/deprotection steps and a carbon-carbon double bond for post-polymerization functionalization and making it an attractive starting point for monomer synthesis. In addition, a Ferrier rearrangement reaction can allow for the incorporation of a seemingly endless variety of functional groups, allowing for an even greater degree of modifications, which increases the utility of the polymer. Finally, removal of an acyloxy functional group during allylic rearrangement leaves behind a masked 1,3 diol, leading to a streamline synthesis with few individual protection and deprotection steps.

4.5.1 Monomer Synthesis

Our approach involves a three step synthesis of a bicyclic carbonate, **3**, from tri-*O*-acetyl-D-glucal, a versatile synthon, for a family of functionalized carbonated monomers. In the presence of Lewis acids, cyclic enol ethers, having leaving groups at the allylic sites, readily undergo nucleophilic displacement reactions, otherwise known as the Ferrier Rearrangement. In the presence of $BF_3.EtO_2$, the departure of an acyloxy leaving group from the C3 position forms a stabilized allyloxycarbenium ion, upon which an *O*- nucleophile species attacks at the C1 position. Initially, methanol was utilized as a nucleophile which afforded the 2,3-unsaturated glycosyl product in high

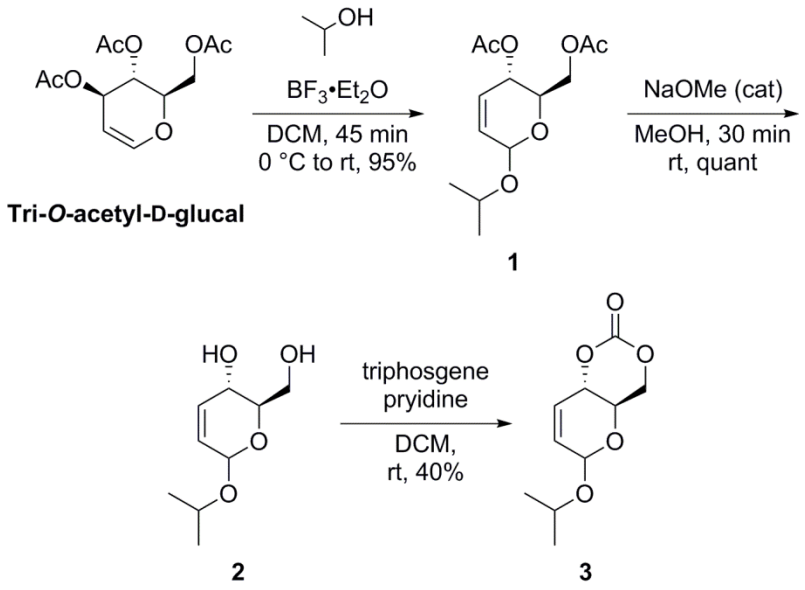

Scheme 4.1. Three-step synthesis of glucal-based cyclic carbonate monomer, **3**.

yields. However, removal of residual glucal proved difficult as the starting material and product share similar R_f and solubility. The ^{1}H NMR signal of the methoxy group also resided in the anticipated area of the methyl group of the intended polymerization initiator, 4-methylbenzyl alcohol, which could have created difficulty when calculating M_n by end group analysis. To avoid these complications, isopropyl alcohol was chosen as an appropriate nucleophile for this proof of concept, which afforded **1** in high yield (95%) favoring the α product in a 9:1 ratio. Bis-deacetylation of **1** under Zemplén conditions, afforded the somewhat unstable pseudoglycal, **2**, in quantitative yields and was used in the next step unpurified. Several conditions have been developed to form cyclic carbonates that do not utilize phosgene as a carbonylation agent, however due the previous difficulty in forming the glucose-bicyclic carbonate[104,105] and the anticipated increase in ring strain due to the double bond, a more reactive carbonylation agent was

employed. The cyclization reaction was performed successfully using triphosgene in the presence of pyridine in DCM at room temperature yielded the cyclic carbonate monomer, **3**, in modest yields (40%). In addition, it is important to note the stability of compounds **2** and **3**. When left under ambient conditions the white solid, **2**, decomposed into a brown sludge within a week and was only stable when stored under dry conditions at -20 °C for 1-2 months. However, after formation of the cyclic carbonate, the monomer proved stable indefinitely (+1 year) when stored in a glovebox (Ar, 30 °C).

4.5.2 Ring-Opening Polymerization Optimization

To test the suitability of these glucal-derived monomers for polymerization, we examined the organocatalyzed ROP of monomer, **3**, to afford glucose-based polycarbonates bearing an endocyclic alkene, or (PDGC-ene) and compared it to the ROP of other glucose-based cyclic carbonates[104,105] and other six-membered cyclic carbonates.[39,55] The ROP of **3** was conducted *via* an initiator/chain-end activation mechanism and studied as a function of time, catalyst type, and catalyst concentration. Table 4.1 summarizes the examination of the two-component catalyst consisting of the Lewis acid 1-(3,5-bis(trifluoromethyl)-phenyl)-3-cyclohexyl-2-thiourea (TU) with the Lewis base 1,8-diazabicyclo[5.4.0]undec-7-ene (DBU) and alternatively the superbase catalyst 1,5,7-triazabicyclo[4.4.0]dec-5-ene (TBD). The number-average molecular weights (M_n) were estimated using gel-permeation chromatography (GPC) and calculated using ^{1}H NMR spectroscopy by comparing the resonance for the methyl

Table 4.1. ROP optimization of glucal based monomer, **3**, *via* organocatalysis by TBD or DBU/TU with initiation by 4-methylbenzyl alcohol.[a]

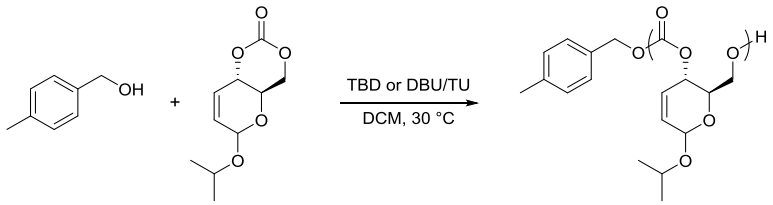

3 **4**

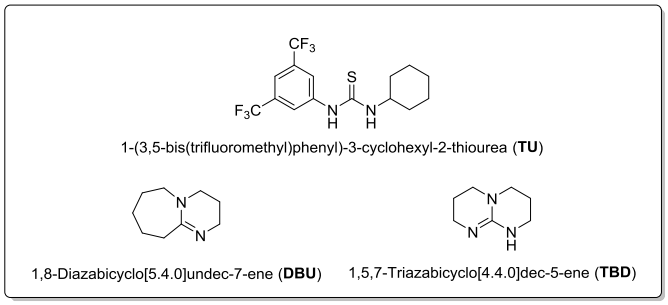

Entry	Polymer	Catalyst	Catalyst mol %	$[M]_0/[I]_0$ [b]	[M] [c]	Time (min)	Conv. (%) [d]	M_n (Da) [e]	M_n (Da) [f]	M_w (Da) [f]	PDI [f]
1	**4**	TBD	2	50	0.3	2	>99	11800	9800	12500	1.31
2	**5**	TBD	1	50	0.3	2	96	7500	8500	10800	1.27
						6	>99	11000	9400	11400	1.21
						10	>99	11000	9900	12900	1.30
3	**6**	DBU	5	25	0.3	1	89	3100	2100	2600	1.24
						5	98	4000	3400	3900	1.15
						10	>99	4000	3800	4300	1.13
4	**7**	TU/DBU	5	25	0.3	1	>99	4600	3300	3700	1.12
						5	>99	4600	3400	3800	1.12
						10	>99	4800	3700	4200	1.14
5	**8**	DBU	2	25	0.3	1	49	800	950	1300	1.37
						5	68	1000	1000	1400	1.40
						10	86	1600	1600	2100	1.31
6	**9**	TU/DBU	2	25	0.3	1	36	1200	780	810	1.03
						5	>99	5300	5000	6000	1.20
						10	>99	5700	5000	5900	1.18
7	**10**	DBU	1	25	0.3	1	29	400	210	220	1.05
						5	41	400	480	590	1.23
						10	57	1200	610	840	1.38

[a]The polymerization of **3** was carried out with TBD or DBU/TU in the presence of 4-methylbenzyl alcohol in CH_2Cl_2 at 30 °C under argon. [b]monomer/initiator feed ratio. [c]Concentration of **3** in mol/L. [d]Estimated by ^{1}H NMR analysis in CDCl3. [e]Estimated using ^{1}H NMR spectra in CDCl3. [f]Estimated by GPC (THF eluent) using polystyrene standards.

protons of the initiator with that of the methine proton on the isopropyl group of the repeat unit. Similar conditions to those used in previously reported glucose-based polycarbonates synthesized in the Wooley lab were used as a starting point (Table 4.1, Entry 1). Despite more dilute conditions (0.3 M as compared to 1.0 M), the conversion of **3** reached >99% within 2 min, much quicker than previously encountered with the methoxy-protected glucose-based cyclic carbonate monomer.[104,105] Lowering the catalyst loading to 1 mol% slowed the reaction, allowing for 96% conversion within 2 min and full conversion within 6 min, which, again, is significantly quicker than glucose-carbonate monomers[104,105] and trimethylene carbonate.[39] The GPC traces showed bimodal polymer peaks with high molecular weight shoulders (Figure 4.2) and PDIs ranging from 1.21 to 1.31, indicating the polymerization proceeded in an uncontrolled fashion. The use of TBD has been reported to broadening of polydispersity *via* transcarbonation of the polymer chains, which could explain the high PDIs.[55] To ensure uniform growth of glucal-based polymer, without allowing for adverse transesterification reactions found with the use of TBD, a less reactive catalyst system, TU-DBU, was explored.

By using TU-DBU catalyst and lowering the concentration to 2 mol %, conversion of **3** was able to be completed within 10 min but at a rate that could be easily monitored. The product, **9**, maintained a comparable number-average degree of polymerization (DP_n = 25) and PDI under 1.2. Under these conditions, transesterification was minimized, allowing for conversion in a controlled fashion. Additionally, conditions that did not utilize the Lewis acid, TU, suffered from slower

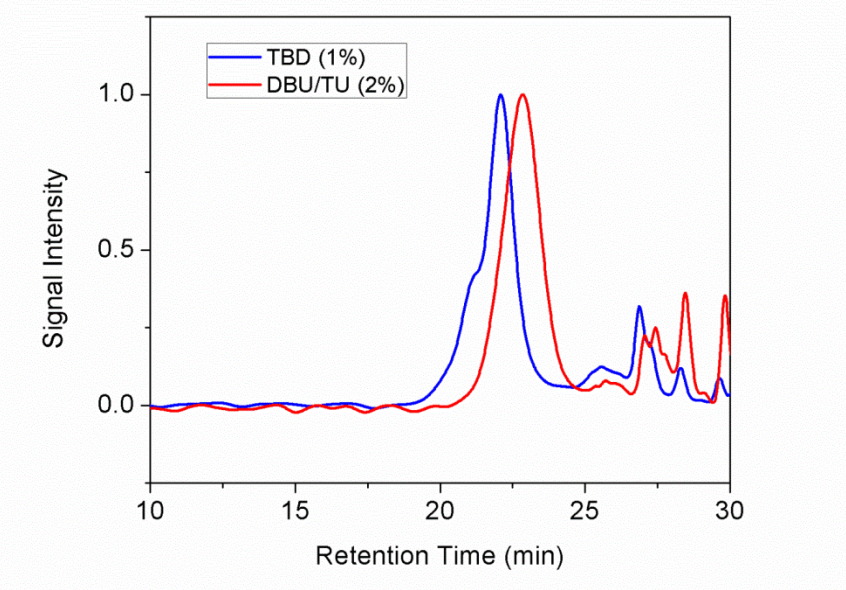

Figure 4.2. GPC traces of **5** (Table 2.1, entry 2, 6 min) and **9** (Table 4.1, entry 6, 10 min).

rates and higher PDIs. This could be due to the introduction of an alternate zwitterionic reaction mechanism. Takashi Endo was able to form linear polycarbonates from glucose-based five membered cyclic carbonates, using such a technique. Traditionally, anionic ring-opening of five-membered cyclic carbonates is more difficult than six- or seven-membered rings and usually require vigorous conditions with higher temperature and often proceed with the elimination of carbon dioxide, however, polymerization took place in the presence of DBU *via* a zwitterionic reaction mechanism, resulting in linear polymers with high PDIs (1.5-2.6).[98,99] The ease of ROP with low amounts of TU-DBU may be explained by the increase in ring strain due to the addition of the double-bond within the bicyclic ring system. Ring strain of the carbonate is evident from a shift in the carbonyl absorption band in the IR spectrum. The carbonyl band of trimethylene

carbonate[151] and various substituted six membered cyclic carbonates[151,152] occur around 1730 cm^{-1} (neat). In the case for fused bicyclic sugar systems shift can be observed in the carbonyl absorption band of about 25 cm^{-1}, occurring at 1755 cm^{-1}(neat), which is also slightly higher than the methoxy-protected glucose based cyclic carbonate monomer (1751 cm^{-1}, neat).[104] An increase in ring strain allowed for the use of a milder TU-DBU catalyst system in low quantities to produce well defined linear polycarbonates in a controlled fashion, with a low degree of transesterification.

The structure of the polycarbonate was confirmed by IR, ^{1}H NMR, and ^{13}C spectroscopies. Assignments of ^{1}H NMR and ^{13}C NMR spectra were performed by using COSY and HSQC NMR analyses. The characteristic carbonyl vibration of the carbonate linkage was observed at 1755 cm^{-1} in the IR spectra. As illustrated by the ^{1}H NMR spectra of **3** and **5** (Figure 4.3) the most significant proton resonance differences between the monomer and the polymer occurred for the pyranoside methine proton (labeled as 4, Figure 4.3), the methylene protons α to the carbonate linkage (6), and the alkenyl proton on C3. Compared to the monomer, the resonance of polymer proton 4 was shifted downfield from *ca*. 4.6 to 5.1 ppm, whereas the methylene protons shifted upfield from two distinct doublet of doublet peaks at 4.5 and 4.3 ppm to a single multiplet at 4.3 ppm. In addition, the alkenyl proton on C3 also had a slight upfield shift from 6.1 to 5.9 ppm. These shifts could arise from an electronic effect of the adjacent carbonyl group and the geometric conformational changes on the glycosidic ring upon opening of the six-membered cyclic carbonate during. Due to the simplicity of the monomer and choice of functional groups, the proton resonances lead to facile

calculations of conversions and molecular weights. The upfield shift of the alkenyl proton 3 created two non-overlapping peaks which allowed for the straightforward calculation of conversion rates. The values of M_n estimated by ^{1}H NMR analysis [based on the ratio of the integral for the methine isopropyl proton in the repeat unit (4.0 ppm) to that of the methyl protons of the initiator at the α-chain end (2.3 ppm)] were in close accord with GPC-estimated values and theoretical values of 10833 Da (DP_{50}) and 5477 Da (DP_{25}).

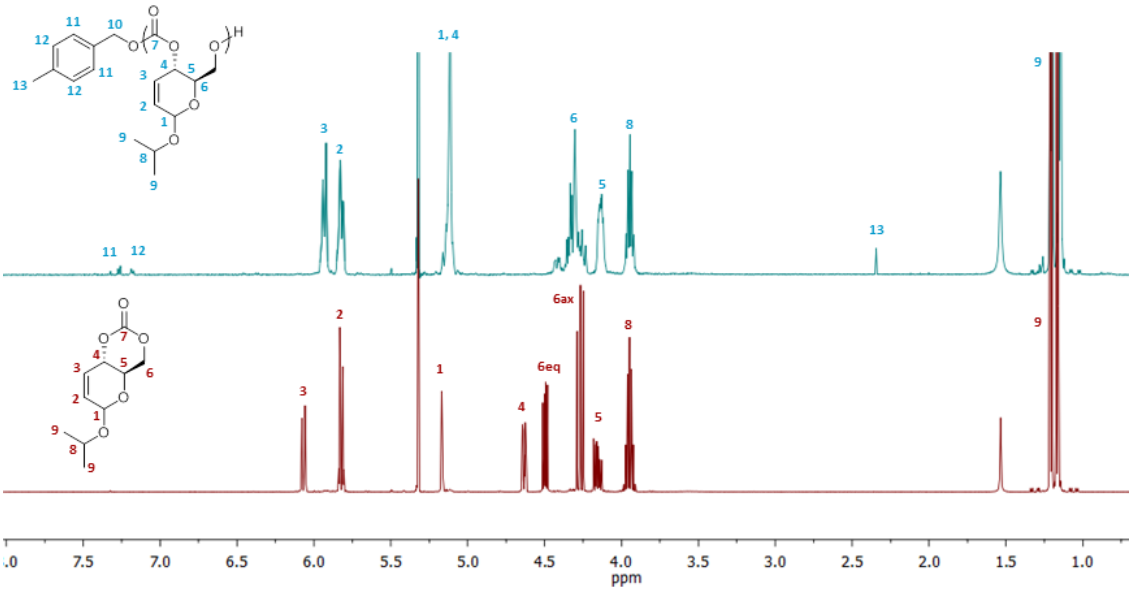

Figure 4.3. ^{1}H NMR spectra (CD_2Cl_2) of glucal-based monomer, **3** (bottom), and PDGC-ene polymer **9** (top).

The ^{13}C NMR spectra showed the characteristic downfield shift, from 148 to 155 ppm, of the carbonate resonance upon ring opening (Figure 4.4). Expanding the carbonyl carbon region shows three sets of observed signals. The dual-activation ring-

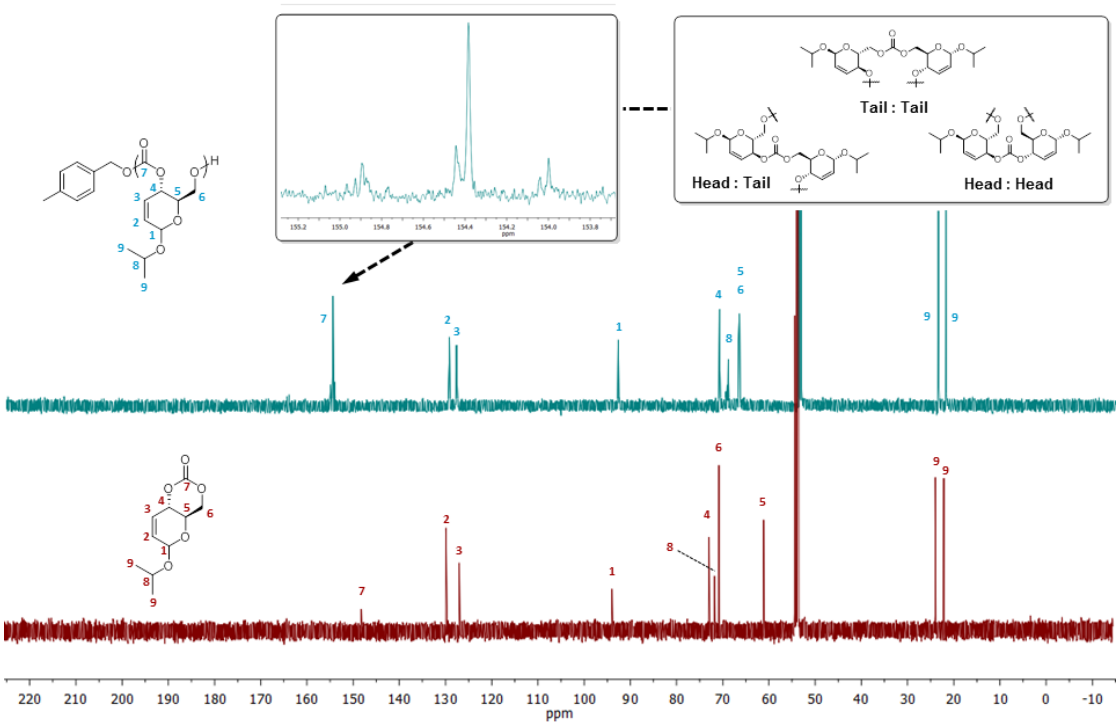

Figure 4.4. ^{13}C NMR spectra (CD_2Cl_2) of glucal-based monomer, **3** (bottom), and PDGC-ene polymer **9** (top).

opening polymerization mechanism catalyzed by TU-DBU involves an activated alcohol attacking the cyclic carbonate in a nucleophilic acyl-substitution reaction whereby the hydroxyl nucleophile first adds to the C=O of the carbonate to give a hydrogen bonded tetrahedral intermediate that subsequently collapses to a hydroxyalkylcarbonate. In this case, acyl oxygen bond cleavage at the different sides of the carbonyl leads to two possible hydroxyalkylcarbonates. Successive addition of glucal based monomers at one of the two types of chain terminal alcohols can lead to three different types of linkages:

head-to-head (HH), head-to-tail (HT) and tail-to-tail (TT) (see Figure 4.4). Similar trends were also observed in the ROP of glucose-based carbonates, which was further supported through ESI tandem MS analysis, which may be influenced by the methoxy protecting groups.[104] It has been demonstrated excessively bulky substituents (*e.g.* 2,2-diphenyl) can impede the ring-opening of six-membered cyclic carbonates and different types of substituents can have an effect on regiochemical preferences. Recently in the Wooley lab, several variations of the glucose-based cylic carbonate monomers, sporting different types of protecting groups on positions 2 and 3, have been synthesized and displayed different trends in regioregularity. The two different classes of side groups (ether and carbonate) showed distinct distributions in terms of regiochemistries of the resulting polymers, as demonstrated by ^{13}C NMR. Ether type protecting groups possessed similar regiorandom distributions, similar to previously reported methoxy protected polymers, whereas the carbonate protected monomers led to regioregular polymers, predominately HT linkages. These trends could be explained by steric or electronic effects created by the carbonyl groups. Interestingly, removal of large side groups and inserting a double bond into the ring has had an effect on the polymer regioregularity. Resonances from all three types of linkages are present in the ^{13}C NMR spectrum; however the intensity of the HT signal is significantly greater than the HH and TT signals. If the acyl-oxygen bond cleavage occurs randomly at either side of the carbonyl, than the probability ratio of HH:HT:TT should be 1:2:1. The integration of the three signals in Figure 4.4 was 1.0 : 4.3 : 0.9, which indicates that the acyl-oxygen bond cleavage occurs preferentially on one side of the carbonate carbonyl.

4.5.3 Thermal Characterization

The thermal properties of the glucal based polycarbonates were evaluated by differential scanning calorimetry (DSC) and thermogravimetric analysis (TGA) under inert atmosphere (Figure 4.5). A single endothermic peak was present in all three heating cycles of the DSC thermogram displayed in Figure 4.5, representing a glass transition (T_g) temperature at 65 °C. The increased chain rigidity due to cyclic structure incorporated into the main chain makes the T_g significantly higher than common aliphatic polycarbonates. However, the absence of side chains on C2 and C3 positions reduces the degree of interchain entanglement, and thus T_g is not as elevated as other homopolymers synthesized from sugar-based six-membered cyclic carbonates. No information to indicate crystallinity was observed, though heating scans did not exceed 150 °C in temperature due to concerns of thermal degradation. These polymers exhibit amorphous properties, like previously synthesized PDGCs, however further studies by X-ray diffraction (XRD) would need to be completed to confirm these observations.

Thermal degradation initiated at relatively low temperatures (200-310 °C for initial to complete mass loss; (Figure 4.5). The addition of the carbon-carbon double bond to the glycosidic ring has made the polymer more thermally sensitive, when compared to previously synthesized PDGCs.[104] The double bond could make the repeat unit prone to elimination and loss of carbon dioxide, which in terms of the percent loss of mass (20%) correlates to the contribution of carbon dioxide to the repeat unit.

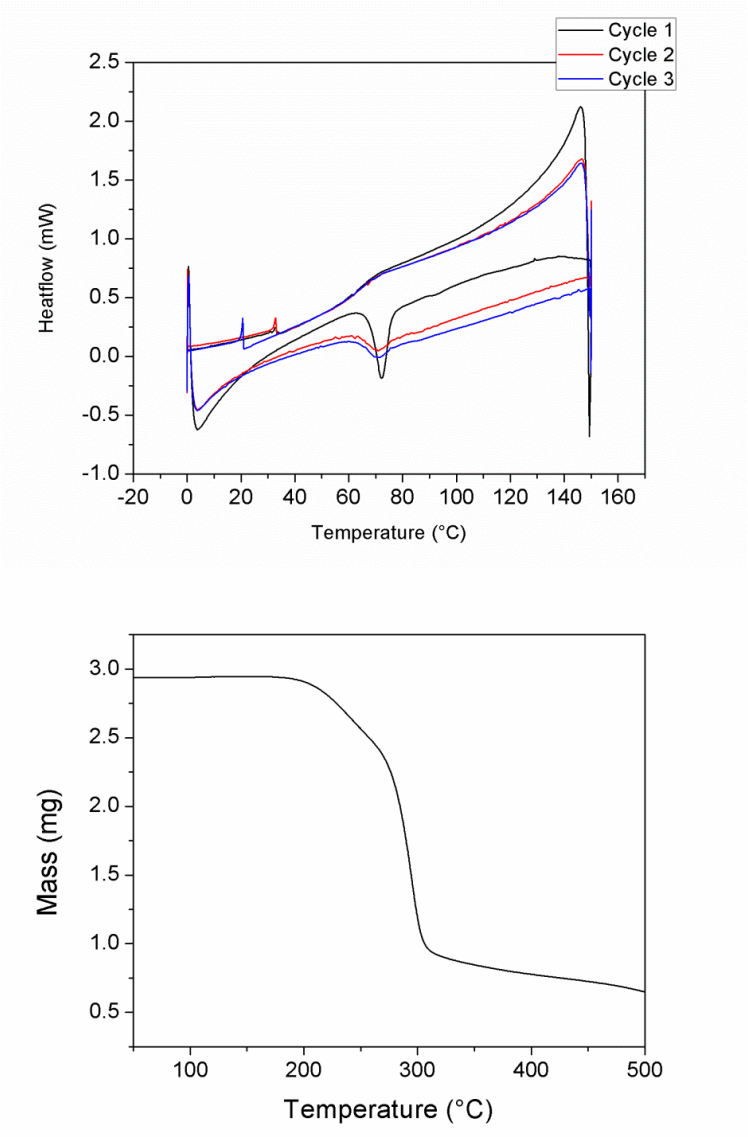

Figure 4.5. Thermal analysis by DSC (top) and mass loss as a function of temperature (bottom) of PDGC-ene polymer **4**.

4.6 Conclusions

In summary, we have demonstrated the synthesis of a glucal-based cyclic carbonate monomer and its controlled ROP *via* the organobase DBU and organic cocatalyst TU to afford a polycarbonate having regioregular properties, well-defined end groups and narrow molecular weight distributions. Design of highly-strained monomers led to rapid reactions that could polymerize in dilute conditions with low catalyst loading. These synthetic methodology developments expanded the use of glucose as a monomer feedstock to create polycarbonate-engineering materials with complex functionalities. Furthermore, thermal analysis revealed that this glucal-based polycarbonate exhibits an amorphous character and comparably high T_g than common aliphatic polycarbonates, making it attractive for a broad range of potential applications. In particular, such materials may impact numerous fields ranging from hydrolytically or thermally degradable materials to tissue engineering and nanotherapeutic delivery vehicles. Moreover, the synthetic design allows for simple modification to incorporate into the monomer a wide range of functionality that allow for the creation of large family of polycarbonates with varying properties. This new architecture constitutes a step towards the next generation of biomaterials, designed from renewable resources with improved properties, biocompatibility, and degradation characteristics.

CHAPTER V

TUNABLE, MULTIFUNCTIONAL, POLY(THIOETHER-CO-CARBONATE) SHAPE MEMORY BIOMATERIALS PREPARED FROM THE NATURAL PRODUCT, QUINIC ACID

5.1 Original Publication Information*

This chapter contains excerpts from the article *Photo-cross-linked Poly(thioether-co-carbonate) Networks Derived from the Natural Product Quinic Acid*. Contents concerning with the synthesis and mechanical testing by DMA found in the article and supporting information, which was originally a separate document, have been included in the chapter, and schemes and figures have been renumbered to the style of this document. Submersion DMA testing, tensile testing, and comparisons to TATATO-based thioether thermosets were excluded. Additional shape memory testing by DMA of select samples, not found in the article, is also included in this chapter.

5.2 Overview

Polycarbonate networks derived from the natural product, quinic acid, that can potentially return to their natural building blocks upon hydrolytic degradation are described herein. Solvent-free thiol–ene chemistry was utilized in the copolymerization of tris(alloc)quinic acid (TAQA), diallyl carbonate (DAC), and a variety of multifunctional thiol monomers to obtain poly(thioether-*co*-carbonate) networks with a wide range of achievable thermomechanical properties including glass transition temperatures from −18 to +65 °C, storage moduli from 357 to 1440 MPa at 25 °C, and rubbery moduli from 3.8 to 20 MPa at 100 °C. Control force cyclic testing by DMA showed excellent shape memory behavior for 1,2-EDT-*co*-TAQA and 1,2-EDT-*co*-TAQA-*co*-DAC materials. High percent recoverable strains were obtained, reaching 100% recovery during fourth and fifth cycles.

5.3 Introduction

Polymers derived from natural resources have attracted increased attention not only for their ability to form renewable commodity plastics, which decrease dependence on petroleum processes, but also for their ability to form biocompatible materials with resorbable degradation products.[153] An important application of degradable polymers is biomedicine, where incorporation of biocompatibility and biodegradability is paramount. Recently the Wooley lab has expressed interest in developing degradable polycarbonates

from renewable resources, such as quinic acid,[133] glucose,[104,105] and ferulic acid.[141] Quinic acid, a naturally occurring compound found in coffee beans and other plants that is known for its growth-promoting properties, was previously investigated as a feedstock for unique degradable polycarbonates. It was originally selected as a starting material because of easy access to a bicyclic diol-monomer by known lactonization and selective silylation, which could lead to materials possessing high-temperature thermal transitions. Polymers with modest high molecular weights (M_n = 7.5-7.7 kDa) were produced with copolymerization with diphosgene in pyridine. As a result of the bicyclic structure of the monomer, these polymers exhibited thermal properties similar to other highly rigid polymers, with glass transition temperatures over 200 °C. However, difficulties arose during initial attempts of mechanical testing. With such high glass transition temperatures and low molecular weights (<7 kDa), the resulting films were brittle and not strong enough to form films that could undergo mechanical characterization by DMA or tensile testing. One possible solution to this problem would be to cross link the polymers to afford more robust films. With this in mind, a synthetic scheme was proposed to modify the existing monomer to form fully crosslinked materials.

Reported herein, are the synthesis and characterization of amorphous polycarbonate thermosets derived from the natural product quinic acid. Solvent-free thiol-ene chemistry was utilized in the copolymerization of tris(alloc)quinic acid (TAQA) and a variety of multifunctional thiol monomers to obtain poly(thioether-*co*-carbonate) three-dimensional networks with a wide range of thermomechanical properties. In addition, diallyl carbonate (DAC) was also used as a potential

comonomer, to allow for additional thermomechanical tunability without changing chemical composition of the system.

5.4 Experimental

5.4.1 Materials

Quinic acid, Amberlyst 15 ion-exchange resin, *N,N,N',N'*-tetramethylethylenediamine, allyl chloroformate, diallyl carbonate, 2,2-dimethoxy-2-phenylacetophenone (DMPA), 1,2-ethanedithiol, 2,3-butanedithiol, 1,6-hexanedithiol, trimethylolpropane tris(3- mercaptopropionate), and triallyl-1,3,5-triazine-2,4,6-trione were purchased from Sigma Aldrich. Tetraethylene glycol bis(3-mercaptopropionate) was purchased from Wako Chemical. These chemicals were used as received.

5.4.2 Characterization

Monomer Synthesis and Characterization. Quinic acid lactone and tris-alloc-quinic acid monomer (TAQA) were characterized by ^{1}H, ^{13}C, COSY, and HSQC nuclear magnetic resonance (NMR) obtained on an Inova 500 MHz spectrometer using the solvent as an internal reference. IR spectra were obtained on a Shimadzu IR Prestige attenuated total reflectance Fourier-Transform infrared spectrometer (ATR-FTIR).

Spectra were analyzed using IRsolution v. 1.40 software (Shimadzu Corp., Japan). High resolution (HRMS) was conducted on an Applied Biosystems PE SCIEX QSTAR.

Thermal Characterization. Differential scanning calorimetric (DSC) studies were performed on a Mettler-Toledo DSC822^e (Mettler-Toledo., Columbus OH), with a heating rate of 10 °C/min. The T_g was taken as the midpoint of the inflection tangent, upon the third heating scan. Thermogravimetric analysis was performed under argon atmosphere using a Mettler-Toledo model TGA/DSC 1 Star^e system, with a heating rate of 10 °C/min. DSC and TGA measurements were analyzed using Mettler-Toledo Star software version 10.00c.

Dynamic Mechanical Analysis. DMA experiments were run in strain mode in tension to determine thermomechanical profiles for the thermoset poly(thioether-*co*-carbonate) samples. Rectangular DMA specimens (4 mm x 25 mm x 0.4 mm) were machined using a Gravograph LS100 40 W CO_2 laser machining device. All laser machined samples were sanded around the edges using 400, then 600 grit sandpaper. DMA was performed using a TA Instruments Q800 Dynamic Mechanical Analyzer in the DMA Multifrequency/Strain mode in tension using a deformation of 0.1% strain, a frequency of 1 Hz, a force track of 150%, and a preload force of 0.01 N. Each experiment was run from -20 to 180°C using a heating rate of 2°C/min.

Shape Memory Characterization. Rectangular DMA specimens (4 mm x 25 mm x 0.4 mm) were machined using a Gravograph LS100 40 W CO_2 laser machining device. All laser machined samples were sanded around the edges using 400, then 600 grit sandpaper. In the DMA strain rate mode in tension, the rectangular samples were

heated to T_g + 10 °C or T_g + 15 °C, allowed to equilibrate for 30 min, and then strained to deformation of 20% and 25%. The strained samples were then cooled to 0 °C and allowed to equilibrate for an additional 30 min. During free strain recovery experiments, which were used to measure the recovery stress of the materials, the drive force of the DMA instrument was set to zero after equilibration at 0 °C, after which 20% or 25% prestrained samples were reheated to 100 °C at 2 °C/min as recoverable strain was measured, and upon reaching 100 °C, the samples were cooled back to $T = T_g$ +10 °C or $T = T_g$ + 15 °C, and four more free strain recovery cycles were subsequently carried out to afford a five-cycle experiment. Percent recoverable deformation was recorded using TA instruments QSeries software.

5.4.3 Synthesis

Quinic acid lactone (1). A mixture of D-(–)-quinic acid (9) (50.0 g, 260.2 mmol), Amberlyst® 15 ion-exchange resin (7 g, 35 mmol), benzene (500 mL) and DMF (125 mL) was refluxed under a Dean-Stark trap for 16 h. The reaction mixture was cooled to 23 °C and filtered over a pad of Celite. The filtrate was then evaporated under reduced pressure to afford a clear thick oil, which was diluted with CH_2Cl_2 (150 mL). Hexanes (250 mL) was added and the resulting mixture was allowed to sit at 23 °C for 2 h. The product was collected by vacuum filtration, and was further dried in *vacuo* to afford lactone in 96% yield. Spectroscopic and MS data are in good accord with previously described synthesis.[154]

Tris-alloc-quinic acid (TAQA). QA lactone (4.081 g, 23.43 mmol) was added to a flame-dried 250-mL schlenk flask nitrogen, DCM (30 mL) was added and the solution was cooled to -5 °C. TMEDA (14.5 mL, 96.8 mmol) was added and allowed to stir at -5 °C for 20 min. To an addition funnel equipped with a pressure equalizing side arm, allyl choroformate (17.8 mL, 168 mmol) was added and diluted with DCM (10 mL). Dropwise addition (*ca.* 1 drop/5 s) of the allyl chloroformate and DCM mixture to the flask proceeded for about 4 h. The reaction was maintained between -5 °C and -10 °C, stirring rapidly for 2 h after the addition was complete. The reaction was allowed to warm to room temperature and stirred overnight. The thick white solid that remained was dissolved in DCM and filtered. The filtrate was washed twice with deionized water, once with a 10 wt% $CuSO_4$ solution, dried with $MgSO_4$, filtered and concentrated. The crude product was purified by column chromatography (SiO_2, hexane-ethyl acetate, 3:2) to afford 7.406 g of tris(alloc) quinic acid (74%).

Tris-alloc-quinic acid (TAQA). T_m = -21 °C. ^{1}H NMR ($CDCl_3$, 300 MHz): δ 5.97-5.88 (m, 3H, H10), 5.41 (t, 1H, *J* = 5.1, 4.6 Hz, H4) 5.41-5.27 (m, 6H, H11), 5.04 (ddd, 1H, *J* = 11.7, 6.9, 4.5 Hz, H5), 4.96-4.94 (dd, 1H, *J* = 6.0, 4.9 Hz, H3), 4.65-4.62 (m, 6H, H9) 3.22-3.18 (ddd, 1H, *J* = 11.6, 6.1, 2.8 Hz, H2), 2.57-2.55 (d, 1H, *J* = 11.4 Hz, H2), 2.46-2.41 (ddd, 1H, *J* = 12.1, 6.9, 2.8, H6), 2.35 (t, 1H, *J* = 11.9, H6); ^{13}C NMR ($CDCl_3$, 125 MHz): δ 170.6 (C7-lactone), 153.8 (C8-carbonate), 153.3 (C8'-carbonate), 152.3 (C8"-carbonate), 131.2 (C10-alkene), 131.0 (C10'-alkene), 130.8 (C10"-alkene), 119.9 (C11-alkene), 119.8 (C11'-alkene), 119.46 (C11"-alkene), 77.5 (C1), 73.4 (C3), 69.6 (C9), 69.5 (C9'), 69.4 (C5), 69.3 (C9"), 67.9 (C4), 33.5 (C2), 33.4

(C6); FTIR-ATR (neat, cm^{-1}): 2985, 2956, 1809 (C=O), 1747 (C=O), 1651, 1448, 1425, 1417, 1367, 1274, 1228, 1211, 1161, 1145, 1103, 1083, 1039, 989, 937, 781, 750; HRMS (+ESI) m/z calc'd for $C_{19}H_{22}O_{11}$ [M+K]+ : 465.08, found 465.0794.

General Procedure for Thermoset Film Fabrication. Mixtures of multifunctional thiol and TAQA and/or DAC were prepared in ratios to afford equal stoichiometric amounts of thiol functional groups to double bonds. The amount of photoinitiator, 2,2-dimethoxy-2-phenylacetophenone (DMPA), was massed to 1 wt% of each mixture. DMPA was first dissolved in the multifunctional thiol and then TAQA was added and blended thoroughly. Neat films were cast by injecting the solutions between two glass slides separated by a 0.5 mm slide-cover spacer, and exposed to UV light (365 nm) for 15 min. A release agent, PDMS, was used in the mold casting of films, to prevent adherence to the glass slides. After exposure to UV light, the glass molds were removed and the freestanding films were post-cured at 100 °C, at ambient pressure for 120 min, or as otherwise noted. Films produced with DAC were made in the same fashion with the exception of the addition of DAC to TAQA before mixing with the multifunctional thiol.

5.5 Results and Discussion

5.5.1 Monomer Synthesis

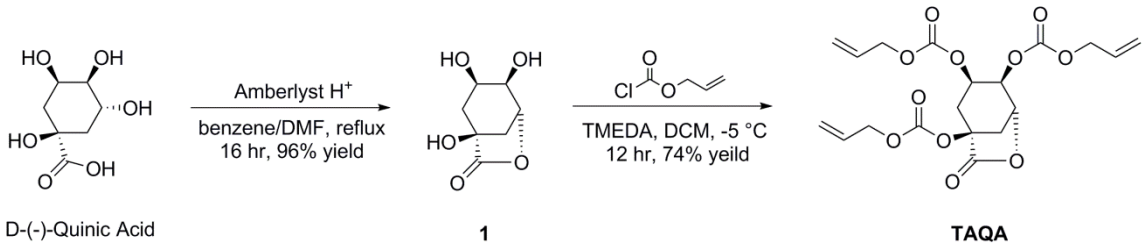

Scheme 5.1. Efficient two-step synthesis of TAQA monomer from D-(-)-quinic acid.

To introduce mechanical robustness into quinic acid materials, a tri-ene-functionalized quinic acid-based monomer was synthesized in two steps (Scheme 5.1). The first step in the monomer synthesis was a well-established lactonization of quinic acid under acidic conditions.[154] Quinic acid and acidic Amberlyst resin were suspended in benzene and *N,N'*-dimethylformamide and heated to reflux with azeotropic removal of water to afford the bicyclic triol quinic acid lactone in 96% yield. To install the three allyloxycarbonyl (alloc) protecting groups, which would ultimately serve as reactive centers during thiol-ene polymerization, allyl chloroformate was added dropwise to quinic acid lactone suspended in *N,N,N'N'*-tetramethylethylenediamine and dichloromethane to give 74% yield of TAQA as a clear, viscous oil. The structure of TAQA was confirmed by FTIR and electrospray ionization mass spectrometry, as well as ^{1}H, ^{13}C, COSY, and HSQC NMR spectroscopies.

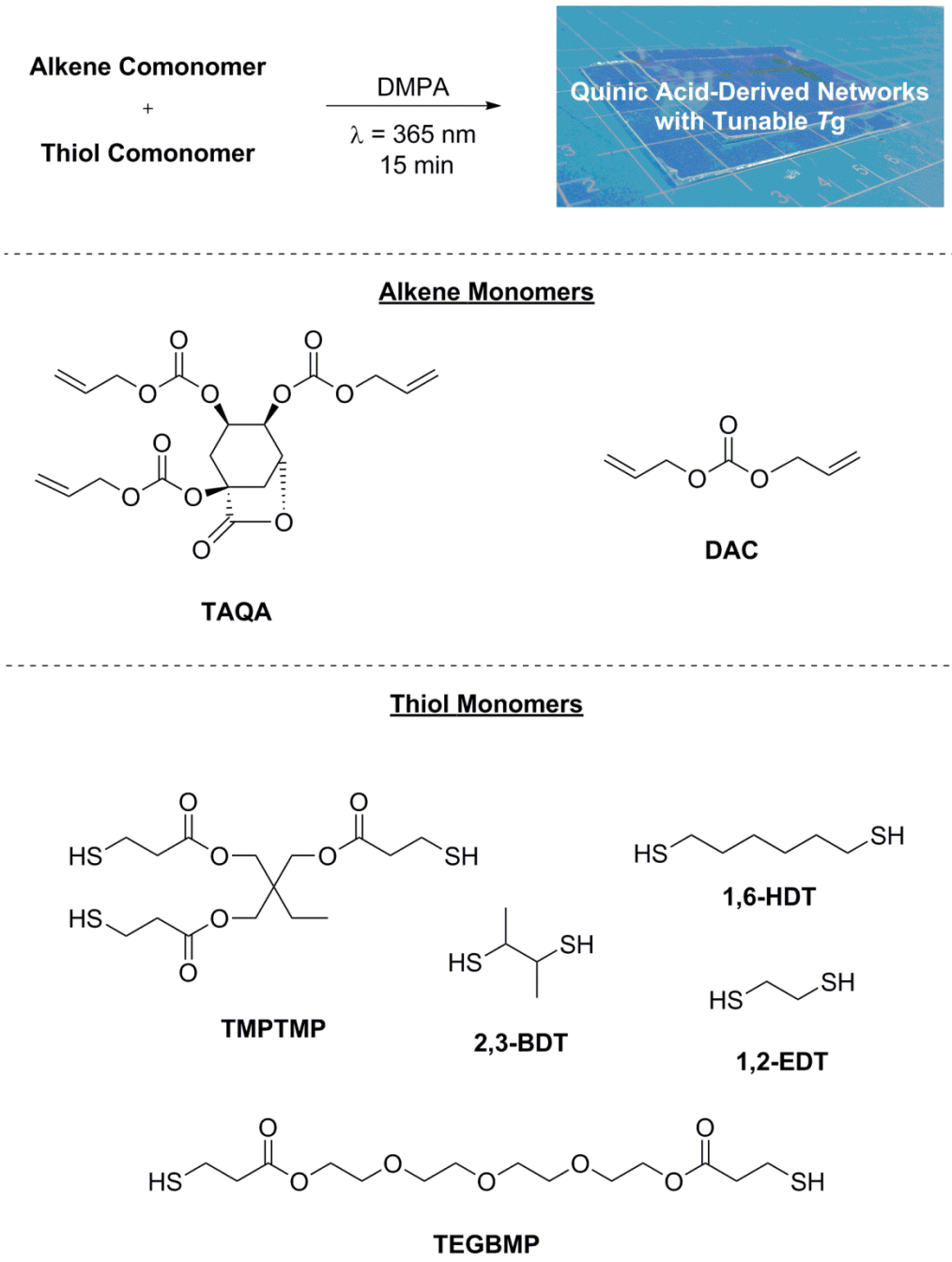

Scheme 5.2. General scheme for photo-crosslinking of poly(thioether-*co*-carbonate) networks and example of resulting cured thermoset (above). Structures and abbreviations of alkene and thiol monomers found below.

.

5.5.2 Polymerization by Solvent Free, UV-catalyzed Thiol-Ene Reaction and Post-Cure Optimization

Three-dimensional networks were formed by photo-catalyzed thiol-ene reaction of TAQA with a series of polythiols. Solvent-free crosslinking copolymerization by thiol-ene radical addition in the presence of 1 wt % 2,2-dimethoxy-2-phenylacetophenone (DMPA) photoinitiator was performed by mixing TAQA and multifunctional thiols based on equal molar functional groups, until a homogenous solution was achieved, mold casted, and exposed to UV light (λ = 365 nm) for five minutes to produce films with uniform thickness (0.4 mm). To ensure complete thiol-ene reaction between comonomers, the films were subjected to an additional post-curing phase at 120 °C. A series of films were produced to study the effect of varying post-cure times and to determine the minimum time needed to ensure complete cross-linking. Four different films were made with TAQA and 1,2-EDT, which were subjected to post-cure for 0 min, 120 min, 6 h, and 24 h (Figure 5.1). Analysis by dynamic mechanical analysis (DMA) revealed that at least 120 min was needed to ensure complete cross-linking; glass transitions, as approximated by the tan delta peaks and storage moduli, shifted from *ca*. 45 °C to 65 °C. In addition, the tan δ went from a broad peak to a sharp monomodal peak, evidence of a formation of a more uniform network. Minimal variation between the glass transition region of the storage modulus and tan δ peak occurred beyond 120 min of post-cure. In addition, samples were characterized by FTIR to verify consumption of alkene (1650 cm^{-1}) and thiol (2750 cm^{-1}) groups upon network

formation. As a result, all film formulations were subjected to at least 120 min of post-cure at 120 °C.

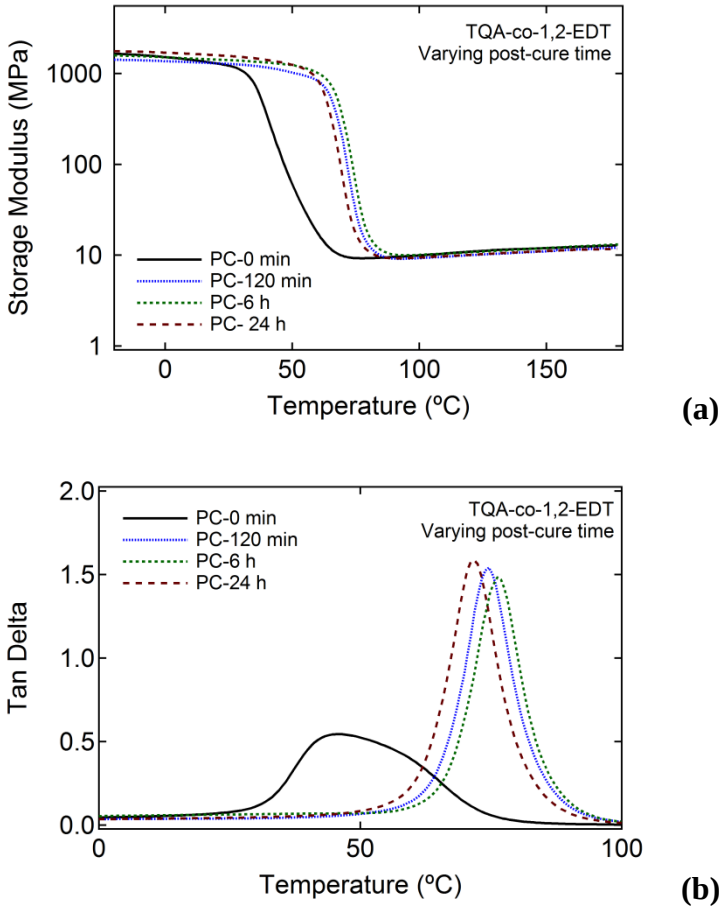

Figure 5.1. Effect of post-cure time at 120°C on storage modulus (a) and tangent delta (b) of TAQA-*co*-1,2-EDT thermosets.

Table 5.1. Thermal transitions and moduli exhibited by poly(thioether-*co*-carbonate) networks derived from quinic acid monomer, TAQA.

Sample	Thiol	Ene	T_g (°C)[a]	Tan δ (°C)[b]	T_d^5 (°C)[c]	E' (MPa)[d]	E_r (MPa)[e]
1	TEGBMP	TAQA	-18	36	264	357	7.3
2	TMPTMP	TAQA	43	55	275	1290	14
3	1,6-HDT	TAQA	48	59	261	1110	12
4	2,3-EDT	TAQA	51	64	261	1440	3.1
5	1,2-EDT	TAQA	65	63	262	1400	10
6	1,2-EDT	TAQA (0.75) DAC (0.25)	-	62	-	1400	10
7	1,2-EDT	TAQA (0.71) DAC (0.29)	-	53	-	1200	10
8	1,2-EDT	TAQA (0.50) DAC (0.50)	-	38	-	1200	10
9	1,2-EDT	TAQA (0.25) DAC (0.75)	-	-15	-	-	4.0

[a]Determined by DSC. [b]Tan δ measured by DMA. [c]Onset of thermal decomposition determined by thermogravimetric analysis. [d]Storage modulus at 25 °C determined by DMA. [e]Rubbery modulus determined by DMA at 100 °C.

5.5.3 Study of Thermomechanical behavior by DMA

A variety of multifunctional thiols was investigated including, 1,2-ethanedithiol (1,2-EDT), 2,3 butanedithiol (2,3-BDT), 1,5 hexanedithiol (1,6-HDT), trimethylolpropane tris(3-mercaptopropionate) (TMPTMP), and tetraethylene glycol bis-(3-mercaptopropionate) (TEGBMP). The DMA results in Table 5.1 show the relative

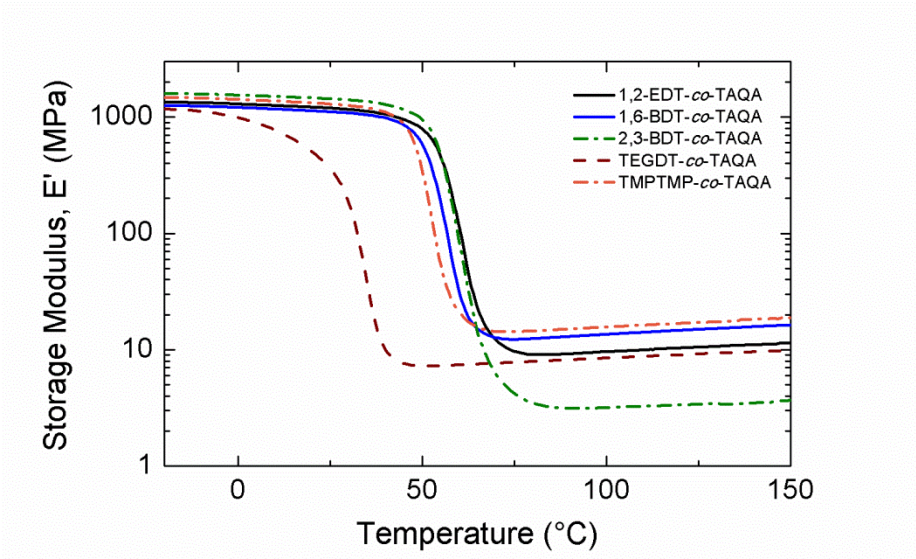

Figure 5.2. Storage modulus measurements of TAQA films copolymerized with various multifunctional thiols by DMA as a function of temperature.

thermomechanical behavior in tension of cured samples synthesized from TAQA and various thiol comonomers. This behavior is consistent with amorphous, crosslinked polymers, which include a glassy modulus plateau at temperatures below the glass transition, a transition region in which the modulus decreases with increasing temperature, and a rubbery region in which the modulus remains relatively constant with increasing temperature. The crosslinking density of a thermosetting polymer is proportional to its rubbery modulus plateau in accordance to an ideal rubber. Materials incorporating TMPTMP had the highest crosslink density because of its increased thiol functionality compared to the other thermosets. The relatively low cross link density of the 2,3-BDT-*co*-TAQA networks, when compared to the other materials, can be attributed to the ineffective cross linking due to the steric hindrance by the secondary

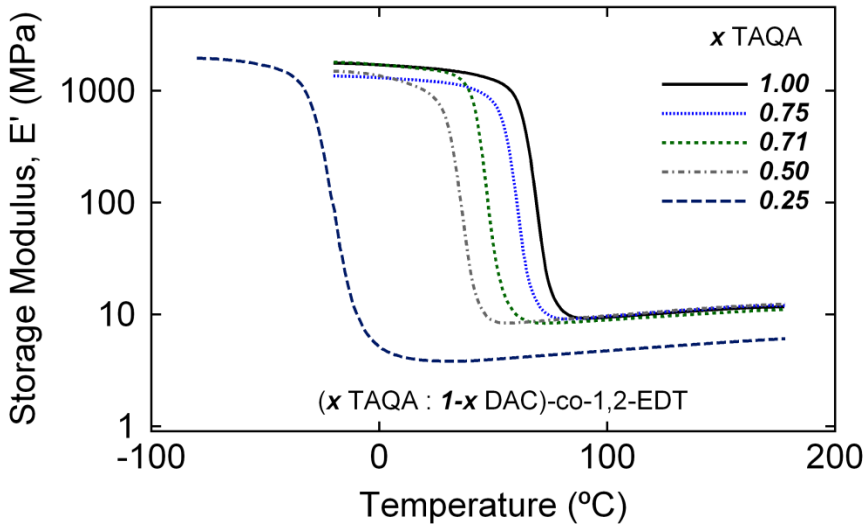

Figure 5.3. Storage modulus measurements of 1,2-EDT-*co*-TAQA films with varying amounts of DAC by DMA as a function of temperature.

thiols of 2,3-BDT. The T_g values, as determined by DSC, are consistent with the onset of the glass transition in the storage modulus of each sample. The 1,2-EDT-*co*-TAQA contained the greatest mass fraction of the rigid, bicylic TAQA monomer and the lowest mass fraction of aliphatic spacer atoms and, thus, exhibited the highest T_g value (65 °C). In contrast, the TEGBMP-*co*-TAQA system's longer and more flexible glycol spacer resulted in an elastomeric material with a T_g well below room temperature (-18 °C).

In addition to variation in thiol-functionality, manipulation of the ene-portion of the polymer system was explored by utilizing diallyl carbonate (DAC) as a third comonomer. Diallyl carbonate was chosen as a potential comonomer in order to modify materials' glass transition without changing the chemical makeup of the polymer system.

Films were formed in the same fashion as previously described, DAC, TAQA, 1,2-EDT, and DMPA were mixed thoroughly to form a homogenous solution, which was then casted between two glass slides, cured under UV light, and post-cured at 120 °C for 2 hours. DAC, along with TAQA was varied to maintain equal molar amounts of ene and thiol functional groups (Table 5.1, Entries 5-8). The 1,2-EDT-*co*-TAQA sample contains the greatest mass amount of the rigid bicyclic monomer and thus, has the highest glass transition of the 1,2-EDT-containing samples. It was hypothesized that the introduction of the flexible DAC comonomer would reduce the mass amount of the rigid TAQA monomer in the system and lower the amount of crosslinking, both of which would afford materials with lower T_gs. Confirmed by DMA, an inverse correlation between DAC amount and T_g was found; as DAC content increased, the T_g of the films decreased. The film with the highest amount of DAC (75% DAC, 25% TAQA), possessed the transition at the lowest temperature, with a tan δ peak at -15 °C. Interestingly, as DAC content was varied from 0% to 50%, in regards to alkene molar concentrations, the tan δ of the material was able to shifted from 65 °C to 38 °C without affecting the rubbery moduli, which was found to be 10 MPa at 100 °C for formulations with 0-50% DAC content. However, materials with higher DAC content exhibited lower rubbery moduli (4.0 MPa at 100 °C) as seen in Figure 5.3.

5.5.4 Study of Shape-Memory Behavior by DMA

Shape memory polymers (SMPs) are a class of stimuli-responsive materials that exhibit geometric transformations in response to subjection to external stimuli such as heating or light exposure, and a number of SMP-based biomedical implant devices are currently being proposed.[155] Various applications may demand SMPs with tailorable actuation temperature, recoverable strain, recovery stress, modulus at physiological conditions and toughness, in addition to good biocompatibility.[156] The moduli, toughness, and processability of many SMP systems has been shown to be highly dependent on the nature and extent of crosslinking in the SMPs.[157] As demonstrated earlier, the thermomechanical behavior of TAQA-based thermosets are highly dependent on the chemical and physical nature of the thiol and alkene comonomers. For a thermally actuated, one-way SMP, the polymer constituents that undergo thermal transitions upon heating or cooling across the SMP switching temperature T_{trans} are referred to as "switching segments," and crosslinks, whether covalent, physical, or other are referred to as "netpoints." Netpoints prevent switching segment chains from permanently sliding past one another during straining to a secondary geometry by effectively acting as anchors that enable shape recovery to occur.[158] Covalently crosslinked SMP systems often exhibit advantages in mechanical behavior over those of physically crosslinked SMP systems, including better cyclic shape memory and greater percent recoverable strains.

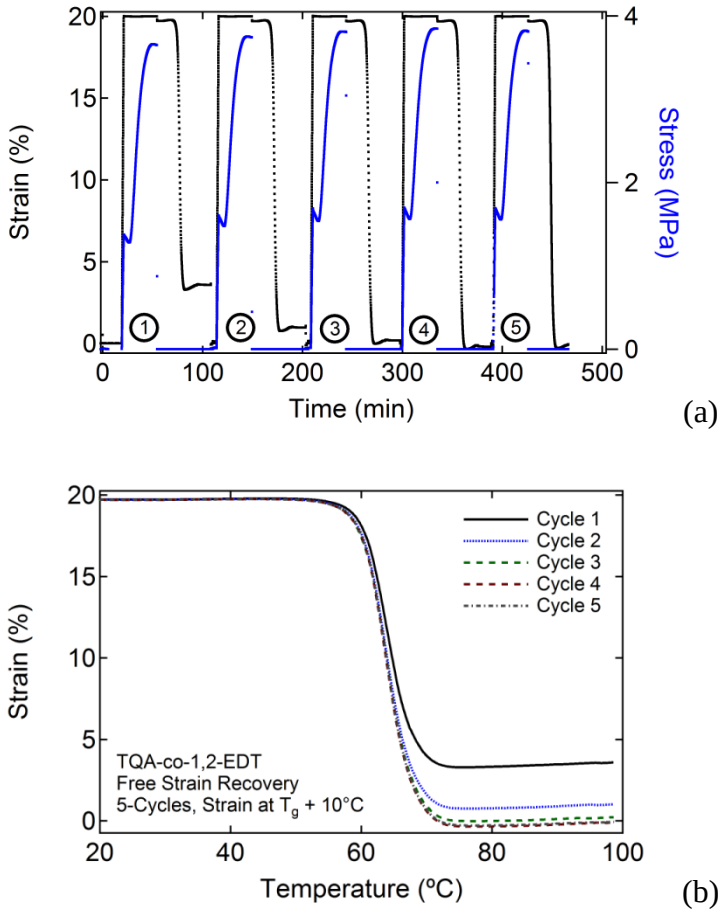

Figure 5.4. Demonstration of the shape memory effect over five cycles of 20% applied strain for poly(thioether-*co*-carbonate) thermoset made from TAQA and 1,2-EDT. Greater than 99% recoverable strains were recovered during cycles 4 and 5.

Select samples (1,2-EDT-*co*-TAQA and 1,2-EDT-*co*-TAQA-*co*-DAC) underwent control force cyclic testing by DMA in order to test their effectiveness as a shape memory material. The shape memory characterization data provided in Figure 5.4 demonstrates that the polymers synthesized from TAQA and 1,2-EDT exhibited good shape memory behavior. In the warm drawing mode, the sample was heated to 75 °C

(T_g + 10 °C) and stretched (to 20% strain) and then cooled to 0 °C before suppressing the applied stress. The free strain recovery data in Figure 5.4 show a five-cycle thermomechanical cycling of 20% prestrained TAQA-1,2-EDT sample in (a) strain-time and stress time and (b) strain-temperature planes. As seen in Figure 5.7b, the recovery strain, ε_{rec}, was 85% for the first cycle, 95% for the second run and greater than 99% for cycles 3-5. According to previous studies, covalent cross-linking is expected to result in good shape recovery and materials with uniform distribution of cross-linking is key to achieving fully recoverable strain capacity, which these thermosets possess.[159] In addition to uniform distribution, identical chain segments between netpoints, as present in these materials, are important to developing predictable shape recovery. Herein, we report similarly behaving materials with narrow transitions.

As it is important to be able to control the temperature at which thermal transition exists, DAC was added in various amounts to reduce the amount of crosslinking and mass content of the rigid bicyclic comonomer, TAQA. Addition of DAC afforded materials with lower T_gs without introducing new chemical functionalities. To confirm that the introduction of DAC would lead facile T_g tuning without affecting shape-memory behavior, which is critical for thermally activated shape-memory systems, the film containing (0.75 TAQA: 0.25 DAC)-*co*-1,2-EDT (Table 5.1, Sample 6) was subjugated to thermomechanical cycling of 20% prestrained sample in (a) strain-time and stress time and (b) strain-temperature planes. As seen in Figure 5.8b, the recovery strain, ε_{rec}, was 90% for the first cycle, greater than 99% for cycles 4-5. The homogeneous nature of the thiol-ene free radical addition polymerization mechanism resulted in thermoset

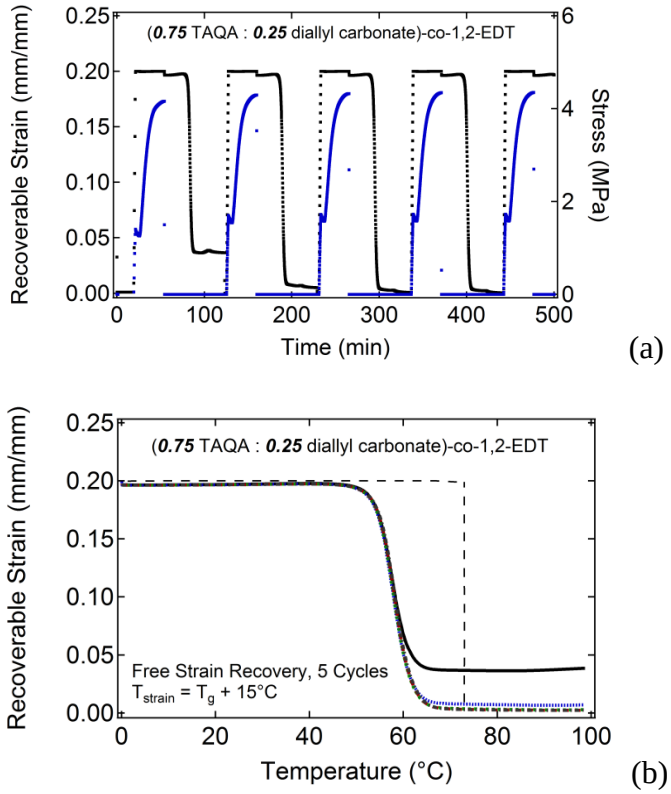

Figure 5.5. Demonstration of the shape memory effect over five cycles of 20% applied strain for poly(thioether-*co*-carbonate) thermoset synthesized from TAQA and DAC (0.75: 0.25 ratio, respectively) and 1,2-EDT. Greater than 99% recoverable strains were recovered during cycles 4 and 5.

networks with sharp glass transition regions, which were tailorable over the range of 35-80°C. The shape memory effect is thus demonstrated to present this novel polycarbonate thermoset system as a platform material system for multi-functional advanced materials applications.

5.6 Conclusions

We presented a series of photo-crosslinked polymer networks derived from the natural product, quinic acid, with controlled T_g values from -18 to 63 °C and rubbery modulus values ranging from 3.8 to 14 MPa by variation in multifunctional thiol comonomers. The network containing the highest weight percent of the rigid bicyclic monomer exhibited the highest T_g of 63 °C and a storage modulus of 1.4 GPa, properties comparable to those of common degradable polyesters currently used in orthopedic applications. Additionally, by varying the ene-component of the network with the introduction of diallyl carbonate, the T_g values of networks of 1,2-EDT-*co*-TAQA-*co*-DAC, fell within a continuum, from 63 to -15 °C without changing the chemical composition of the resulting materials. Interestingly, films with ≥50% TAQA, in terms of ene molar functionality, exhibited decreasing T_gs with increasing DAC content, without a decrease in rubbery moduli. Early studies revealed that these materials exhibit shape-memory properties and show promise as thermal responsive actuating materials. The homogenous nature of the highly crosslinked network led to materials with sharp T_g regions and fast actuation speeds. Control force cyclic testing by DMA showed high percent recoverable strains, reaching 100% recovery during fourth and fifth cycles for 1,2-EDT-*co*-TAQA and 1,2-EDT-*co*-TAQA-*co*-DAC materials. This system of alloc-protection and synthesis of poly(thioether-*co*-carbonate) represents a viable way to produce materials with a wide-range of achievable properties from non-petroleum based products. In fact, this method has already been applied to the production of elastic

materials produced from isosorbide, a bicyclic diol produced from the dehydration of glucose. These compounds represent an expansion of this polymerization system, allowing for the production of additional elastic materials with further tuning of existing quinic acid-based networks *via* copolymerization.

CHAPTER VI

CONCLUSIONS

This body of work has expanded on the field of polycarbonates synthesized from carbohydrates and other naturally occurring polyhydroxyl products. Linear polycarbonates incorporating glucose into the main chain were synthesized by AA'/BB polymerizations of phosgene, diphosgene or triphosgene with one of four different regioisomeric diols. Monomers were synthesized by selective protection of D-glucose, affording 2,3,6-tri-*O*-benzyl-α-D-glucopyranoside (*1,4* diol), 2,3,4-tri-*O*-benzyl-α-D-glucopyranoside (*1,6* diol), methyl 3,4-di-*O*-benzyl-α-D-glucopyranoside (*2,6* diol), and methyl 2,4-di-*O*-benzyl-α-D-glucopyranoside (*3,6* diol). Polymerization screening with the *1,4* monomer failed in the production of high molecular weight polymers (>10 kDa). Initial attempts at polymerization of the *1,4* monomer proved unsuccessful due to the reactivity of the anomeric hemiacetal group in pyridine. It was later discovered, that monomers with hemiacetal functional groups (*1,4* and *1,6* monomers) were significantly less reactive than the *2,6* and *3,6* diols (which possessed primary and secondary alcohols), producing polymers with lower molecular weights (≤10 kDa) when polymerized with triphosgene. Reaction conditions involving stoichiometric amounts of triphosgene in DCM were conducive for producing large molecular weight polymers (≥30 kDa) with *2,6* and *3,6* monomers.

Thermal analysis by DSC and TGA demonstrated that the thermal properties of resulting polycarbonates were dependent on the monomer composition. Depending on

connectivity and molecular weight, polymers with varying T_g values were produced, ranging from 44 to 85 °C. In addition, the thermal stability also was affected by the connectivity of each polymer. Polymers with carbonate linkages connected to the anomeric center of the glycosidic ring were more thermally sensitive and possessed low onset decomposition temperatures. We hypothesized that polymers made from *1,4* and *1,6* monomers would be more sensitive to thermal and hydrolytic degradation as the acetal linkage at the anomeric position would accelerate the decomposition of the backbone, however, the mass loss and tandem TGA-MS data did not fully support our proposals. Additional observed MS signals indicated a more complicated degradation mechanism, in which the carbonate group interacts with the benzyl protecting groups, leading to loss of carbon dioxide and benzaldehyde compounds.

Using lessons learned from the first family of glucose-diol monomers, changes in the synthetic design were made to give AA'A'A monomers bearing to primary alcohols with the expectations that the more nucleophilic and less hindered hydroxyl groups would lead to higher molecular weight polymers. As predicted, bis-adduct monomers with led to higher molecular weight polymers, exceeding 100 kDa in one case, with high T_g values and high thermal stability. As a result of this step-wise monomer synthesis, polymers with only head-to-head and tail-to-tail connections were produced. Direct comparison could be made with previous generation of polymers shedding more light on their regiorandom connectivites. The stepwise synthesis not only allowed for the synthesis of larger molecular weight polymers but also gives us greater flexibility in their design. Different linkages or monomers can be incorporated into the main chain to

alter the chemical composition and chain length, allowing for a great deal of control over the final properties of the resulting material.

Our initial goal was to form glucose-based polycarbonates with the glucose ring incorporated into the main chain in order to mimic the structure of cellulose, leading to strong renewable materials. Ideally we could produce robust polymers that have the similar degrees of intermolecular hydrogen bonding and crystallinity as cellulose, while introducing the ability for hydrolytic degradation by the replacing β1→4 glycosidic linkages with carbonate groups. To this point, we have been successful in formation protected polymers. Further studies would need to be performed to assess the utility of the polymer in hard tissue biomedical applications and other engineering materials. Removal of benzyl protecting groups through hydrogenolysis is currently being performed. It will be interesting to see how the increased degree in intermolecular hydrogen bonding will affect the mechanical properties of the polymers or amplify any morphological differences between polymers with different stereo- or regiochemistries.

We have demonstrated the synthesis of a glucal-based cyclic carbonate monomer and it's controlled ROP *via* the organobase DBU and organic cocatalyst TU to afford polymers with well-defined end groups and narrow molecular weight distributions. Analysis by ^{13}C NMR revealed the formation of polycarbonates having regioregular properties, favoring the formation of head-to-tail polymers. This finding was surprising, considering previously synthesized glucose analogues with sterically larger side groups polymerized in a random fashion. Absence of 2,3-*O*-functionality and introduction of a double-bond in the glycosidic ring introduced ring strain to the six-membered cylic

carbonate, allowing for the monomer to polymerize at a much faster rate with much lower catalyst concentrations than other monomer systems. Thermal analysis revealed that this glucal-based polycarbonate exhibited an amorphous character and comparably high T_g than common aliphatic polycarbonates, making it attractive for a broad range of potential applications.

Design of highly-strained monomers led to rapid reactions that could polymerize in dilute conditions with low catalyst loading, expanding the use of glucose as a monomer feedstock to create polycarbonate materials with complex functionalities. In order to understand the role of the double bond during the polymerization, further assessment of the ring strain of cyclic carbonate is needed. Computational studies are currently being performed to better understand how the double bond affects the polymerization thermodynamics and ring-opening mechanism. Furthermore, to truly assess the novelty of this monomer system as a platform for the synthesis of tunable materials, preparation of copolymers and post-polymerization functionalization should take place to assess the compatibility of this monomer with other monomer systems and the viability of the cyclic-ene group, or any other functional group added *via* Ferrier reaction, for polymer modification.

In Chapter V, we presented a series of photo-crosslinked polymer networks derived from the natural product, quinic acid, with controlled T_g values from -18 to 63 °C and rubbery modulus values from 3.8 to 14 MPa. The network containing the highest weight percent of the rigid bicyclic monomer exhibited the highest T_g of 63 °C and a storage modulus of 1.4 GPa, properties comparable to those of common

degradable polyesters currently used in orthopedic applications. By varying the ene-component of the network, by introduction of diallyl carbonate, the T_g values of networks of 1,2-EDT-*co*-TAQA-*co*-DAC, were also able to varied, from 63 to -15°C, without significantly altering the rubbery modulus or changing the chemical composition of the resulting materials. Early studies revealed that these materials exhibit shape-memory properties and show promise as thermal responsive actuating materials. The homogenous nature of the highly crosslinked network led to materials with sharp T_g regions and fast actuation speeds. Control force cyclic testing by DMA showed excellent shape memory behavior for 1,2-EDT-*co*-TAQA and 1,2-EDT-*co*-TAQA-*co*-DAC materials. High percent recoverable strains were obtained, reaching 100% recovery during fourth and fifth cycles. This system of alloc-protection and synthesis of poly(thioether-*co*-carbonate) represents a viable way to produce materials with a wide-range of achievable properties from non-petroleum based products. In fact, this method has already been applied to the production of elastic materials produced from isosorbide, a bicyclic diol produced from the dehydration of glucose. These compounds represent an expansion of this polymerization system, allowing for the production of additional elastic materials with further tuning of existing quinic acid-based networks *via* copolymerization.

These materials show promise as degradable biomedical materials, however little is known of their degradation dynamics. Future investigations will need to focus on the degradation kinetics in vitro and in vivo of these materials, as well as on strategies for incorporating other chemistries and other functional components. In addition, we need

to test the biodegradability and cytotoxicity of these polymer systems, which can be elucidated by cell viability studies. Utilizing naturally occurring poly-hydroxyl compounds should benefit in the production of benign biomedical materials. However, the thiol comonomers, the aliphatic thioether segments of the crosslinked material, or processing methods could cause undesirable cytotoxicity. Copolymerization with alternate comonomers, synthesized from naturally occurring thiol-bearing compounds, such as cysteine, could not only help improve the biological compatibility of these materials, but also further expand the field of green materials.

In all, this body of work will impact how next-generation renewable materials are synthesized, characterized and modified to generate a family of renewable degradable polycarbonates that are of interest for both fundamental studies and numerous applications. These novel polymeric structures are interesting materials that are not found in nature and provide new molecular architectures to be explored.

REFERENCES

(1) Pellis, A.; Herrero Acero, E.; Gardossi, L.; Ferrario, V.; Guebitz, G., M. *Polymer International* **2016**, *65*, 861-871.

(2) Rabie, A. B. M.; Wong, R. W. K.; Hägg, U. *British Journal of Oral and Maxillofacial Surgery* **2000**, *38*, 565-570.

(3) Cavalcanti, S. C. S. X. B.; Pereira, C. L.; Mazzonetto, R.; de Moraes, M.; Moreira, R. W. F. *Journal of Craniomaxillofacial Surgery* **2008**, *36*, 354-359.

(4) *National Hospital Discharge Survey 2010*, U.S. Department of Health and Human Services Centers for Disease Control and Prevention, National Center for Health Statistics: Washington DC, 2010.

(5) Scholz, M. S.; Blanchfield, J. P.; Bloom, L. D.; Coburn, B. H.; Elkington, M.; Fuller, J. D.; Gilbert, M. E.; Muflahi, S. A.; Pernice, M. F.; Rae, S. I.; Trevarthen, J. A.; White, S. C.; Weaver, P. M.; Bond, I. P. *Composites Science and Technology* **2011**, *71*, 1791-1803.

(6) Schaschke, C.; Audic, J.-L. *International Journal of Molecular Sciences* **2014**, *15*, 21468-21475.

(7) Yeung, K. W. K.; Wong, K. H. M. *Technology and Health Care* **2012**, *20*, 345-362.

(8) Goodrich, J. T.; Sandler, A. L.; Tepper, O. *Child's Nervous System* **2012**, *28*, 1577-1588.

(9) Curtis, R.; Goldhahn, J.; Schwyn, R.; Regazzoni, P.; Suhm, N. *Osteoporosis International* **2005**, *16*, S54-S64.

(10) Sheikh, Z.; Najeeb, S.; Khurshid, Z.; Verma, V.; Rashid, H.; Glogauer, M. *Materials* **2015**, *8*, 5744-5794.

(11) Ganesh, V. K.; Ramakrishna, K.; Ghista, D. N. *BioMedical Engineering OnLine* **2005**, *4*, 1-15.

(12) Ohlin, A.; Karlsson, M.; Duppe, H.; Hasserius, R.; Redlund-Johnell, I. *Spine* **1994**, *19*, 2774-2779.

(13) McAfee, P. C.; Cunningham, B. W.; Lee, G. A.; Orbegoso, C. M.; Haggerty, C. J.; Fedder, I. L.; Griffith, S. L. *Spine* **1999**, *24*, 2147-2153.

(14) Wuisman, P. I. J. M.; Smit, T. H. *European Spine Journal* **2005**, *15*, 133-148.

(15) Balamurugan, A.; Rajeswari, S.; Balossier, G.; Rebelo, A. H. S.; Ferreira, J. M. F. *Materials and Corrosion* **2008**, *59*, 855-869.

(16) Park, H.; Temenoff, J. S.; Mikos, A. G. In *Engineering of Functional Skeletal Tissues*; Bronner, F., Farach-Carson, M. C., Mikos, A. G., Eds.; Springer London: London, 2007; pp 55-68.

(17) Kulkarni, R. K.; Pani, K. C.; Neuman, C. C.; Leonard, F. F. *Archives of Surgery* **1966**, *93*, 839-843.

(18) Rokkanen, P.; Vainionpää, S.; Törmälä, P.; Kilpikari, J.; Böstman, O.; Vihtonen, K.; Laiho, J.; Tamminmäki, M. *The Lancet* **1985**, *325*, 1422-1424.

(19) Middleton, J. C.; Tipton, A. J. *Biomaterials* **2000**, *21*, 2335-2346.

(20) Törmälä, P. *Clinical Materials* **1992**, *10*, 29-34.

(21) Ikada, Y.; Tsuji, H. *Macromolecular Rapid Communications* **2000**, *21*, 117-132.

(22) Chu, C. C. In *Biomaterials: Principles and Applications*; Park, J. B., Bronzino, J. D., Eds.; CRC Press: Boca Raton, 2003; pp 95-115.

(23) Gogolewski, S. *Injury, International Journal of the Care of the Injured* **2000**, *31*, D28-D32.

(24) Huiskes, R.; van Rietbergen, B. In *Basic Orthopaedic Biomechanics and Mechano-biology*; Third Edition ed.; van Mow, C., Huiskes, R., Eds.; Lippincott Williams & Wilkins: Philidelphia, 2005; pp 123-179.

(25) Park, S. H.; Llinás, A.; Goel, V. K.; Keller, J. C. In *Biomaterials: Principles and Applications*; Park, J. B., Bronzino, J. D., Eds.; CRC Press: Boca Raton, 2003; pp 173-206.

(26) Pietrzak, W. S.; Sarver, D. R.; Verstynen, M. L. *Journal of Craniofacial Surgery* **1997**, *8*, 87-91.

(27) Turvey, T. A.; Bell, R. B.; Tejera, T. J.; Proffit, W. R. *Journal of Oral and Maxillofacial Surgery*, **2002**, *60*, 59-65.

(28) Ambrose, C. G.; Clanton, T. O. *Annals of Biomedical Engineering* **2004**, *32*, 171-177.

(29) Gupta, A. P.; Kumar, V. *European Polymer Journal* **2007**, *43*, 4053-4074.

(30) Lasprilla, A. J. R.; Martinez, G. A. R.; Lunelli, B. H.; Jardini, A. L.; Filho, R. M. *Biotechnology Advances* **2012**, *30*, 321-328.

(31) Ren, J. In *Biodegradable Poly(Lactic Acid): Synthesis, Modification, Processing and Applications*; Ren, J., Ed.; Springer Berlin Heidelberg: Berlin, Heidelberg, 2010; pp 240-272.

(32) Grijpma, D. W.; Nijenhuis, A. J.; van Wijk, P. G. T.; Pennings, A. J. *Polymer Bulletin* **1992**, *29*, 571-578.

(33) Gunatillake, P. A.; Adhikari, R. *European Cells and Materials* **2003**, *5*, 1-16.

(34) Lee, S. J.; Khang, G.; Lee, Y. M.; Lee, H. B. *Journal of Biomaterials Science, Polymer Edition* **2002**, *13*, 197-212.

(35) Dobrzynski, P.; Kasperczyk, J. *Journal of Polymer Science Part A: Polymer Chemistry* **2006**, *44*, 98-114.

(36) Yang, J.; Liu, F.; Tu, S.; Chen, Y.; Luo, X.; Lu, Z.; Wei, J.; Li, S. *Journal of Biomedical Materials Research Part A* **2010**, *94A*, 396-407.

(37) Pospiech, D.; Komber, H.; Jehnichen, D.; Häussler, L.; Eckstein, K.; Scheibner, H.; Janke, A.; Kricheldorf, H. R.; Petermann, O. *Biomacromolecules* **2005**, *6*, 439-446.

(38) Darensbourg, D. J.; Choi, W.; Karroonnirun, O.; Bhuvanesh, N. *Macromolecules* **2008**, *41*, 3493-3502.

(39) Nederberg, F.; Lohmeijer, B. G. G.; Leibfarth, F.; Pratt, R. C.; Choi, J.; Dove, A. P.; Waymouth, R. M.; Hedrick, J. L. *Biomacromolecules* **2007**, *8*, 153-160.

(40) Thomas, C.; Bibal, B. *Green Chemistry* **2014**, *16*, 1687-1699.

(41) Shi, R.; Chen, D.; Liu, Q.; Wu, Y.; Xu, X.; Zhang, L.; Tian, W. Recent Advances in Synthetic Bioelastomers. *International Journal of Molecular Sciences* **2009**, *10*, 4223-4256.

(42) Carothers, W. H.; Natta, F. J. V. *Journal of the American Chemical Society* **1930**, *52*, 314-326.

(43) Xu, J.; Feng, E.; Song, J. *Journal of Applied Polymer Science* **2014**, *131*, 39822. DOI: 10.1002/app.39822.

(44) Feng, J.; Zhuo, R.-X.; Zhang, X.-Z. *Progress in Polymer Science* **2012**, *37*, 211-236.

(45) Tempelaar, S.; Mespouille, L.; Coulembier, O.; Dubois, P.; Dove, A. P. *Chemical Society Reviews* **2013**, *42*, 1312-1336.

(46) Fukuoka, S.; Kawamura, M.; Komiya, K.; Tojo, M.; Hachiya, H.; Hasegawa, K.; Aminaka, M.; Okamoto, H.; Fukawa, I.; Konno, S. *Green Chemistry* **2003**, *5*, 497-507.

(47) Bisht, K. S.; Svirkin, Y. Y.; Henderson, L. A.; Gross, R. A.; Kaplan, D. L.; Swift, G. *Macromolecules* **1997**, *30*, 7735-7742.

(48) Yamamoto, Y.; Kaihara, S.; Toshima, K.; Matsumura, S. *Macromolecular Bioscience* **2009**, *9*, 968-978.

(49) Darensbourg, D. J. *Chemical Reviews* **2007**, *107*, 2388-2410.

(50) Park, J. H.; Jeon, J. Y.; Lee, J. J.; Jang, Y.; Varghese, J. K.; Lee, B. Y. *Macromolecules* **2013**, *46*, 3301-3308.

(51) Sun, J.; Kuckling, D. *Polymer Chemistry* **2016**, *7*, 1642-1649.

(52) Wang, X.-L.; Zhuo, R.-X.; Liu, L.-J.; He, F.; Liu, G. *Journal of Polymer Science Part A: Polymer Chemistry* **2002**, *40*, 70-75.

(53) Wang, L.-S.; Cheng, S.-X.; Zhuo, R.-X. *Macromolecular Rapid Communications* **2004**, *25*, 959-963.

(54) Mindemark, J.; Bowden, T. *Polymer Chemistry* **2012**, *3*, 1399-1401.

(55) Pratt, R. C.; Nederberg, F.; Waymouth, R. M.; Hedrick, J. L. *Chemical Communications* **2008**, 114-116.

(56) Tempelaar, S.; Mespouille, L.; Dubois, P.; Dove, A. P. *Macromolecules* **2011**, *44*, 2084-2091.

(57) Tempelaar, S.; Barker, I. A.; Truong, V. X.; Hall, D. J.; Mespouille, L.; Dubois, P.; Dove, A. P. *Polymer Chemistry* **2013**, *4*, 174-183.

(58) Venkataraman, S.; Veronica, N.; Voo, Z. X.; Hedrick, J. L.; Yang, Y. Y. *Polymer Chemistry* **2013**, *4*, 2945-2948.

(59) Engler, A. C.; Chan, J. M. W.; Coady, D. J.; O'Brien, J. M.; Sardon, H.; Nelson, A.; Sanders, D. P.; Yang, Y. Y.; Hedrick, J. L. *Macromolecules* **2013**, *46*, 1283-1290.

(60) Wang, R.; Chen, W.; Meng, F.; Cheng, R.; Deng, C.; Feijen, J.; Zhong, Z. *Macromolecules* **2011**, *44*, 6009-6016.

(61) Xu, J.; Prifti, F.; Song, J. *Macromolecules* **2011**, *44*, 2660-2667.

(62) Zhang, X.; Cai, M.; Zhong, Z.; Zhuo, R. *Macromolecular Rapid Communications* **2012**, *33*, 693-697.

(63) Bartolini, C.; Mespouille, L.; Verbruggen, I.; Willem, R.; Dubois, P. *Soft Matter* **2011**, *7*, 9628-9637.

(64) Chiu, F.-C.; Lai, C.-S.; Lee, R.-S. *Journal of Applied Polymer Science* **2007**, *106*, 283-292.

(65) Ong, Z. Y.; Fukushima, K.; Coady, D. J.; Yang, Y.-Y.; Ee, P. L. R.; Hedrick, J. L. *Journal of Controlled Release* **2011**, *152*, 120-126.

(66) Seow, W. Y.; Yang, Y. Y. *Journal of Controlled Release* **2009**, *139*, 40-47.

(67) Varma, A. J.; Kennedy, J. F.; Galgali, P. *Carbohydrate Polymers* **2004**, *56*, 429-445.

(68) Narain, R.; Jhurry, D.; Wulff, G. *European Polymer Journal* **2002**, *38*, 273-280.

(69) Ladmiral, V.; Melia, E.; Haddleton, D. M. *European Polymer Journal* **2004**, *40*, 431-449.

(70) Jain, K.; Kesharwani, P.; Gupta, U.; Jain, N. K. *Biomaterials* **2012**, *33*, 4166-4186.

(71) Slavin, S.; Burns, J.; Haddleton, D. M.; Becer, C. R. *European Polymer Journal* **2011**, *47*, 435-446.

(72) Galbis, J. A.; García-Martín, M. d. G.; de Paz, M. V.; Galbis, E. *Chemical Reviews* **2016**, *116*, 1600-1636.

(73) LeGrand, D. G.; Bendler, J. T. *Handbook of Polycarbonate Science and Technology*; Marcel Dekker: New York, 2000.

(74) Brunelle, D. J. In *Advances in Polycarbonates*; American Chemical Society: **2005**; *898*, 1-5.

(75) vom Saal, F. S.; Nagel, S. C.; Coe, B. L.; Angle, B. M.; Taylor, J. A. *Molecular and Cellular Endocrinology* **2012**, *354*, 74-84.

(76) Buckley, J. P.; Herring, A. H.; Wolff, M. S.; Calafat, A. M.; Engel, S. M. *Environment International* **2016**, *91*, 350-356.

(77) Menale, C.; Mita, D. G.; Diano, N.; Diano, S. *Open Biotechnology Journal* **2016**, *10*, 122-130.

(78) Fukuoka, S.; Fukawa, I.; Tojo, M.; Oonishi, K.; Hachiya, H.; Aminaka, M.; Hasegawa, K.; Komiya, K. *Catalysis Surveys from Asia* **2010**, *14*, 146-163.

(79) Chatti, S.; Schwarz, G.; Kricheldorf, H. R. *Macromolecules* **2006**, *39*, 9064-9070.

(80) Ignatov, V. N.; Tartari, V.; Carraro, C.; Pippa, R.; Nadali, G.; Berti, C.; Fiorini, M. *Macromolecular Chemistry and Physics* **2001**, *202*, 1946-1949.

(81) Woo, B. G.; Choi, K. Y.; Song, K. H.; Lee, S. H. *Journal of Applied Polymer Science* **2001**, *80*, 1253-1266.

(82) Eo, Y. S.; Rhee, H.-W.; Shin, S. *Journal of Industrial and Engineering Chemistry* **2016**, *37*, 42-46.

(83) Li, Q.; Zhu, W.; Li, C.; Guan, G.; Zhang, D.; Xiao, Y.; Zheng, L. *Journal of Polymer Science, Part A: Polymer Chemistry* **2013**, *51*, 1387-1397.

(84) Betiku, O.; Jenni, M.; Ludescher, K.; Meierdierks, E.; Lunt, J.; Schroeder, J. *Polym Prepr (Am Chem Soc Div Polym Chem)* **2007**, *48*, 802-803.

(85) Terado, Y.; Wada, M.; Urakami, T. Aliphatic Polyester Copolymer. U.S. Patent US20080015331 A1, Jan 17, 2008.

(86) Medem, H.; Schreckenberg, M.; Dhein, R.; Nouvertne, W.; Rudolph, H. Thermoplastic Polycarbonates: Their Preparation and Their Use as Shaped Articles and Films. U.S. Patent US4506066 A, Mar 19 1985.

(87) Fenouillot, F.; Rousseau, A.; Colomines, G.; Saint-Loup, R.; Pascault, J. P. *Progress in Polymer Science (Oxford)* **2010**, *35*, 578-622.

(88) Zamora, F.; Hakkou, K.; Alla, A.; Rivas, M.; Roffé, I.; Mancera, M.; Muñoz-Guerra, S.; Galbis, J. A. *Journal of Polymer Science Part A: Polymer Chemistry* **2005**, *43*, 4570-4577.

(89) Bou, J. J.; Iribarren, I.; Munoz-Guerra, S. *Macromolecules* **1994**, *27*, 5263-5270.

(90) García-Martín, M. a. d. G.; Pérez, R. o. R.; Hernández, E. B.; Galbis, J. A. *Carbohydrate Research* **2001**, *333*, 95-103.

(91) Acemoglu, M.; Bantle, S.; Mindt, T.; Nimmerfall, F. *Macromolecules* **1995**, *28*, 3030-3037.

(92) García-Martín, M. G.; Pérez, R. R.; Hernández, E. B.; Espartero, J. L.; Muñoz-Guerra, S.; Galbis, J. A. *Macromolecules* **2005**, *38*, 8664-8670.

(93) Suzuki, M.; Sekido, T.; Matsuoka, S.-i.; Takagi, K. *Biomacromolecules* **2011**, *12*, 1449-1459.

(94) Chen, X.; Gross, R. A. *Macromolecules* **1999**, *32*, 308-314.

(95) Shen, Y.; Chen, X.; Gross, R. A. *Macromolecules* **1999**, *32*, 2799-2802.

(96) Shen, Y.; Chen, X.; Gross, R. A. *Macromolecules* **1999**, *32*, 3891-3897.

(97) Kumar, R.; Gao, W.; Gross, R. A. *Macromolecules* **2002**, *35*, 6835-6844.

(98) Haba, O.; Tomizuka, H.; Endo, T. *Macromolecules* **2005**, *38*, 3562-3563.

(99) Azechi, M.; Matsumoto, K.; Endo, T. *Journal of Polymer Science Part A: Polymer Chemistry* **2013**, *51*, 1651-1655.

(100) Haba, O.; Furuichi, N.; Akashika, Y. *Polymer Journal* **2009**, *41*, 702-708.

(101) Tezuka, K.; Komatsu, K.; Haba, O. *Polymer Journal* **2013**, *45*, 1183-1187.

(102) Tezuka, K.; Koda, K.; Katagiri, H.; Haba, O. *Polymer Bulletin* **2015**, *72*, 615-626.

(103) Gregory, G. L.; Jenisch, L. M.; Charles, B.; Kociok-Köhn, G.; Buchard, A. *Macromolecules* **2016**, *49*, 7165-7169.

(104) Mikami, K.; Lonnecker, A. T.; Gustafson, T. P.; Zinnel, N. F.; Pai, P.-J.; Russell, D. H.; Wooley, K. L. *Journal of the American Chemical Society* **2013**, *135*, 6826-6829.

(105) Gustafson, T. P.; Lonnecker, A. T.; Heo, G. S.; Zhang, S.; Dove, A. P.; Wooley, K. L. *Biomacromolecules* **2013**, *14*, 3346-3353.

(106) Zhang, S.; Li, A.; Zou, J.; Lin, L. Y.; Wooley, K. L. *ACS Macro Letters* **2012**, *1*, 328-333.

(107) Zhang, S.; Zou, J.; Zhang, F.; Elsabahy, M.; Felder, S. E.; Zhu, J.; Pochan, D. J.; Wooley, K. L. *Journal of the American Chemical Society* **2012**, *134*, 18467-18474.

(108) Nair, L. S.; Laurencin, C. T. *Progress in Polymer Science* **2007**, *32*, 762-798.

(109) Yu, L.; Dean, K.; Li, L. *Progress in Polymer Science* **2006**, *31*, 576-602.

(110) Langer, R. *Advanced Materials* **2009**, *21*, 3235-3236.

(111) Balasundaram, G.; Webster, T. J. *Macromolecular Bioscience* **2007**, *7*, 635-642.

(112) Elsabahy, M.; Wooley, K. L. *Chemical Society Reviews* **2012**, *41*, 2545-2561.

(113) Williams, C. K. *Chemical Society Reviews* **2007**, *36*, 1573-1580.

(114) Stanford, M. J.; Dove, A. P. *Chemical Society Reviews* **2010**, *39*, 486-494.

(115) Vert, M. *Journal of Material Science: Materials in Medicine* **2009**, *20*, 437-446.

(116) Galbis, J. A.; García-Martín, M. G. Synthetic Polymers from Readily Available Monosaccharides. In *Carbohydrates in Sustainable Development II*; Rauter, A. P., Vogel, P., Queneau, Y., Eds.; Topics in Current Chemistry; Springer: Berlin; 2010; Vol. 295, pp 147-176.

(117) Wu, G.-M.; Kong, Z.-W.; Huang, H.; Chen, J.; Chu, F.-X. *Journal of Applied Polymer Science* **2009**, *113*, 2894-2901.

(118) Wilbon, P. A.; Chu, F.; Tang, C. *Macromolecular Rapid Communications* **2013**, *34*, 8-37.

(119) Lowe, J. R.; Martello, M. T.; Tolman, W. B.; Hillmyer, M. A. *Polymer Chemistry* **2011**, *2*, 702-708.

(120) Shin, J.; Lee, Y.; Tolman, W. B.; Hillmyer, M. A. *Biomacromolecules* **2012**, *13*, 3833-3840.

(121) Mecking, S. *Angewandte Chemie International Edition* **2004**, *43*, 1078-1085.

(122) Suriano, F.; Pratt, R.; Tan, J. P. K.; Wiradharma, N.; Nelson, A.; Yang, Y.-Y.; Dubois, P.; Hedrick, J. L. *Biomaterials* **2010**, *31*, 2637-2645.

(123) Ong, Z. Y.; Yang, C.; Gao, S. J.; Ke, X.-Y.; Hedrick, J. L.; Yan Yang, Y. *Macromolecular Rapid Communications* **2013**, *34*, 1714-1720.

(124) Kricheldorf, H. R.; Sun, S.-J.; Gerken, A.; Chang, T.-C. *Macromolecules* **1996**, *29*, 8077-8082.

(125) Chen, X.; Gross, R. A. *Macromolecules* **1999**, *32*, 308-314.

(126) Yokoe, M.; Aoi, K.; Okada, M. *Journal of Polymer Science Part A: Polymer Chemistry* **2005**, *43*, 3909-3919.

(127) Haba, O.; Furuichi, N.; Akashika, Y. *Polymer Journal* **2009**, *41*, 702-708.

(128) Wu, J.; Eduard, P.; Jasinska-Walc, L.; Rozanski, A.; Noordover, B. A. J.; Van Es, D. S.; Koning, C. E. *Macromolecules* **2013**, *46*, 384-394.

(129) Fenouillot, F.; Rousseau, A.; Colomines, G.; Saint-Loup, R.; Pascault, J. P. *Progress in Polymer Science* **2010**, *35*, 578-622.

(130) Beguin, P.; Aubert, J.-P. *FEMS Microbiology Reviews* **1994**, *13*, 25-58.

(131) Lam, S. N.; Gervay-Hague, J. *The Journal of Organic Chemistry* **2005**, *70*, 2387-2390.

(132) Plackett, R. L.; Burman, J. P. *Biometrika* **1946**, *33*, 305-325.

(133) Besset, C. J.; Lonnecker, A. T.; Streff, J. M.; Wooley, K. L. *Biomacromolecules* **2011**, *12*, 2512-2517.

(134) Inaba, S.; Yamada, M.; Yoshino, T.; Ishido, Y. *Journal of the American Chemical Society* **1973**, *95*, 2062-2063.

(135) Iimori, T.; Shibazaki, T.; Ikegami, S. *Tetrahedron Letters* **1996**, *37*, 2267-2270.

(136) Yoon, S. J.; Kim, S. H.; Ha, H. J.; Ko, Y. K.; So, J. W.; Kim, M. S.; Yang, Y. I.; Khang, G.; Rhee, J. M.; Lee, H. B. *Tissue Engineering Part A* **2008**, *14*, 539-547.

(137) Agrawal, C. M.; Ray, R. B. *Journal of Biomedical Materials Research* **2001**, *55*, 141-150.

(138) Fu, K.; Pack, D.; Klibanov, A.; Langer, R. *Pharmaceutical Research* **2000**, *17*, 100-106.

(139) Tinsley-Bown, A. M.; Fretwell, R.; Dowsett, A. B.; Davis, S. L.; Farrar, G. H. *Journal of Controlled Release* **2000**, *66*, 229-241.

(140) Walter, E.; Moelling, K.; Pavlovic, J.; Merkle, H. P. *Journal of Controlled Release* **1999**, *61*, 361-374.

(141) Noel, A.; Borguet, Y. P.; Raymond, J. E.; Wooley, K. L. *Macromolecules* **2014**, *47*, 2974-2983.

(142) Link, L. A.; Lonnecker, A. T.; Hearon, K.; Maher, C. A.; Raymond, J. E.; Wooley, K. L. *ACS Applied Materials & Interfaces* **2014**, *6*, 17370-17375.

(143) Zelikin, A. N.; Putnam, D. *Macromolecules* **2005**, *38*, 5532-5537.

(144) Daniel, J. B.; Michael, R. K. *Advances in Polycarbonates*; American Chemical Society, 2005; Vol. 898.

(145) Zhang, Z.; Kuijer, R.; Bulstra, S. K.; Grijpma, D. W.; Feijen, J. *Biomaterials* **2006**, *27*, 1741-1748.

(146) Suyama, T.; Tokiwa, Y. *Enzyme and Microbial Technology* **1997**, *20*, 122-126.

(147) Acemoglu, M. *International Journal of Pharmaceutics* **2004**, *277*, 133-139.

(148) Artham, T.; Doble, M. *Macromolecular Bioscience* **2008**, *8*, 14-24.

(149) Dadsetan, M.; Christenson, E. M.; Unger, F.; Ausborn, M.; Kissel, T.; Hiltner, A.; Anderson, J. M. *Journal of Controlled Release* **2003**, *93*, 259-270.

(150) Pratt, R. C.; Lohmeijer, B. G. G.; Long, D. A.; Lundberg, P. N. P.; Dove, A. P.; Li, H.; Wade, C. G.; Waymouth, R. M.; Hedrick, J. L. *Macromolecules* **2006**, *39*, 7863-7871.

(151) Whiteoak, C. J.; Kielland, N.; Laserna, V.; Escudero-Adán, E. C.; Martin, E.; Kleij, A. W. *Journal of the American Chemical Society* **2013**, *135*, 1228-1231.

(152) Ray, W. C.; Grinstaff, M. W. *Macromolecules* **2003**, *36*, 3557-3562.

(153) Tschan, M. J. L.; Brule, E.; Haquette, P.; Thomas, C. M. *Polymer Chemistry* **2012**, *3*, 836-851.

(154) Garg, N. K.; Caspi, D. D.; Stoltz, B. M. *Journal of the American Chemical Society* **2004**, *126*, 9552-9553.

(155) Small IV, W.; Singhal, P.; Wilson, T. S.; Maitland, D. J. *Journal of Materials Chemistry* **2010**, *20*, 3356-3366.

(156) Safranski, D. L.; Smith, K. E.; Gall, K. *Polymer Reviews* **2013**, *53*, 76-91.

(157) Safranski, D. L.; Gall, K. *Polymer* **2008**, *49*, 4446-4455.

(158) Lendlein, A.; Kelch, S. *Angewandte Chemie International Edition* **2002**, *41*, 2034-2057.

(159) Hearon, K.; Wierzbicki, M. A.; Nash, L. D.; Landsman, T. L.; Laramy, C.; Lonnecker, A. T.; Gibbons, M. C.; Ur, S.; Cardinal, K. O.; Wilson, T. S.; Wooley, K. L.; Maitland, D. J. *Advanced Healthcare Materials* **2015**, *4*, 1386-1398.

APPENDIX

VITA

Name:	Alexander Thomas Lonnecker
Address:	Department of Chemistry Texas A&M University Mailstop 3255 Ross St. @ Spence St. College Station, TX, 77842
Email Address:	alonnecker@gmail.com

Education: B.S., Chemistry, Rhodes College, 2009